To the Graduate Council:

I am submitting herewith a thesis written by Wei Liu entitled "Unmixed Zone in Arc Weld, Significance on Corrosion Resistance and Mechanical Properties." I have examined the final copy of this thesis for form and content and recommend that it be accepted in partial fulfillment of the requirement for the degree of Masters of Science, with a major in Metallurgical Engineering.

Carl D. Lundin, Major Professor

We have read this thesis and recommend its acceptance:

Charlie R. Brooks

Charlie R. Brooks

R. A. Buchanan

Raymond A. Buchanan

Accepted by the Council:

Associate Vice Chancellor and
Dean of The Graduate School

UNMIXED ZONE IN ARC WELDS: SIGNIFICANCE ON CORROSION RESISTANCE AND MECHANICAL PROPERTIES

A Thesis Presented for the

Master of Science

Degree

The University of Tennessee, Knoxville

Wei Liu

August 1996

DEDICATION

This thesis is dedicated to my parents

Mr. Zixiang Liu

刘子祥

and

Mrs. Meina R. Liu

阮梅娜

who have given me love, opportunities, and have always encouraged me in my life.

This thesis is also dedicated to my husband

Gang Zhou

周钢

who has been my best friend, and has always understood and supported me.

ACKNOWLEDGMENT

I would like to thank my major professor, Dr. Carl D. Lundin, for his guidance. I would also like to thank the other committee members, Dr. Charlie R. Brooks and Dr. Raymond A. Buchanan, for their comments and assistance. I would like to express my appreciation to Dr. Paul C. Y. Qiao and Mr. G. Zhou who have helped me with this project and also to BoB McGill for SEM work.

ABSTRACT

The nature and the effect of the unmixed zone in dissimilar fusion welds, especially its significance with regard to corrosion resistance, has been studied in this Welding Research Council sponsored program. Three types of super-austenitic stainless steel (high Mo), (AL-6XN, 254SMO and 654SMO) and five types of fully austenitic nickel based weld filler metals (Inconel 625, C-22, C-276, 686CPT and P16) were evaluated. Shielded Metal Arc (SMA), Gas Metal Arc (GMA), Gas Tungsten Arc (GTA) (filler added) and Gas Tungsten Arc (GTA) autogenous welding processes were utilized for fabricating weldments of each super-austenitic stainless steel. The employment of these welding techniques provided a full range of unmixed zone formation.

The unmixed zone formation was metallographically evaluated using both Optical Light Microscopy (OLM) and Scanning Electron Microscopy (SEM) with varied etchants and etching techniques. It was found that an unmixed zone, with the identical chemical composition of the base metal, is distributed along and adjacent to the fusion boundary in the dissimilar welds. The distribution (width) of the unmixed zone along the weld interface is widest near the root of the SMA Bead-on-plate (BOP) welds and near the mid-plane of the sheet for GTA and GMA open root welds.

The formation of the unmixed zone is dependent on a number of factors which are highly reflective of the welding process, welding heat input and the physical properties of filler metal, such as melting range. The unmixed zone in GTA welds is wider than that in GMA welds for the same welding heat input. A wider unmixed zone has also been observed for welds fabricated using

a filler metal with a higher melting range than that with a lower melting range.

Depletion of Mo in the core of the cellular dendrites in the unmixed zone has been clearly defined by energy dispersive spectroscopy (EDS) analysis. It is believed that depletion of Mo in the core of the cellular dendrites in the unmixed zone is the major reason for reduced localized corrosion resistance in the unmixed zone. However, upon proper solution heat treatment, the extent of Mo segregation is reduced and the localized corrosion resistance of the unmixed zone is improved.

The pitting corrosion behavior of the unmixed zone was evaluated using immersion corrosion tests in 10% $FeCl_3$. For GTA BOP welds, the critical pitting temperature (CPT) of the unmixed zone is lower than that of respective base metal. However, GTA autogenous BOP welds show that the CPT of the fusion zone is lower than that of the unmixed zone (the entire fusion zone of the autogenous weld is an unmixed zone). These experiments indicate that the unmixed zone has an inferior pitting corrosion resistance compared to the base metal.

The pitting corrosion behavior of the unmixed zone was confirmed using cyclic polarization scanning tests. The pitting corrosion resistance of the unmixed zone was evaluated based on measurement of the hysteresis loop area and passive current density in comparison with the respective base metal. The results obtained from the cyclic polarization scanning tests are consistent with that obtained from the immersion corrosion tests.

Pit initiation and propagation behavior was investigated for AL-6XN SMA BOP welds (C-22 filler metal) in 10% $FeCl_3$ at the unmixed zone CPT of 80°C as a function of time. Pits initiated at the core of the cellular dendrites in the

unmixed zone and a "cave propagation" behavior beneath the surface was observed. Upon an increased extent of "cave propagation" beneath the surface, corrosion breaks through to the surface at the other locations due to continuous corrosion along the core of the cellular dendrites. In addition, pit propagation is always oriented vertically downward, independent of the weld or base metal orientation.

The crevice corrosion behavior of the unmixed zone was evaluated for GTA filler added open root welds. Test results showed that a deeper and wider corroded area is characteristic of the unmixed zone compared to the HAZ and base metal. These results define that the unmixed zone has a lower crevice corrosion resistance than that of the base metal and HAZ. This is the case for all the three super-austenitic stainless steels.

It was found that surface condition has a significant influence on the pitting and crevice corrosion behavior of the unmixed zone. Greater surface roughness exacerbates pitting and crevice corrosion in the unmixed zone because a greater surface roughness creates micro-crevices and a higher surface energy condition, which can cause instability of the passive film on the specimen surface. Surface oxidation (i.e. HAZ tinting) also exacerbates the localized corrosion. It is believed that there are some physical defects, such as pores and/or cracks in the oxide film of the heat tinted zone, which can trigger and facilitate the localized corrosion in the heat tinted zone. Reducing surface roughness before welding by grinding (600 grit) and removal of heat tint after welding by pickling causes a significant reduction in the corrosion sensitivity of the unmixed zone.

Solution heat treatments at 2100°F, 2150°F and 2200°F for 30 minutes were performed on all weldment types to define the effect of solution treatment on the localized corrosion behavior in the unmixed zone (related to reduction of the extent of Mo segregation). A thirty minute solution heat treatment at 2100°F is recommended for both dissimilar and autogenous welds to eliminate the pitting corrosion sensitivity in the unmixed zone. After solution treatment at 2100°F for 30 min, the pitting resistance of the unmixed zone is equivalent to that of the base metal, while the pitting resistance of autogenous fusion zone is close to that of the respective base metal. Under the crevice condition, a thirty minute solution heat treatment at 2100°F is recommended for dissimilar welds to eliminate the crevice corrosion in the unmixed zone. A 2200°F solution heat treatment for 30 min is suggested for autogenous weld to avoid the crevice corrosion in autogenous fusion zone. After the recommended solution treatments, the crevice corrosion resistance of the unmixed zone and the autogenous fusion zone is basically equivalent to that of the base metal.

Bend tests and hardness measurements on AL-6XN welds show that there is virtually no influence of the unmixed zone on mechanical properties (although there is a significant effect of the unmixed zone on localized corrosion behavior). The bend ductility and hardness of the unmixed zone were equivalent to that of the base metal for all three super-austenitic stainless steels.

TABLE OF CONTENTS

CHAPTER Page

I. INTRODUCTION 1
1.1 Background 1
1.2 Scope of the program 3

II. LITERATURE REVIEW 5
2.1 The base metals 5
2.1.1 Microstructure of base metals 5
2.1.2 Mechanical properties of base metals 7
2.1.3 Corrosion behavior of base metals 7
• Pitting and crevice corrosion 7
• General corrosion 9
• Stress corrosion cracking 11
2.1.4 Physical properties of base metals 15
2.2 Welding 15
2.2.1 Welding procedures and techniques 15
2.2.2 Filler metals 18
2.3 Unmixed zone 19
2.3.1 Unmixed zone formation 19
2.3.2 Unmixed zone evaluation techniques 23
2.3.3 Unmixed zone corrosion resistance 23
2.4 Localized corrosion 25
2.4.1 Localized corrosion initiation and propagation mechanisms 25
• Pitting corrosion 25
• Crevice corrosion 28
2.4.2 Factors related to localized corrosion 31
2.4.3 Localized corrosion test methods and ASTM standards .. 32
• Electrochemical tests 32
• Chemical tests 40

III. MATERIALS AND EXPERIMENTAL PROCEDURES 41

3.1 Materials and weld preparation..... 41
3.2 Sample preparation..... 43
3.2.1 Metallographic sample preparation..... 43
3.2.2 Corrosion test sample preparation..... 46
• Pitting corrosion test specimen..... 46
• Crevice corrosion test specimen..... 46
3.2.3 Mechanical property test sample preparation..... 47
• Hardness test specimen..... 47
• Bending test specimen..... 47
3.3 Testing methods..... 48
3.3.1 Pitting corrosion testing..... 48
• Test for determining the critical pitting temperature (CPT) of the unmixed zone..... 48
• Electrochemical corrosion testing..... 50
• Pitting initiation and propagation testing..... 52
3.3.2 Crevice corrosion testing..... 52
3.3.3 Solution heat treatment..... 55
3.3.4 Microhardness testing..... 56
3.3.5 Bend testing..... 56

IV. EXPERIMENTAL RESULTS AND DISCUSSIONS..... 60
4.1 Evaluation of unmixed zone..... 60
4.1.1 Metallographic evaluation of unmixed zone..... 60
4.1.2 Extent and distribution of unmixed zone..... 61
4.1.3 Evaluation of unmixed zone using SEM with EDS analysis..... 75
4.1.4 Solidification and segregation in unmixed zone..... 76
• Solidification in unmixed zone..... 76
• Segregation in unmixed zone..... 78
4.1.5 Effect of solution heat treatment on unmixed zone..... 81
4.1.6 Effect of welding technique on unmixed zone Occurrence..... 87
4.1.7 Summary of evaluation of unmixed zone..... 91
4.2 Pitting corrosion behavior of unmixed zone..... 92

4.2.1 Critical pitting temperature of unmixed zone..... 92
• Immersion Corrosion Testing..... 92
• Electrochemical Corrosion Testing..... 96
4.2.2 Pit initiation and propagation behavior in unmixed zone..... 105
4.2.3 Effect of solution heat treatment on pitting behavior of unmixed zone..... 114
4.2.4 Effect of surface finish on pitting behavior of unmixed zone..... 123
4.2.5 Summary of unmixed zone pitting corrosion behavior..... 126
4.3 Crevice corrosion behavior of unmixed zone..... 129
4.3.1 Evaluation of crevice corrosion behavior of unmixed zone..... 129
4.3.2 Effect of surface condition on crevice corrosion behavior of unmixed zone..... 144
4.3.3 Effect of heat treatment on crevice corrosion behavior of unmixed zone..... 150
4.3.4 Summary of unmixed zone crevice corrosion behavior..... 163
4.4 Effect of welding technique on unmixed zone corrosion behavior..... 164

4.5 Effect of unmixed zone on mechanical properties..... 166
4.5.1 Effect of unmixed zone on hardness..... 166
4.5.2 Effect of the unmixed zone on ductility..... 169
4.5.3 Summary the effect of unmixed zone on mechanical properties..... 171

V. CONCLUSIONS..... 172
5.1 Evaluation of Unmixed Zone..... 172
5.2 Pitting Corrosion Behavior of Unmixed Zone..... 174
5.3 Crevice Corrosion Behavior of Unmixed Zone..... 176
5.4 Effect of Unmixed Zone on Mechanical properties..... 178

REFERENCES..... 179

VITA..... 186

LIST OF TABLES

TABLE	Page
1. Chemical Compositions of Austenitic Stainless Steels	6
2. Typical Tensile Properties for Superaustenitic Stainless Alloy Sheet	8
3. Pitting and Crevice Corrosion Indices	10
4. Corrosion Resistance in Boiling Solution	12
5. Lowest temperature (°F) at which the corrosion rate exceeds 5 mpy	13
6. U-bend Stress Corrosion Cracking Test	14
7. SCC Resistance of Stainless Steels	16
8. Physical Properties of Superaustenitic Stainless Steels at Room Temperature	17
9. Chemical Compositions (wt%) of High Mo Content Filler Metals	20
10. Chemical Compositions of Base Metals and Filler Metals (wt.%).	42
11. Welding Parameters for Different Welding Techniques	45
12. Etchants and Etching Techniques Used in This Study	65
13. Welds Selected for Solution Heat Treatment	93
14. Polarization Characteristics of Different Specimens	103
15. Corrosion Test Results for Different Surface Condition	127
16. Weight Loss of Test Specimens after Crevice Corrosion Tests	134

LIST OF FIGURES

FIGURE page

1. Regions Consisted in a Dissimilar Weld..... 21

2. (a) Illustration of a process leading to pit initiation. M: metal, MO: passive film, MX: metal halide, Sol: solution; (b) Schematic representation of processes occurring within the system consisting of the metal, the passive film, the halide nucleus, and the solution..... 29

3. Typical electrochemical polarization curve for an active-passive alloy (with cathodic trace) showing active, passive, and transpassive regions and other important features such as E_B = breakdown potential and E_p = repassivation potential as well as E_{pp} = primary passive potential and E_{corr} = freely corroding potential..... 33

4. Schematic representation of anodic polarization curves obtained using all three potentiokinetic methods. (a) Potential sweep in anodic direction only (b) Anodic potential sweep followed by the reverse sweep..... 35

5. Schematic representation of anodic polarization curves obtained using galvanokinetic methods. (a) Galvanodynamic and quasi-stationary methods (b) Stationary methods..... 36

6. Schematic representation of current vs. time curves obtained using potentiostatic methods. (a) Determination of E_B; (b) Determination of E_p..... 38

7. Schematic representation of potential time curve obtained using galvanostatic method..... 39

8. The sketch of weld groove for open root welds..... 44

9. The sketch of bending test specimens. (a) Transverse root bend test specimen. (b) Longitudinal root bend test samples..... 49

10. The electrochemical testing cell..... 51

11. UT crevice corrosion device..... 53

12. Crevice corrosion test specimen. (a) Weld face. (b) Weld root..... 54

13. Calculation of solution heat treatment time as a function of temperature..... 57

14. Bend Test Jig..... 59

15. Longitudinal cross-section of AL-6XN SMA BOP weld..... 62

16. Transverse cross-section of AL-6XN SMA BOP weld..... 63

17. Top-view of AL-6XN SMA BOP weld..... 64

18. The unmixed zone revealed using electrolytic glyceregia, (a) weld with C-22 filler metal, (b) weld with Inconel 625 filler metal..... 66

19. The unmixed zone revealed using electrolytic oxalic acid, (a) weld with C-22 filler metal, (b) weld with Inconel 625 filler metal..... 67

20. The unmixed zone revealed using chemical aqua-regia, (a) weld with C-22 filler metal, (b) weld with Inconel 625 filler metal..... 68

21. The area for measurement of distribution of the unmixed zone along welding interface on transverse cross-section of AL-6XN SMA BOP weld (C-22 filler metal)..... 70

22. The area for measurement of distribution of the unmixed zone along welding interface on transverse cross-section of AL-6XN GTA open root weld (C-22 filler metal)..... 71

23. Width of the unmixed zone along welding interface on transverse cross-section of AL-6XN SMA BOP weld with C-22 and Inconel 625 filler metals..... 72

24. Width of the unmixed zone along welding interface on transverse cross-section of GTA open root welds on AL-6XN (C-22 filler) and 654SMO (P16 filler)..... 73

25. Variation of viscosity of some metals with temperature..... 75

26. (a) SEM micrograph at weld interface of CN-3MN SMA BOP weld with Inconel 112 filler metal, (b) chemical profile of alloying elements along line AB in Figure 26 (a)..... 77

27. Solidification morphology in CN-3MN SMA BOP (casting) weld with 112 electrode, transverse cross-section, (a) bright field image, (b) dark field image 79

28. (a). Micrograph at weld interface of CN-3MN SMA BOP weld (Inconel 112 electrode), (b). Molybdenum profile along line XY in the unmixed zone in Figure (a) 82

29. The unmixed zone distributed along weld interface - AL-6XN GTA open root weld (C-22 filler) on transverse cross-section, (a) as-welded condition, (b) solution heat treated condition (2100°F for 30 min) 84

30. The unmixed zone distributed along weld interface - AL-6XN GTA open root weld (C-22 filler) on transverse cross-section, (a) as-welded condition, (b) solution heat treated at 2100°F for 30 min 86

31. (a) SEM micrograph at weld interface of 654SMO GTA open root weld (P16 filler metal) in as-welded condition, (b) chemical profile of alloying elements along line AB in Figure 31 (a) 88

32. (a) SEM micrograph at weld interface of 654SMO GTA open root weld (P16 filler metal) after solution treatment at 2100°F for 30 min, (b) chemical profile of alloying elements along line AB in Figure 31 (a) 89

33. Width of the unmixed zone along weld interface on transverse cross-section - AL-6XN GMA open root weld (C-22 filler) and AL-6XN manual GTA open root weld (C-22 filler) 90

34. Critical pitting temperature of the unmixed zone as a function of pitting resistance equivalent of base metals. (Test solution: 10% $FeCl_3$, Test time: 24 hours and surface condition: 0.05 μm) 94

35. Pitted sample surface of AL-6XN SMA BOP autogenous weld - Test solution: 10% $FeCl_3$, test time: 24 hours, test temperature: 60°C 97

36. Pitted sample surface of AL-6XN SMA BOP weld (C-22 filler metal) - Test solution: 10% $FeCl_3$, test time: 24 hours, test temperature: 80°C 98

37. Cyclic polarization curve of AL-6XN dissimilar welded specimen with the unmixed zone on surface in comparison with that of AL-6XN un-welded base metal..... 100

38. Cyclic polarization curve of AL-6XN autogenous fusion zone in comparison with that of the dissimilar welded specimen with the unmixed zone on the surface..... 101

39. Cyclic polarization curve of AL-6XN dissimilar welded specimen with the unmixed zone on surface in comparison with that of AL-6XN dissimilar welded specimen without the unmixed zone on surface..... 102

40. Pit initiation in the core of the cellular dendrite in the unmixed zone after 2 minutes at 80°C in 10% $FeCl_3$ solution..... 106

41. Pit propagation in the unmixed zone after 4 minutes at 80°C in 10% $FeCl_3$ solution..... 107

42. Pit propagation in the unmixed zone after 30 minutes 80°C in 10% $FeCl_3$ solution, (a) top view, (b) transverse cross-section..... 108

43. Pit propagation in the unmixed zone after 60 minutes in 10% $FeCl_3$ solution, top view..... 110

44. Pit propagation in the unmixed zone after 720 minutes in 10% $FeCl_3$ solution, top view..... 111

45. Pit propagation orientation - AL-6XN SMA BOP welded specimen after 60 minutes in 10% $FeCl_3$ solution at 80°C, (a) with the weld oriented horizontally, (b). with the weld oriented horizontally..... 115

46. Pitting corrosion tested specimen - AL-6XN autogenous GTA BOP weld without solution heat treated, test at 60 °C for 24 hours in 10% $FeCl_3$ solution. (a). as-welded surface, (b). 600 grit surface..... 118

47. Pitting corrosion tested specimen - AL-6XN autogenous GTA BOP weld with 600 grit surface, solution heat treated at (a). 2100°F, (b). 2150 °F and (c). 2200°F, test at 60 °C for 24 hours in 10% $FeCl_3$ solution..... 119

48. Pitting corrosion tested specimen - AL-6XN GTA BOP weld (C-22 filler) without solution heat treated, test at 80 °C for 24 hours in 10% $FeCl_3$ solution. (a). as-welded surface, (b). 600 grit surface..... 121

49. Pitting corrosion tested specimen - AL-6XN GTA BOP weld (C-22 filler) with 600 grit surface, solution heat treated at (a). 2100°F, (b). 2150 °F and (c). 2200°F, test at 80 °C for 24 hours in 10% $FeCl_3$ solution..... 122

50. Pitting corrosion tested specimen - 254SMO GTA BOP weld (C-22 filler) without solution heat treated, test at 64 °C for 24 hours in 10% $FeCl_3$ solution. (a). as-welded surface, (b). 600 grit surface..... 124

51. Pitting corrosion tested specimen - 254SMO GTA BOP weld (C-22 filler) with 600 grit surface, solution heat treated at (a). 2100°F, (b). 2150 °F and (c). 2200°F, test at 64 °C for 24 hours in 10% $FeCl_3$ solution..... 125

52. Crevice corrosion tested specimen - AL-6XN GTA open root welds (C-22 filler), as-welded surface, tested at 45°C for 72 hours in 6% $FeCl_3$ solution..... 131

53. Crevice corrosion tested specimen - AL-6XN GTA open root welds (C-22 filler), as-welded surface, tested at 23°C for 72 hours in 6% $FeCl_3$ solution..... 132

54. Crevice corrosion tested specimen - AL-6XN GTA open root welds (C-22 filler), as-welded surface, tested at 0°C for 72 hours in 6% $FeCl_3$ solution..... 133

55. Crevice corrosion tested specimen - AL-6XN GTA open root welds (Inconel 112 filler), transverse cross-section, tested at 45°C for 72 hours in 6% $FeCl_3$ solution..... 136

56. Comparison of the unmixed zone appearances before and after crevice corrosion test at 45°C in 6% $FeCl_3$ for 72 hours, AL-6XN GTA open root welds (Inconel 112 filler), transverse cross-section, (a) location A, (b) location C..... 137

57. AL-6XN GTA open root welds (686CPT filler), test at 45°C in 6% $FeCl_3$ for 72 hours, (a). transverse cross-section of tested specimen, (b). crevice corrosion depth distribution..... 139

58. AL-6XN GTA open root welds (686CPT filler), test at 45°C in 6% $FeCl_3$ for 72 hours, (a). weld root surface of tested specimen, (b). crevice corrosion width distribution..... 140

59. Comparison of crevice corrosion depth distribution of 254SMO and AL-6XN GTA open root welds (686CPT filler), test at 45°C in 6% $FeCl_3$ for 72 hours..... 142

60. Comparison of crevice corrosion width distribution of 254SMO and AL-6XN GTA open root welds (686CPT filler), test at 45°C in 6% $FeCl_3$ for 72 hours..... 143

61. Crevice corrosion tested specimen - AL-6XN GTA open root weld (C-22 filler), test at 23°C in 6% $FeCl_3$ for 72 hours, (a) as-welded on as-received (mill) surface, (b) as-welded on 600 grit surface, (c) pickled after welding on as-received (mill) surface, (d) pickled after welding on 600 grit surface..... 145

62. Crevice corrosion tested specimen - AL-6XN autogenous GTA BOP weld, test at 45°C in 6% $FeCl_3$ for 72 hours on pickled surface, (a). as-welded, (b). 30 min solution treated at 2100°F, (c). 30 min solution treated at 2150°F, (d). 30 min solution treated at 2200°F..... 151

63. Crevice corrosion tested specimen - AL-6XN autogenous GTA BOP weld, test at 45°C in 6% $FeCl_3$ for 72 hours on 600 grit surface, (a). as-welded, (b). 30 min solution treated at 2100°F, (c). 30 min solution treated at 2150°F, (d). 30 min solution treated at 2200°F..... 153

64. Crevice corrosion tested specimen - 254SMO GTA open root weld (C-22 filler), test at 45°C in 6% $FeCl_3$ for 72 hours, (a) as-welded, (b) solution treated at 2100°F, (c) solution treated at 2150°F, (d) solution treated at 2200°F..... 157

65. Crevice corrosion tested specimen - 654SMO GTA open root weld (P16 filler), test at 80°C in 6% $FeCl_3$ for 72 hours, (a) as-welded, (b) solution treated at 2100°F..... 161

66. Hardness distribution across the unmixed zone in AL-6XN GTA open root weld (Inconel 625 filler metal)..... 167

67. Hardness distribution across the weld fusion zone in AL-6XN autogenous GTA BOP weld..... 168

68. Bend tested specimens - (a) AL-6XN GTA open root welded coupons (C-22 filler), (b) AL-6XN autogenous GTA BOP welded coupons..... 170

CHAPTER I
INTRODUCTION

1.1 Background

Super-austenitic stainless steels, such as AL-6XN, 254SMO and 654SMO, are austenitic stainless steels with a high level of molybdenum (>6%), chromium (>20%), nickel (>18%) plus nitrogen (>0.22%). With their excellent resistance to localized corrosion and stress corrosion cracking, these super-austenitic stainless steels are a better choice than the conventional stainless steels for applications in highly aggressive environments. Examples of such usage include chloride containing cooling waters in chemical process industry, offshore platform heat exchangers and piping using seawater and crude oil, piping and tanks for the paper industry and power plant gas scrubber environments. The super-austenitic stainless steels are also a cost effective alternative to more expensive nickel-base alloys in applications where excellent formability, weldability and strength are essential.

As emphasized above, the super-austenitic stainless steels with higher nitrogen, molybdenum, and chromium are chosen for their excellent resistance to localized corrosion, general corrosion, and stress-corrosion cracking combined with their excellent formability and strength. In arc welding, an over-matched nickel-base filler metal, such as Inconel 625 or Hastelloy C-22, is generally used for making dissimilar welds to provide good corrosion resistance. These dissimilar weld joints have been used for applications in sour hydrocarbon service. Although both base metal and composite fusion zone

individually have been proven to be satisfactory in sour service, the adequacy of dissimilar welds is still in question. The problem area in dissimilar welds is a narrow region in the fusion zone along the fusion boundary [1]. This thin fusion region is called the "unmixed zone", and it has the same chemical composition as the base metal but has been completely melted and resolidified during welding [2, 3]. It has been found that corrosion can preferentially occur in the unmixed zone in an environment where the base metal and composite zone are resistant to corrosion. Due to its inferior localized corrosion resistance as compared to the respective base metal, concerns of corrosion in the unmixed zone have been raised. No matter how excellent the base metals or filler metal individually is, when they welded together, the unmixed zone will form along the fusion boundary and the preferential corrosion in the unmixed zone can eventually degrade the whole weldments.

Another unmixed zone concern is mechanical properties. However, there is no literature available on mechanical properties of the unmixed zone because the unmixed zone is narrow and difficult to evaluate using conventional methods.

Based on the information from the literature review, it is evident that, although the existence of the unmixed zone in arc welds has been recognized for many years, investigations of the unmixed zone corrosion behavior have not been definitive. Observations of preferential attack of the unmixed zone in the super-austenitic stainless steel welds with high alloyed filler metals has been reported in several papers, but the localized corrosion behavior of the unmixed zone in super-austenitic stainless steel weldments is not understood in terms of pit initiation and propagation behavior and crevice corrosion behavior. Also, no

research work has been performed to characterize the mechanical properties of the unmixed zone in super-austenitic stainless steel weldments. Thus, it is evident that further research is necessary to provide a better understanding of localized corrosion behavior and mechanical properties of the unmixed zone in arc welds and to develop optimum solutions to the problem.

1.2 Scope of the Program

This program has extensively studied the localized corrosion behavior of the unmixed zone in arc welds in super-austenitic stainless steels under oxidizing chloride environments to define the influence of the unmixed zone on localized corrosion behavior of super-austenitic stainless steel joints with and without crevice condition. The effect of filler metals and welding techniques on the formation of the unmixed zone and the effect of surface conditions and solution heat treatment on the localized corrosion behavior of the unmixed zone were investigated. In addition, mechanical properties of the unmixed zone were evaluated in this study.

The investigations were designed to obtain enhanced understanding of the following aspects:

1) Metallographic evaluation and distribution of unmixed zone in super-austenitic stainless steel arc welds.
2) Pit initiation and propagation behavior in unmixed zone.
3) Crevice corrosion behavior in unmixed zone.
4) Effect of the solution heat treatment on formation and localized corrosion behavior of unmixed zone.

5) Effect of surface condition on localized corrosion behavior of unmixed zone.

6) Effect of welding technique and welding heat input on formation of unmixed zone.

7) Influence of unmixed zone on mechanical properties of entire weld joint.

CHAPTER II

LITERATURE REVIEW

2.1 The Base Metals

2.1.1 Microstructure of base metals

The super-austenitic stainless steels such as AL-6XN alloy (UNS NO8367), 254SMO (UNS S31254), and 654SMO (UNS S32654) are low carbon, high purity, nitrogen-bearing stainless alloys. Table 1 shows the typical chemical composition of three super-austenitic stainless steels . For comparison, the composition of standard type 304L (UNS S30403) and 316L (UNS S31603) are also listed in Table 1.

Compared to conventional stainless steels, super-austenitic stainless steels contain higher chromium, molybdenum, and nickel contents. High levels of molybdenum and chromium endow the super-austenitic stainless steel with extremely good resistance to pitting and crevice corrosion. The high nickel content of the super-austenitic stainless steels serves to inhibit the formation of sigma, to stabilize the austenite, and to improve resistance to stress-corrosion cracking as well as general corrosion. Nitrogen is also added In super-austenitic stainless steels. Nitrogen has been found to be effective in reducing the formation of secondary phases and enhance the effects of chromium and molybdenum to improve localized corrosion resistance and stress-corrosion cracking resistance.

AL-6XN alloy, 254SMO and 654SMO are stable austenitic stainless steels showing no transformation even under extensive deformation.

Table 1. Chemical Composition of Austenitic Stainless Steels.

Element	C	Mn	P	S	Si	Cr	Ni	Mo	N	Cu	Fe	Nb	Co	W	V	Melting Range (°F)
AL-6XN	.02	.40	.025	.002	.40	20.5	24.0	6.3	.220	0.10	Bal	-	-	-	-	2410-2550
254SMO	.010	.460	.020	.001	.36	19.87	18.3	6.11	.200	0.67	Bal	-	0.25	-	-	2420-2550
654SMO	.015	.200	.010	.001	.29	24.6	21.9	7.3	.487	0.4	Bal	-	-	-	-	2417-2498
304L	.030	2.00	.045	.030	1.00	18-20	8-12	-	-	-	Bal	-	-	-	-	-
316L	.030	2.00	.045	.030	1.00	16-18	10-14	2-3	-	-	Bal	-	-	-	-	-

At elevated temperatures (1000°F, 540°C) [4, 5], they are metallurgical stable. On long exposures to higher temperatures, in the 1200-1800°F (650-980°C) range, sigma phase may precipitate at grain boundaries. Sigma phase can have an adverse effect on corrosion resistance as well as mechanical properties.

2.1.2 Mechanical Properties of Base Metals

The super-austenitic stainless steels are stronger with comparable ductility and harder relative to conventional austenitic stainless steels. Table 2 shows typical transverse tensile properties at room temperature for the three super-austenitic stainless steels: AL-6XN sheet (thickness: 0.026 to 0.139" or 0.066 to 0.353 cm), 654SMO sheet (thickness: 1" or 2.54 cm), and 254SMO sheet in comparison to Type 316 austenitic stainless flat rolled products [5, 7, 8].

2.1.3 Corrosion Behavior of Base Metals

Super-austenitic stainless steels show exceptional resistance to localized corrosion and stress corrosion cracking in high chloride and various acid, alkali, and salt solutions in chemical processing and other industrial environments. The corrosion behavior of super-austenitic stainless steel from laboratory and field tests is summarized in the following subsections.

- Pitting and Crevice Corrosion

One of the most important characteristics of super-austenitic stainless steels is their resistance to pitting and crevice corrosion. The pitting and crevice corrosion resistance of an austenitic stainless steel can be correlated to its alloy composition in terms of the Pitting Resistance Equivalent (PRE_N):

Table 2. Typical Tensile Properties for Super-austenitic Stainless Alloy Sheet [5, 7, 8].

Properties at Room Temperature	AL-6XN Alloy	254 SMO	654 SMO	Type 316
Yield Strength (ksi)	53	44	62	45
Ultimate Tensile Strength (ksi)	108	94	109	88
% Elongation in 2"	47	35	40	57
Hardness Rockwell B	88	210	250	81

$$PRE_N = Cr\% + 3.3\ Mo\% + 30\ N\%.$$

The PRE_N values for AL-6XN, 254 SMO, 654 SMO and several 300 series alloys are given in Table 3 [5] along with other common pitting and crevice corrosion indices. The temperature of a solution at which pitting is first observed is defined as the critical pitting temperature (CPT). The CPT^1 and CPT^2 values of AL-6XN, 254 SMO, and 654 SMO listed in Table 4 have been determined in ferric chloride (ASTM G-48A 6% $FeCl_3$, boiling point of this solution is 103°C) and in an acidic mixture of chlorides and sulfate (4% NaCl + 1% $Fe_2(SO_4)_3$ + 0.01M HCl), respectively. The temperature of a solution at which crevice corrosion is first observed is defined as the critical crevice corrosion temperature (CCCT). The CCCT values of AL-6XN, 254 SMO, and 654 SMO presented in Table 3 were determined in ferric chloride solution (ASTM G-48B 6% $FeCl_3$) [5,9].

From Table 3, it is evident that the pitting and crevice corrosion resistance of AL-6XN and 254 SMO alloys in ferric chloride solution is superior to 300 series austenitic stainless steels and Alloy 904L. The chloride pitting and crevice corrosion resistance of 654 SMO is far superior to 300 series austenitic stainless steels. The relative ranking according to all indices listed in Table 3 is consistent and demonstrates the superior pitting and crevice corrosion resistance of the super-austenitic stainless steels.

• General Corrosion

In contrast to localized corrosion, general corrosion is rather predictable. The uniform attack of an entire area exposed to a corrosive environment is

Table 3. Pitting and Crevice Corrosion Indices [5, 9].

Alloy	Composition (wt%) Cr	Mo	N	PRE_N	CCCT (°C)	CPT^1 (°C)	CPT^2 (°C)
Type 304	18.0	-	0.06	19.8	<-2.5	-	-
Type 316	16.5	2.1	0.05	24.9	-2.5	15.0	-
Type 317	18.5	3.1	0.06	30.5	1.7	18.9	25
904L	20.5	4.5	0.05	36.9	20.0	40.0	45
AL-6XN	20.5	6.3	0.23	47.9	43.0	80.5	78
254 SMO	20.0	6.1	0.2	46.1	37.5	75	-
654 SMO	24.0	7.3	0.5	63.1	>60	>BP (103)	-

Note: BP---Boiling point

expressed in terms of an average loss-of-metal-thickness for a given period of time in units of mils per year (mpy). The general corrosion resistance of AL-6XN to various environments has been evaluated in laboratory tests conducted according to ASTM Standard G-31[5]. The test results are reviewed in Table 4 in comparison with Type 316L, Type 317L, Alloy 904L, and Alloy 276. Compared to the general corrosion behavior of Type 316L, Type 317L, Alloy 904L, and Alloy 276 in terms of corrosion rate, the performance of the AL-6XN alloy is excellent (<5 mpy) in acetic, formic, and phosphoric acids, satisfactory (5-20 mpy) in oxalic acid and sodium hydroxide, useful (20-50 mpy) in sodium bisulfate, and poor (>50 mpy) in boiling 10% sulfuric acid.

Table 5 compares the performance of 254 SMO and 654 SMO alloys with other stainless steels in a variety of common corrosive environments in terms of the lowest temperature at which the corrosion rate exceeds 5 mpy [7]. It is to be noted that the higher the temperature at which the corrosion rate exceeds 5 mpy the better the general corrosion resistance. It is evident that, in high chloride containing environments, super-austenitic stainless steels show superior corrosion resistance compared to conventional stainless steels.

• Stress Corrosion Cracking

Stress corrosion cracking (SCC) is the primary mode of material failure in the chemical process and power industries, particularly where chlorides and high temperatures are encountered, such as in flue gas reheaters and scrubbers, gas generators, and inlets to spray towers. Table 6 shows the results of a series of U-bend tests on AL-6XN and other materials [6]. It is evident that AL-6XN has improved stress corrosion cracking resistance

Table 4. Corrosion Resistance in Boiling Solution [5].

ASTM G-31 Test Solution	Corrosion Rate in Mils per Year for Cited Material				
	Type 316L	Type 317L	Alloy 904L	AL-6XN	Alloy 276
20% Acetic Acid	0.12	0.48	0.59	0.12	0.48
45% Formic Acid	23.41	18.37	7.68	4.56	2.76
10% Oxalic Acid	48.03	44.90	27.13	10.92	11.24
20% Phosphoric Acid	0.60	0.72	0.47	0.24	0.36
10% Sodium Bisulfate	71.57	55.76	8.88	24.00	2.64
50% Sodium Hydroxide	77.69	32.78	9.61	15.96	17.77
10% Sulfuric Acid	124.3	93.26	9.13	29.38	2.64
10% Sulfuric Acid	635.7	298.28	100.8	84.36	13.93

Table 5. Lowest temperature (°F) at which the corrosion rate exceeds 5 mpy [7].

Test Solution	Lowest temperature (°F) at which the corrosion rate exceeds 5 mpy				
	654 SMO	254 SMO	Alloy 904L	Type 316L	Type 304
1% Hydrochloric Acid	203	158	122	86	86
10% Sulfuric Acid	158	140	140	122	-
96% Sulfuric Acid	86	68	95	113	-
85% Phosphoric Acid	194	230	248	203	176
65% Nitric Acid	221	212	212	212	212
10% Sulfuric Acid + 2000ppm Cl^-+N_2	149	104	131	77	-
WPA1, High Cl content	203	176	122	<50	<<50
WPA2, High F content	176	140	95	<50	<<50

Table 6. U-bend Stress Corrosion Cracking Test [6].

Test solution	Type 316	904L	AL-6XN
33% Lithium Chloride, Boiling	Fail (<150 Hours)	Fine Cracks (<170 Hours)	Resist (500 Hours)
26% Sodium chloride, Boiling	Fail (<150 hours)	Resist (1000 Hours)	Resist (1075 Hours)

compared to Type 316 stainless steel as well as Alloy 904L.

For 254SMO and 654SMO, the drop-evaporation test (DET) has been used by Avesta Sheffield Inc. to evaluate stress-corrosion cracking resistance in comparison with Type 316 and Type 904L. The test results are shown in Table 7 [8]. The results reveal that 254SMO and 654SMO super-austenitic stainless steels have higher stress-corrosion cracking resistance than conventional stainless steels.

2.1.4 Physical Properties of Base Metals

Super-austenitic stainless steels have a stable face-centered cubic crystal structure similar to other austenitic stainless alloys. They are non-magnetic in both the fully annealed and the cold-worked condition. The physical properties of super-austenitic stainless steels are presented in Table 8 [5, 7, 8]. The physical properties of the super-austenitic stainless steels are similar to those of other austenitic stainless steels.

2.2 Welding

2.2.1 Welding Procedures and Techniques [5, 10, 11, 12]

Super-austenitic stainless steels are highly weldable using normal welding procedures for conventional stainless steels. The acceptable arc-welding processes for fabrication of super-austenitic stainless steels are the following:

a) Gas Tungsten Arc Welding (GTAW).

b) Gas Metal Arc Welding (GMAW).

Table 7. SCC Resistance of Stainless Steels [8].

Material	Applied Stress R, N/mm^2 200°C	Time to failure, hour
316	21	155
904L	194	230
254 SMO	221	>500
654 SMO	300	>500

Table 8. Physical Properties of Super-austenitic Stainless Steels at Room Temperature.

Physical Properties	AL-6XN	254 SMO	654 SMO	Unites
Density	0.291	0.287	0.289	(lb/in^3)
Modulus of elasticity	$28.2X10^6$	29X10-6	29X10-6	(psi)
Melting Range	2410-2550	2420-2550	2444-2498	(°F)
Coefficient of Expansion (77-212°F)	7.9	9.4	-	(10^{-6}/°F)
Specific Heat Capacity	0.11	0.119	500 J/kg°C	(Btu/lb-°F)
Magnetic Permeability (Fully annealed 0.5" plate)	1.0028	1.003	-	(Oersted)

c) Shielded Metal Arc Welding (SMAW).

d) Submerged Arc Welding (SAW).

e) GTA-Autogenous Welding.

The following cautions must be taken in welding super-austenitic stainless steels:

- Oxyacetylene welding can not be used for welding super-austenitic stainless steels because carbon pick-up from the flame lowers corrosion resistance.
- In Submerged Arc Welding, carbon and silicon pick-up from the flux must be minimized to avoid loss of corrosion resistance and ductility.
- GTAW-PAW Autogenous welding, is not recommended because microsegregation within the weld metal during solidification will reduce corrosion resistance. Thus, autogenous welding should normally be followed by solution annealing between 2100 and 2200°F followed by rapid quenching and pickling.

2.2.2 Filler Metals

Wrought super-austenitic stainless steel products have homogeneous compositions as commercially available. However, when the alloy is melted during welding, elements such as chromium, nickel, and particularly molybdenum are segregated during resolidification, which results in susceptibility to preferential attack in severely corrosive environments. A filler metal which compensates for chemical segregation in the weld bead will provide resistance to hot cracking and improved corrosion resistance. Consequently, filler metals containing at least 9% Mo are recommended for

welding super-austenitic stainless steels or joining them to other austenitic, ferritic, and duplex stainless steels and most nickel-base alloys. The choice of the best filler for individual super-austenitic stainless steel depends on the service environment and the fabrication situation. The most widely used filler metals for super-austenitic stainless steels are listed in Table 9. It is believed that the filler metals in Table 9 when used with proper welding procedures and welding parameters should provide weld joints with equivalent pitting and crevice corrosion resistance to that of the base metal. In certain applications, such as oxidizing acid chlorides, the chromium and molybdenum content of the filler metal is extremely important.

2.3 Unmixed Zone

2.3.1 Unmixed Zone Formation

An unmixed zone with the chemical composition of the base metal, which has melted and resolidified, exists along the fusion boundary in dissimilar welds. This zone has been recognized for more than 25 years [13, 14, 15]. Figure 1 [2] shows a sketch for the regions which exist in a dissimilar weld. A dissimilar weld is actually comprised of four regions: a composite fusion zone, an unmixed zone (UNMZ), a partially-melted zone, and a "true" heat affected zone (HAZ). The definitions of these zones are given as follows:

Composite Fusion Zone: The bulk portion of the weld metal within which the chemical composition is modified by dilution of the filler metal with material melted from the surrounding base metal.

Unmixed Zone: A zone at the outer extremities of the weld metal, consisting of

Table 9. Chemical Composition (wt%) of High Mo Content Filler Metals.

Filler Metal	C	Mn	P	S	Si	Cr	Ni	Mo	Cu	Fe	Nb	Co	W	V	Melting Range (°F)
In 625	.10	1.0	.03	.02	.75	20.0-23.0	Bal	8.0-10.0	0.5	7.0	3.15-4.15	.12	-	-	2350-2460
C-22	.02	1.0	.003	.015	.20	20.0-22.5	Bal	12.5-14.5	0.5	2.0-6.0	-	2.5	2.5-3.5	.35	2475-2550
C-276	.02	1.0	.04	.03	.20	14.5-16.5	Bal	15.0-17.0	0.5	4.0-7.0	-	2.5	3.0-4.5	.35	2415-2550
686CPT	.02	1.0	.002	.002	.25	19.0-23.0	Bal	15.0-17.0-	0.5	5.0	-	2.5	3.0-4.4	-	2440-2516
P16	.004	0.14	.004	.002	.03	22.5	Bal	15.5	-	0.64	-	-	-	-	-
Alloy59	.01	-	-	-	-	23	Bal	16	-	-	-	-	-	-	-

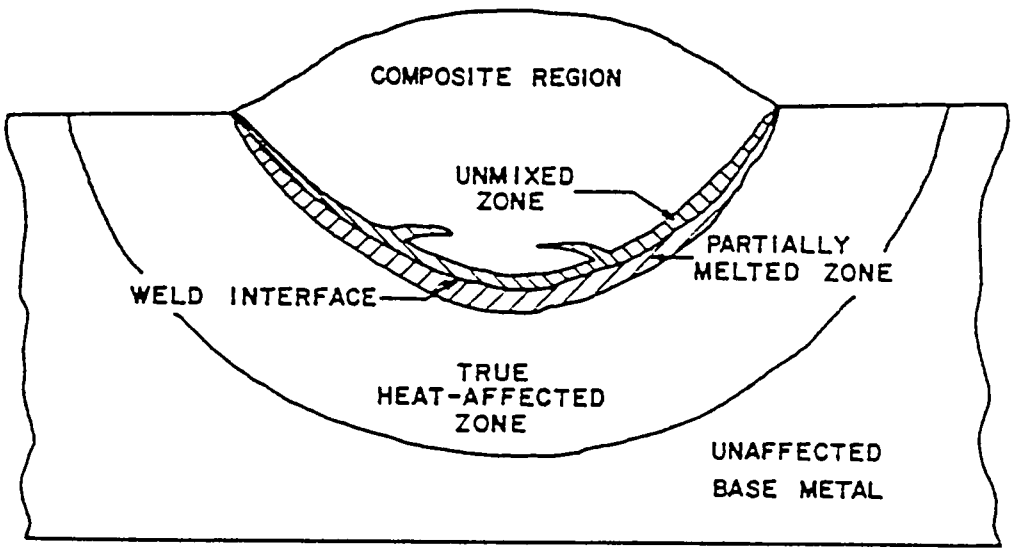


Figure 1. Regions Consisted in a Dissimilar Weld.

Source: Savage, W.F., Nippwa, E.F. and Szekeres, E.S. "A Study of Weld Interface Phenomena in a Low Alloy Steel," Weld Journal, 55, 1976, pp 260s-268s.

base metal which has been melted and solidified during welding without experiencing mechanical mixing with the filler metal.

Weld Interface: The surface bounding the region within which complete melting was experienced during welding as evidenced by the presence of a definite solidification substructure.

Partially Melted Zone: The portion of the base metal located just outside the weld interface, within which the degree of melting ranges from 0 to 100%.

True Heat-Affected Zone: That portion of the base metal within which all microstructure changes produced by welding occur in the solid state.

It has been previously reported that, as a fundamental phenomenon, the unmixed zone formation in welding of stainless steels can be expected to occur for all combinations of filler and base materials and for all fusion welding techniques [16]. However, the extent of the unmixed zone is dependent on a number of factors that are highly reflective of the welding process and the specific welding parameters together with the filler metal (its composition and physical properties such as melting range). In a study of the effect of welding techniques on the location and width of the unmixed zone in 304 base metal with 316 filler metal, Lukkari and Moisio [17] found that the widest unmixed zone was observed associated with the SMA welding technique and narrowest with GMA short arc welding. They also found that the width of the unmixed zone increased with an increase in energy input and penetration. The unmixed zone occurs all along the fusion interface with a maximum width occurring at about

the mid-plane of the 4 mm plate where the shape of the interface is concave and also near the root.

2.3.2 Unmixed Zone Evaluation Techniques

Chemical etching is the most widely used technique to reveal the unmixed zone [2, 17]. When using this technique, attention must be taken for selecting proper etchants because the unmixed zone can remain indistinguishable and would be mistakenly identified as part of the heat-affected zone by improper etchants because the unmixed zone is nominally the same in composition as the adjacent base metal HAZ. The difference in the as-etched appearance between the unmixed zone and the HAZ is the revelation of solidification substructure in the unmixed zone. Thus, selection of specific solute sensitive etchants that can show the segregation resulting from solidification is important [2]. In addition, both optical microscopy and SEM with EDS are common techniques, which have been used for metallographic evaluation of the unmixed zone [2, 18].

2.3.3 Unmixed Zone Corrosion Resistance

The influence of the unmixed zone in dissimilar welds on the corrosion resistance of welded joints has been reported by several researchers. Takalo and Moisio [19, 20] reported that preferential attack occurred along the fusion boundary in welds on austenitic stainless steels. In Tuthill's and Avery's work [21], corrosion occurring near the fusion boundary of the root pass was reported when AL-6XN was welded with Alloy 625. It is believed that corrosion which occurred in the root bead fusion boundary was due to insufficient mixing in the

molten weld pool. Unmixed zone attack was also found by Liljas, Holmberg, Ulander [22] and Gooch [23] in welding of 254 SMO despite use of overalloyed consumables (Avesta P12 and Inconel 625 filler metal).

In the evaluation of bleach plant piping materials, Tuthill and Garner [24, 25, 26] not only observed preferential pitting corrosion in the unmixed zone in Nitronic 50 and 50W welded with Inconel 112 filler metal (Alloy 625), but also indicated the necessity for further work to establish an inside root pass procedure to avoid or minimize the formation of the unmixed zone. They have pointed out that preferential corrosion in the unmixed zone is primarily a problem when enriched filler metals are used to combat preferential corrosion in the fusion zone. In order to avoid or minimize the occurrence of the unmixed zone, TAPPI is currently formulating and evaluating GTA welding procedures for open root joint configuration of 6% Mo piping materials for bleach plant service [27].

Kearns and Moller [28] summarized the factors which can affect the corrosion resistance of stainless steel weldments. The formation of the unmixed zone is one of the factors which results in the inferior corrosion resistance of the welds compared to that of the corresponding base metal. They also indicated that the potential for preferential attack in the unmixed zone may be reduced by maintaining a constant and adequate supply of filler metal to the weld, controlling the heat input sufficient to mix filler with base metal, and completely filling the weld joint to avoid undercutting and to flow molten over-alloyed filler metal over the root and face surface of the unmixed zone to form a barrier to the service environment.

From the above literature review, it is evident that unmixed zone has lower corrosion resistance than the respective base metal. Preferential corrosion in the fusion zone has been noted to occur in autogenous welds in austenitic stainless steels. In addition, preferential fusion zone corrosion in autogenous welds of 304 austenitic stainless steel was also reported by Takalo and Moisio [19, 20].

Recently developed high molybdenum and nitrogen bearing super-austenitic stainless steels such as AL-6XN, 254 SMO and 654 SMO are designed for critical corrosion service. However, localized corrosion in the unmixed zone of these super-austenitic stainless steel weldments is currently a serious problem [29].

2.4 Localized Corrosion

2.4.1 Localized corrosion Initiation and Propagation Mechanisms

• Pitting Corrosion

Pitting corrosion is a result of the breakdown of the passive film that protects a given metal or alloy. Chloride anions are especially known to cause film breakdown in aqueous environments, but the exact mechanism of that action is not quite clear.

Several models for the damage of passive films on metals in the environment containing halogen ions have been proposed [30, 31, 32]. While each model is supported by experimental results, often it is invalidated by others, and numerous conflicting results have been reported. The reported results indicate the nature of the complexity of the processes involved in pitting.

The existing models for pitting can be divided into two groups [33]: one assumes that pits initiate at the metal/oxide interface, and the other assumes that pits initiate at the oxide/electrolyte interface. In the first case, the metal is primarily attacked, and in the second case the oxide suffers dissolution of the outermost layer.

For the first case [33], the ideals of the models (such as the point defect model and the penetration model) are summarized as follows:

(1) Imperfections of the passive film are assumed to be caused by the presence of pores, flaws, and fissures. These defects act as occluded cells in which the anodic and cathodic reactions occur.

The anodic reaction: $M \rightarrow M^{m+} + me$

The cathodic reaction: $\frac{m}{4} O_2 + \frac{m}{2} H_2O + me \rightarrow mOH^-$

The overall reaction: $M + \frac{m}{4} O_2 + \frac{m}{2} H_2O \rightarrow M^{m+} + mOH^-$

In the occluded region, the increase in the local concentration of M^{m+} tends to hydrolyze according to reactions of the following:

$$M^{m+} + xH_2O \rightarrow [M(OH)_x]^{(m-x)+} + xH^+$$

However, the depletion of O_2, caused by its slow diffusion, make the cathodic reaction in the flaws difficult to maintain. Thus, there is not enough OH^- that can react with H^+ produced by hydrolysis reaction, which causes the decreasing pH in the occluded region. Acidification in the occluded cell occurs, which make it difficult for the passive film to remain insoluble.

(2) Chloride ions, Cl^-, migrate into the occluded cell and enhance the hydrolysis reaction of the metal. This causes the further decrease of the pH in the occluded cell.

(3) When chloride ions migrate through the pores, the direct reaction of chloride ions and metal can occur when chloride ions reach the bare metal surface. The direct reaction between chloride ions and metal can also occur when the film is destroyed mechanically by cracks and when aggressive anions reach the metal at the crack bottom. By this reaction, the soluble complex metal-chloride ions form and pass into the solution, which results in localized corrosion. In addition, the acidification due to hydrolysis of the metal ions reduces the stability of the oxide and build-up of positive charge because increased cation concentration attracts negative chloride ions. Local conditions thereby exacerbate both the initiation and propagation of pitting.

(4) Chloride ions can also be incorporated into the passive film by occupying anion vacancies. This results in the decreasing density of anion vacancies and increasing density of cation vacancies. The cation vacancies pile up at the film/metal interface. When the voids grow to a certain critical site, the passive film suffers local collapse. Thus, the pit initiation occurs.

For the second case [33], pits are believed to nucleate at the solution/oxide interface. According to the models, the mechanism of pit initiation is described as follows:

(1) The first step in pit initiation is the adsorption of the halogen ions, mostly Cl^-, on the passivated metal surface.

When a passivated metal is immersed in water, its adsorption on the oxide film leads to the formation of a "hydrolated" surface layer. The

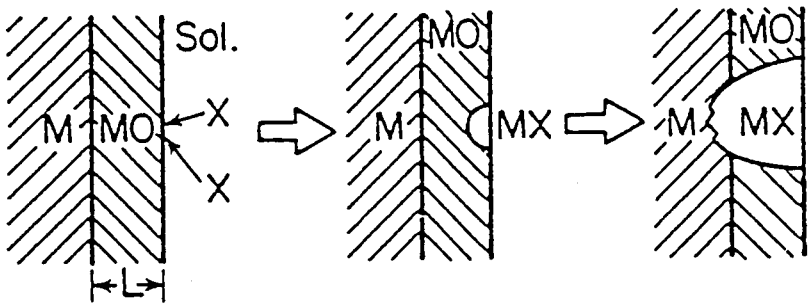
concentration of OH^- on the oxide surface equals that of H^+ at a pH of zero charge (pH_{zch}). At pH higher than pH_{zch}, the oxide surface is charged negatively. The adsorption of Cl^- does not occur in this case. At pH lower than pH_{zch}, Cl^- and other halogen anions are susceptible to adsorption.

(2) The initiation of a pit is caused by the formation and dissolution of soluble salt produced by the reaction of the chloride ions with metal cations in the passive film.

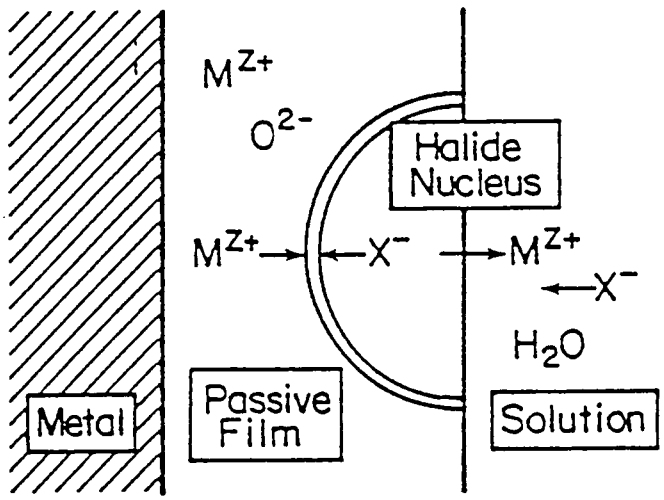
As shown in Figure 2, chloride ions adsorbed on the passive film react with metal ions. As a result, salt nuclei are formed and grow. When the nucleus is stable and grows continuously, it permeates the passive film, and dissolution of the metal occurs through the salt film. A critical size of pit nuclei supposedly exists, below which pit nuclei do not grow. The thicker the film, the greater the nuclei would be. The model predicts that, in the case of very thick film, it would not be possible to obtain large enough nuclei to develop pits. However, this prediction does not agree well with the majority of the experimental results. Another disadvantage of this model is that it does not consider the presence of physical defects in passive films.

• Crevice Corrosion

Compared to pitting corrosion, crevice corrosion is also involved in occluded cells. Thus, the crevice corrosion initiation and propagation mechanisms are similar to that of pitting corrosion. However, crevice corrosion exhibits several distinguishing features. A significant difference is that a crevice has the geometry of a pre-existing site for the occluded cell. As a consequence, the initiation stages for the two types of localized corrosion differ. Generally, the



A



B

Figure 2. (a) Illustration of a process leading to pit initiation. M: metal, MO: passive film, MX: metal halide, Sol: solution; (b) Schematic representation of processes occurring within the system consisting of the metal, the passive film, the halide nucleus, and the solution.

Source: Smialowska, Z. S. "Pit Initiation," Proceeding of the Second International Conference on Localized Corrosion, Orlando, Florida, June 1-5, 1987, pp 41-45.

mechanism of crevice corrosion is believed to involve the following sequence [34]:

(1) In a pre-existing crevice (such as overlapping metal/metal or non-metal surface, flanged joints, bolts, nuts and washers), the metal ion concentration increases and the oxygen concentration decreases immediately following access of the environment into the crevice. Since a pre-existing crevice with its geometry makes the diffusion of ions into the occluded region much easier than that for pitting corrosion, crevice corrosion usually occurs ahead of pitting corrosion.

In view of this sequence, the crevice geometry in terms of gap width and depth becomes important. If the gap is sufficiently wide and shallow, oxygen depletion and chloride ion influx will decrease and metal ion build-up will be less due to increased diffusion of corrosion products from the crevice. The decrease in pH due to hydrolysis of cations will be less, the passive film may be preserved, and if so, crevice corrosion will not occur. These factors are reversed for deep narrow crevices, and at some critical geometry, crevice corrosion will occur.

(2) The metal ions will hydrolyze, but the effect in the lowering of the pH caused by hydrolysis is initially countered by the OH^- ions resulting from the oxygen reduction. After the occluded oxygen is consumed, the cathodic reaction is predominantly on the outer surfaces. With continued dissolution of the metal in the crevice, decreasing the local pH by hydrolysis becomes more serious. At a sufficiently low pH in the crevice, any passive film that might have been present will be destroyed and active corrosion becomes the mechanism of propagation of corrosive attack.

2.4.2 Factors Related to Localized Corrosion

Localized corrosion can be related to the chemical composition in alloys, the microstructure of a metal or alloy, and the physical condition of the surface. These factors are listed below:

a) The variations in chemical composition in alloys.

b) Preferred dissolution sites such as dislocations and grain boundaries.

c) Dispersed phases such as carbides, sulfides, and intermetallic components.

d) Chemical segregation in materials.

e) Irregular surface coatings such as discontinuous oxide coatings, deposits of more noble metals, and deposits of conducting materials such as graphite resulting from fabrication processes.

f) Irregular deposits such as dirt, scale, and biological growths.

g) Junction of dissimilar metals.

h) Existence of crevice caused by overlapping metal/metal or metal/non-metal surface, flanged joints, bolts, nuts and washers.

Environmental conditions also can lead to localized corrosion. These conditions are usually associated with non-uniform concentrations of cathodic reactant species or corrosion product ions. These conditions can be brought about by the following:

a) Non-uniform access of the cathodic species due to the location of the source of the species. For example, a gradient in the dissolved-oxygen concentration exists along the wall of an open tank, providing more oxygen near the top and inducing anodic regions just below the water line. Similar conditions may exist near entrance piping into

tanks and heat exchangers where the concentration of cathodic reactants will be higher.

b) Induction of the local anodic and cathodic regions caused by non-uniform fluid velocity.

c) Localized restriction of the cathodic reactant caused by overlapping surfaces, accumulated porous scale, dirt and corrosion product deposits.

2.4.3 Localized Corrosion Test Methods and ASTM Standard

Accelerated localized corrosion tests fall into two broad groups: electrochemical corrosion and chemical corrosion.

• Electrochemical Tests

The majority of electrochemical tests for localized corrosion revolve around the determination of breakdown potential E_B and protection potential (or repassivation potential) E_p. The localized corrosion behavior can be described based on the corrosion potential relative to E_B and E_p:

$E \geq E_B$	Stable pits initiate and propagate.
$E \leq E_p$	No initiation or propagation of pits. Pits formed above E_B will eventually repassivate below E_p.
$E_p < E < E_B$	Pit will not initiate, but if it already exists, it will propagate.

The typical electrochemical polarization curve for an active-passive alloy is shown in Figure 3 [35]. As summarized by J. W. Oldfield [36], S. Smialowska and M. Czachor et al. [37, 38], the experiment methods for determining these potentials are given below.

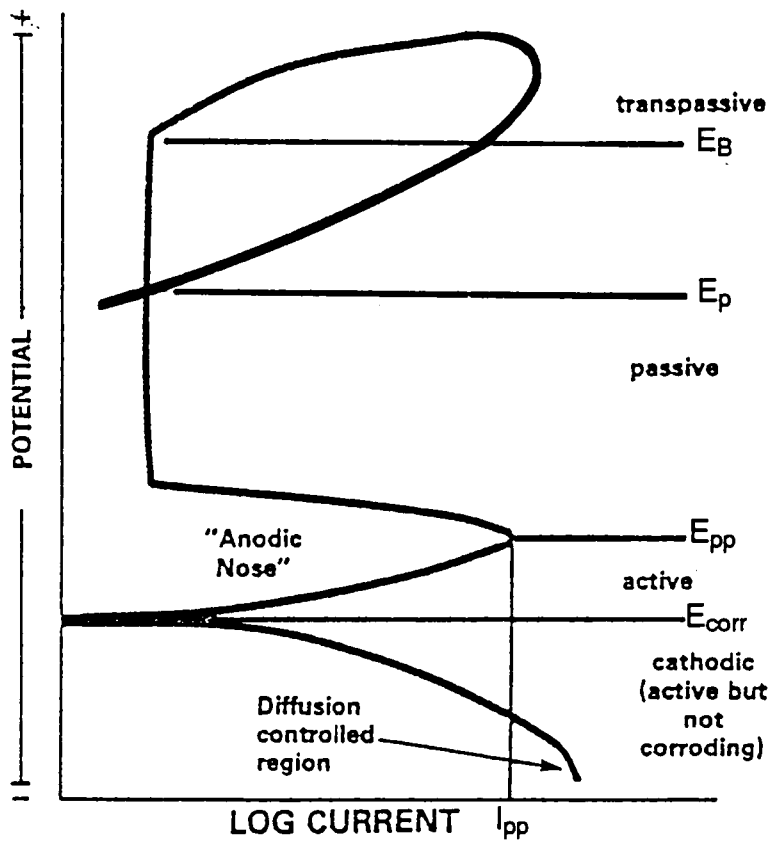


Figure 3. Typical electrochemical polarization curve for an active-passive alloy (with cathodic trace) showing active, passive, and transpassive regions and other important features such as E_B = breakdown potential and E_p = repassivation potential as well as E_{pp} = primary passive potential and E_{corr} = freely corroding potential.

Source: Siebert, O. W. "Laboratory Electrochemical Test Methods," Laboratory Corrosion Tests and Standards. ASTM STP 866, G. S. Haynes and R. Baboian. Eds. American Society for Testing and Materials, Philadelphia, 1985, pp 65-90.

a) Potentiokinetic Methods

Potentiokinetic techniques, as a group, determine current as a function of potential (I = f (E)), as illustrated schematically in Figure 4. There are three methods by which this relationship can be obtained:

i) The potentiodynamic method, where there is a continuous change in potential at a fixed rate.

ii) The quasi-stationary method, where there is a stepwise change of potential at a certain rate.

iii) The stationary method, where there is a stepwise change of potential that is maintained until a stable current is established.

These methods are the ones most commonly used in determining both E_B and E_p in a single experiment. A detailed standard procedure for carrying out cyclic potentiodynamic polarization measurement for localized corrosion (method i) is documented in ASTM Standard G61 [39].

b) Galvanokinetic Methods

Gavlanokinetic methods, as a group, determine potential as a function of current (E = f (I)), as illustrated schematically in Figure 5. There are also three methods by which this relationship can be obtained:

i) The galvanodynamic method, where there is a continuous change in current at a fixed rate.

ii) The quasi-stationary method, where there is a stepwise change in current at a certain rate.

iii) The stationary method, where there is a stepwise change in current which is maintained until a stable potential is established. In general

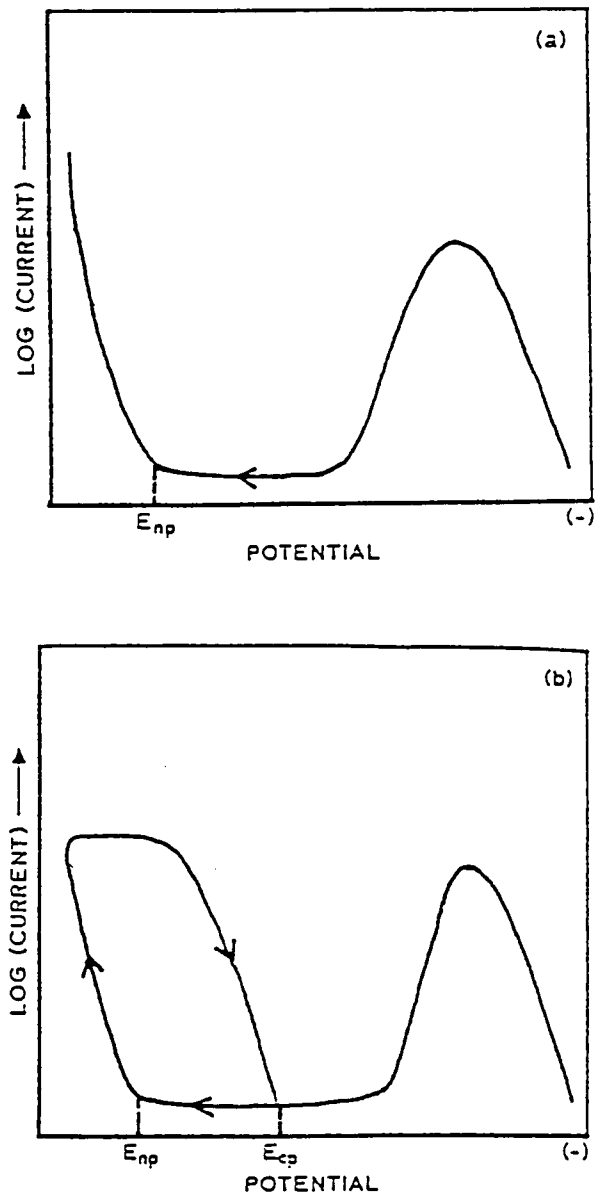


Figure 4. Schematic representation of anodic polarization curves obtained using all three potentiokinetic methods. (a) Potential sweep in anodic direction only (b) Anodic potential sweep followed by the reverse sweep.

Source: Oldfield, J. W. " Test Techniques for Pitting and Crevice Corrosion Resistance of Stainless Steels and Nickel-Base Alloys in Chloride-Containing Environments," International Materials Reviews, Vol. 32, No. 3, 1987, pp 153-170.

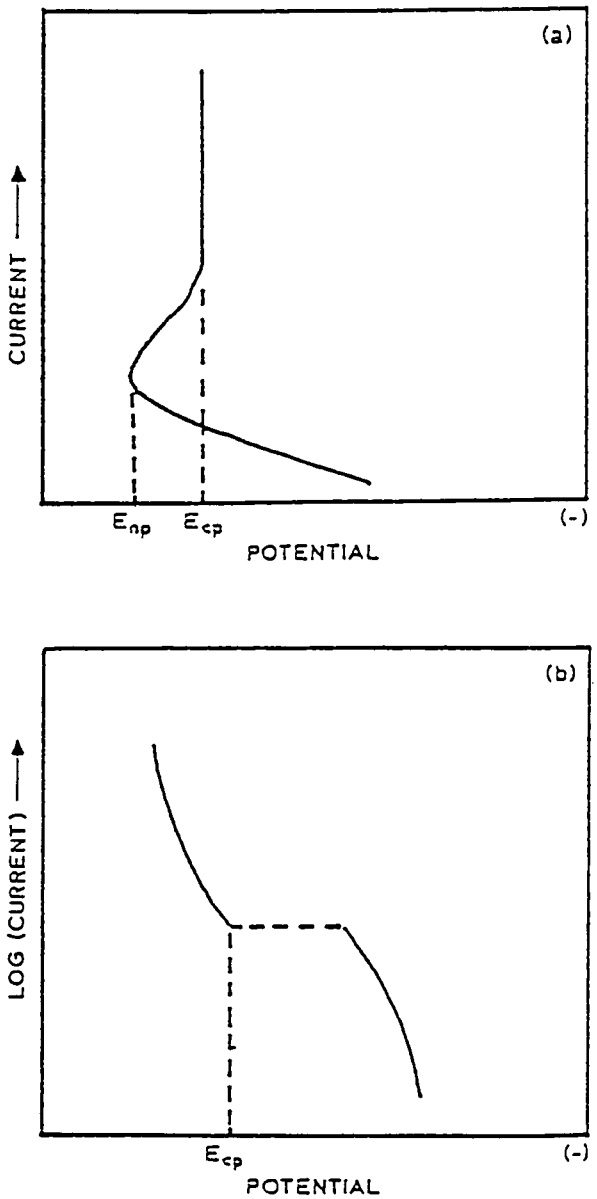


Figure 5. Schematic representation of anodic polarization curves obtained using galvanokinetic methods. (a) Galvanodynamic and quasi-stationary methods (b) Stationary methods.

Source: Oldfield, J. W. " Test Techniques for Pitting and Crevice Corrosion Resistance of Stainless Steels and Nickel-Base Alloys in Chloride-Containing Environments," International Materials Reviews, Vol. 32, No. 3, 1987, pp 153-170.

these methods are not widely used in connection with E_B and E_p determinations.

c) Potentiostatic Methods

Potentiostatic techniques, as a group, determine current (I) as a function of time (t) at constant potential (E = constant, I = f(t),), as shown in Figure 6. There are two general methods, one is for determining E_B and the other is for determining E_p. These are the followings:

i) The determination of E_B by recording I versus t curves at different constant potentials using a new specimen for each potential.

ii) The determination of E_p by recording current (I) versus time (t) curves at different constant potentials using electrodes on which active pits have been initiated.

With method i), a series of current versus time curves are obtained at a constant potential but at increasing temperatures until breakdown (signified by an increase in current) is observed. In this way, the temperature is obtained where the constant potential is equal to E_B. By doing a series of runs at different constant potentials, E_B can be obtained as a function of temperature. These data are then viewed with the temperature, rather than the potential, as the ranking parameter named "critical pitting temperature" (CPT) [40, 41, 42].

d) Galvanostatic Methods

Galvanostatic techniques determine the potential as a function of time at constant current (I = constant, E = f (t)), as shown in Figure 7. There are two general methods: one that determines both E_B and E_p and the other that

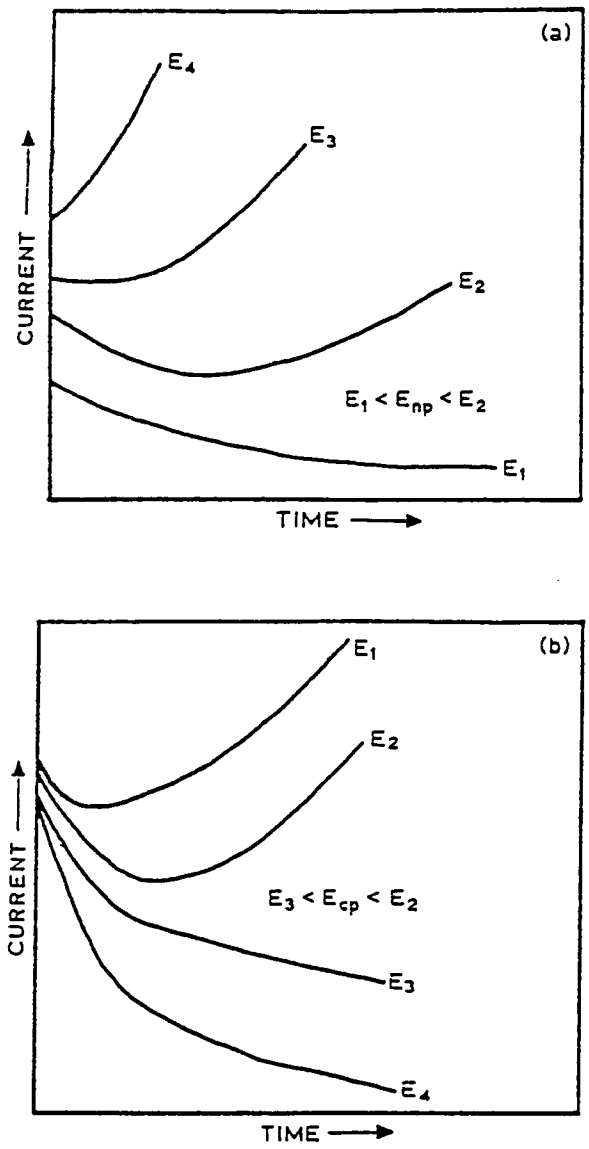


Figure 6. Schematic representation of current vs. time curves obtained using potentiostatic methods. (a) Determination of E_B; (b) Determination of E_p.

Source: Oldfield, J. W. " Test Techniques for Pitting and Crevice Corrosion Resistance of Stainless Steels and Nickel-Base Alloys in Chloride-Containing Environments," International Materials Reviews, Vol. 32, No. 3, 1987, pp 153-170.

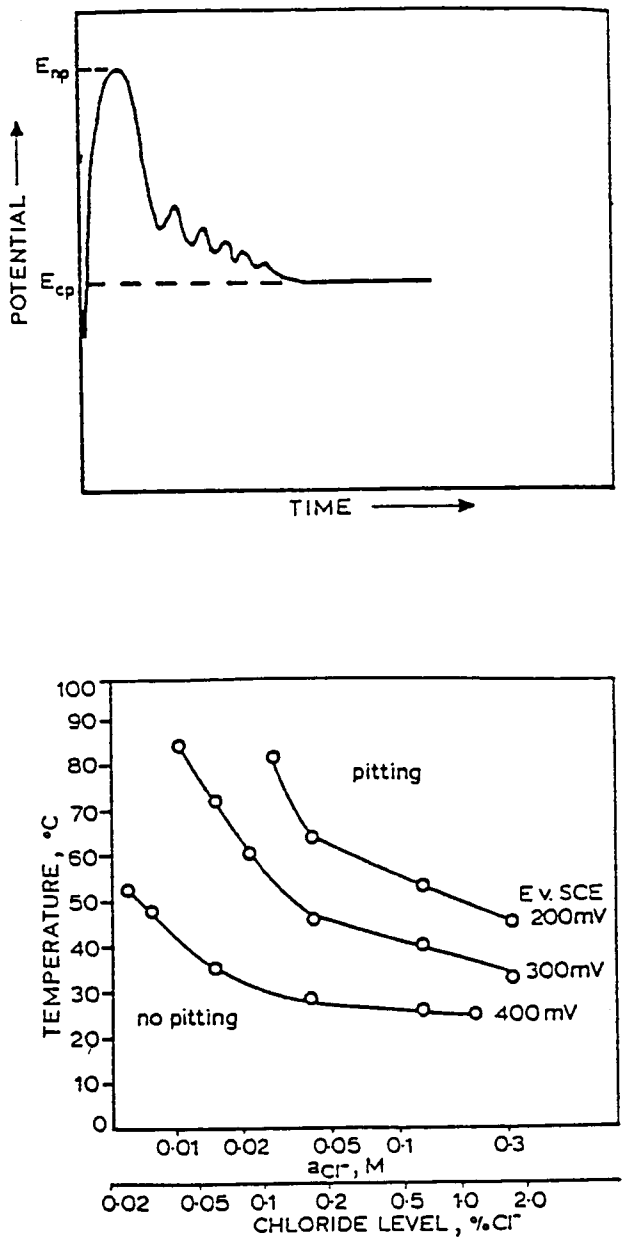


Figure 7. Schematic representation of potential time curve obtained using galvanostatic method.

Source: Oldfield, J. W. " Test Techniques for Pitting and Crevice Corrosion Resistance of Stainless Steels and Nickel-Base Alloys in Chloride-Containing Environments," International Materials Reviews, Vol. 32, No. 3, 1987, pp 153-170.

determines E_p only. These are the followings:

i) The determination of E_B and E_p by recording E versus t curves at constant current starting from the corrosion potential.

ii) The determination of E_p by recording E versus t curves at constant current starting from a fixed potential.

Note that neither of these techniques is in general use.

• Chemical Tests

Chemical methods used for assessing resistance to pitting and crevice corrosion are based on solutions containing an activator, which is usually Cl^- and an oxidizing agent in definite concentrations. For this reason, such methods cannot be used to predict pitting and crevice corrosion resistance in natural environments, but can only be used to provide a ranking. However, this method has been used extensively for determining the pitting and crevice corrosion resistance of stainless steels and related alloys because the corrosion test results can be observed directly on the tested specimens [43, 44, 45]. Different chemicals can be used for this test. The most common chemical used is ferric chloride, and the best known test using ferric chloride is given in ASTM Standard G48 [46].

CHAPTER III

MATERIALS AND EXPERIMENTAL PROCEDURES

3.1 Materials and Weldment Preparation

Three types of super-austenitic stainless steels were selected as the base metals for this study: AL-6XN (12"X12"X1/8" wrought sheet, provided by Allegheny Ludlum), 254SMO (12"X12"X1/4" wrought sheet, provided by Avesta Sheffield) and 654SMO (12"X12"X1/8" wrought sheet, provided by Avesta Sheffield). Five types of Mo rich filler metals were chosen for welding the super-austenitic stainless steels: Inconel 625, C-22, C-276, Inco-weld 686CPT, and P16. The chemical composition of the base metals and filler metals are listed in Table 10.

Welds in this study were made using following welding techniques:

1) SMA bead-on-plate (BOP) welding process.
2) GTA bead-on-plate (BOP) autogenous welding process.
3) GTA open root filler added welding process.
4) GMA open root welding process.

BOP welds were made on 1" wide strips extracted from AL-6XN, 254SMO and 654SMO sheets. Welding was conducted using SMAW, GMAW and autogenous GTAW. All the welding coupons were clamped in a fixture with copper backing plate during welding to prevent full penetration. SMA BOP welding was performed using a Powcon 250 AC/DC welding power source. Autogenous GTA BOP welding was conducted automatically with an ASTRO-

Table 10. Chemical Composition of Base Metals and Filler Metals (wt.%).

Alloy	C	Mn	P	S	Si	Cr	Ni	Mo	N	Cu	Fe	Nb	Co	W	V	Melting Range (°F)
AL-6XN	.02	.40	.025	.002	.40	20.5	24.0	6.3	.220	.10	Bal	-	-	-	-	2410-2550
CN-3MN	013	.19	.015	.002	.73	20.8	24.8	6.2	.200	.10	Bal	-	-	-	-	2410-2550
254SMO	010	.460	.020	.001	.36	19.87	18.3	6.11	.200	.67	Bal	-	0.25	-	-	2420-2550
654SMO	015	.200	.010	.001	.29	24.6	21.9	7.3	.487	.40	Bal	-	-	-	-	2417-2498
P16	004	.14	.004	.002	.03	22.5	Bal	15.5	-	-	.64	-	-	-	-	-
C-22	.02 max	1.0 max	.003 max	.015 max	.20 max	20.0-22.5	Bal	12.5-14.5	-	0.5 max	2.0-6.0	-	2.5 max	2.5-3.5	.35 max	2475-2550
C-276	.02 max	1.0 max	.04 max	.03 max	.20 max	14.5-16.5	Bal	15.5-17.5	-	0.5 max	4.0-6.0	-	2.5 max	3.0-4.5	.35 max	2415-2550
686CPT	.02 max	1.0 max	.002 max	.002 max	.25 max	19.0-23.0	Bal	15.0-17.0	-	0.5 max	5.0 max	-	2.5 max	-	-	2440-2516
Inconel 625	0.10 max	1.0 max	0.03 max	0.02 max	0.75 max	20.0-23.0	55.0 min	8.0-10.0	-	0.50 max	7.0 max	3.15-4.15	0.12 max	-	-	2350-2460

ARC Model 3P-300-PE welding machine.

Open root welds were fabricated using two 1" wide strips. The weld groove for open root weld is illustrated in Figure 8. Welding coupons were clamped in a fixture with copper backing plate and back-purged with pure argon gas during welding. For 1/8" thick sheet a single-pass is deposited in the groove for open root welds, and for 1/4" thick sheet two-pass open root welds were fabricated. GTA open root welding was conducted manually using pure argon as the shielding gas. GMA open root welds were made automatically using Miller-Maxtron 450 CC/CV DC Inverter Arc Welder and S-64M Microprocessor Controlled Wire Feeder with a gas mixture of helium (75%) and argon (25%) as the shielding gas.

Welding parameters for each welding technique are listed in Table 11. The employment of these techniques provides the full range of the unmixed zone formation behavior. All specimens for metallographic evaluation of the unmixed zone, localized corrosion testing and mechanical property testing were extracted from these welds.

3.2 Sample Preparation

3.2.1 Metallographic Sample Preparation

Specimens, 1"X1/2" in size, for metallographic evaluation were extracted from SMA BOP weldments as well as GTA and GMA open root welded coupons and mounted (in epoxy) in both weld face and transverse orientations. The metallographic specimens were polished to 0.05 μm, and then etched chemically or electrolytically with solute sensitive etchants to reveal the

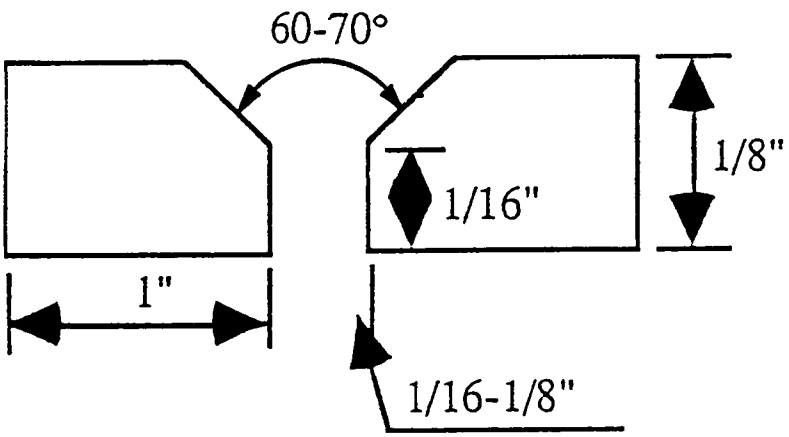


Figure 8. The sketch of weld groove for open root welds.

Table 11. Welding Parameter for Different Welding Techniques

Welding Technique	Current [A]	Voltage [v]	Wire Feed [in/min]	Welding Speed [in/min]	Gas Flow [CFH]	Heat Input [KJ/in]
GMAW open root	65	32	190	3.7	50	32
	65	32	190	6.5	50	18
	65	32	190	9.1	50	13
	65	32	190	12.0	50	10
GTAW open root	125	12	-	9.2	40	10
GTAW BOP (autogenous)	85	12	-	6.4	40	9.6
SMAW BOP	75	12	-	6.4	-	8.4

unmixed zone. Before metallographic evaluation, the specimens were rinsed in distilled water, cleaned using methanol, and dried in air.

The metallographic evaluations were conducted using both optical light microscopy (OLM) and scanning electron microscopy (SEM). Alloy element distribution across the unmixed zone was evaluated using an automated EDS technique on polished and etched specimens.

3.2.2 Corrosion Test Sample Preparation

• Pitting corrosion test sample

For pitting corrosion tests, 1" square welded specimens were extracted from both SMA BOP welds and GTA BOP autogenous welds. Before test, the corrosion specimens were prepared with different surface treatments in order to study surface condition effects and solution heat treatment effects:

i) 0.05 μm surface polishing followed by etching (as-welded).

ii) 6 micron diamond polishing without etching (as-welded).

iii) 600 grit (emery) grinding (as-welded & solution treated).

iv) 240 grit (emery) grinding (as-welded).

v) as-welded surface condition.

• Crevice corrosion test sample

Crevice corrosion samples were extracted from both GTA open root filler added welds and GTA BOP autogenous welds. Sample sizes of 1"X2"X1/8" and 1"X1"X1/8" were cut from the open root and BOP welds. Before crevice corrosion testing, the following surface conditions were imposed to evaluate the

effect of the surface condition and solution heat treatment on crevice corrosion behavior:

i) as-welded condition (welded on as-received mill surface) with and without pickling (10% HNO_3 + 2% HF, 43°C, 1 hour).

ii) as-welded condition (welded on 600 grit surface) with and without pickling (10% HNO_3 + 2% HF, 43°C, 1 hour).

iii) solution heat treated condition with pickling (10% HNO_3 + 2% HF, 43°C, 1 hour).

iv) 600 grit grinding (as-welded and solution treated).

For both the pitting and crevice corrosion test samples, after obtaining each desired surface condition, the samples were rinsed with water, cleaned using methanol, and dried in air. In addition, it is to be noted that all sharp edges of the corrosion samples were ground to avoid edge effects.

3.2.3 Mechanical Property Test Sample Preparation

• Hardness Test Sample

Microhardness test samples were extracted from both GTA open root filler added welds and GTA BOP autogenous welds. The sample was cut to 1"X1/2" and mounted. Before hardness testing, the top and bottom surfaces of the sample were ground or machined parallel, and the samples were polished to 0.05 μm and etched to reveal the unmixed zone.

• Bend Test Sample

Bend test samples were extracted from GTA open root filler added weldments and GTA BOP autogenous weldments (3 1/2"X1 1/2"X1/8"). To

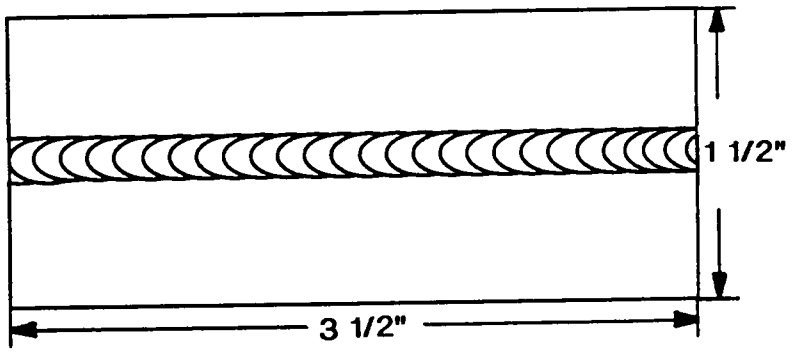
study the effect of the unmixed zone on the ductility of the weld joint, the bend tests were conducted in the as-welded condition. Both transverse root bend and longitudinal root bend test samples were used. A sketch of bend test specimens (transverse root bend and longitudinal root bend) is shown in Figure 9.

3.3 Testing Methods

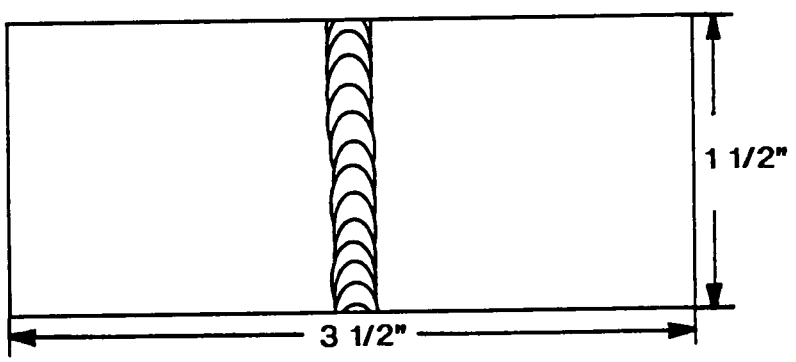
3.3.1 Pitting Corrosion Testing

- Chemical Corrosion Testing for Determining the Critical Pitting Temperature (CPT) of Unmixed Zone

For determination of the CPT of the unmixed zone, immersion corrosion tests were conducted on 1" square weld coupons. Test specimens were polished to 0.05 μm and electrolytically etched with oxalic acid to reveal the unmixed zone before testing. 10% (dry) $FeCl_3$ by weight (made by dissolving 167g $FeCl_3 \cdot 6\ H_2O$ in 900 ml distilled water) was principally used as the test solution instead of 6% dry $FeCl_3$ which is the ASTM G-48B recommended solution because 6% $FeCl_3$ solution is too dilute for optimum evaluation of the pitting behavior of high Mo (>6%) and Cr (>20%) super-austenitic stainless steels, especially for specimens with a 0.05 μm polished surface. Before testing, the container with the test solution is preheated in a constant temperature water bath (±1°C accuracy). After the water bath reaches the test temperature of interest, the solution is held at the desired temperature for 12 hours to let any precipitates settle completely. Then, the test specimen, in a glass cradle, is immersed in the test solution.



(a)



(b)

Figure 9. The sketch of bending test specimens. (a) Transverse root bend test specimen. (b) Longitudinal root bend test samples.

The critical pitting temperature (CPT: the lowest temperature at which pitting is first observed) is used to evaluate the pitting resistance of the weld specimens. Corrosion tests were conducted for 24 hours at various test temperatures to determine the CPT with a 2°C increment between tests. Pitting was determined using optical microscopy at a magnification of 100X.

• Electrochemical Corrosion Testing

The cyclic polarization scans were used to determine the pitting corrosion tendency of the unmixed zone. Polarization data were generated using a computer controlled EG & G model 273 potentiostat. The test cell, as shown in Figure 10, was used with a saturated (KCl) silver/silver-chloride reference electrode and a electrolyte test solution (6% $FeCl_3$, 2 liters) which was aerated by purging air into the solution. All electrochemical measurements were made at 23°C (room temperature). All potentials were converted to the standard hydrogen electrode (SHE) scale. The scans are represented in the form of E (SHE potential) verses $\mu A/cm^2$ (current density) plots.

Prior to the polarization scan for each test, the specimen was allowed to corrode freely for at least 45 minutes to stabilize E_{corr} (free corrosion potential). After E_{corr} stabilization, the potential was scanned in the noble direction beginning 35 mV below the established E_{corr} value. The scan rate was 0.17 mV/s. The reversing current density was kept at 1000 μA/sq.cm. The final potential on each reverse scan was programmed to be 20 mV (vs. reference electrode) below the initial free corrosion potential (E_{corr}).

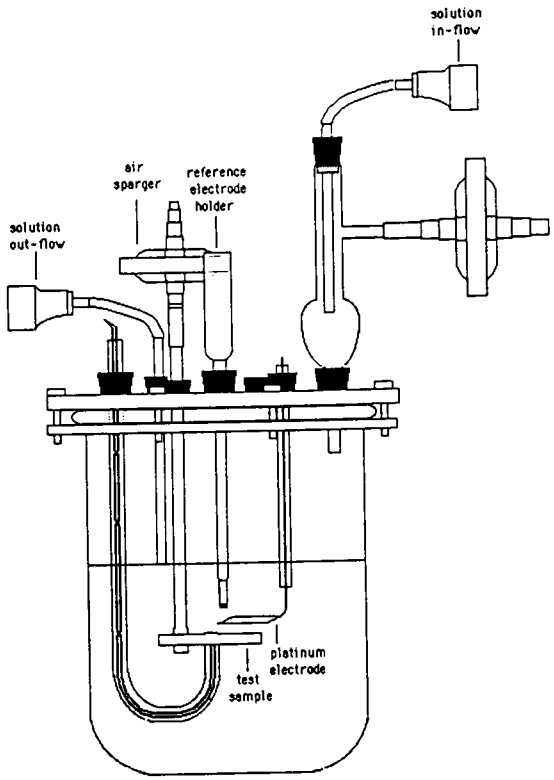


Figure 10. The electrochemical testing cell.

• Pit Initiation and Propagation Testing

The immersion corrosion test was used to investigate pit initiation and propagation behavior. 1" square weld specimens were polished to 0.05 μm and electrolytically etched with oxalic acid to reveal the unmixed zone on the weld face before the pitting tests. Then, the immersion corrosion tests were conducted in 10% $FeCl_3$ solution at the CPT of the unmixed zone as a function of test time. After a designated testing time at the CPT in 10% $FeCl_3$, the corrosion specimens were examined using optical microscopy to evaluate pit initiation and propagation behavior. In addition, pit propagation orientation was also investigated under the same conditions.

3.3.2 Crevice Corrosion Testing

The crevice corrosion testing was conducted using the UT Crevice Corrosion Device for welded specimens. The UT Crevice Corrosion Device and welded specimens are shown in Figures 11 and 12. The specimen (1"X2") was placed in between two 3/8" diameter low-halide silicone rubber rods (GE RTV 664 - formed by casting into PTFE molds).

The silicone rubber rods can only be re-used when there is no observation of discoloration on its surface after a crevice corrosion test. It is strongly recommend that the used rubber rods be cleaned in boiling distilled water in a glass container for 30 minutes before reuse in crevice corrosion testing. Through boiling in distilled water, water-soluble ingredients which can affect the corrosion test results are removed from the used rubber rods.

The specimen with silicone rubber rods was held in place by bolted titanium backing plates at a torque of 32 in-oz applied to each bolt. Two

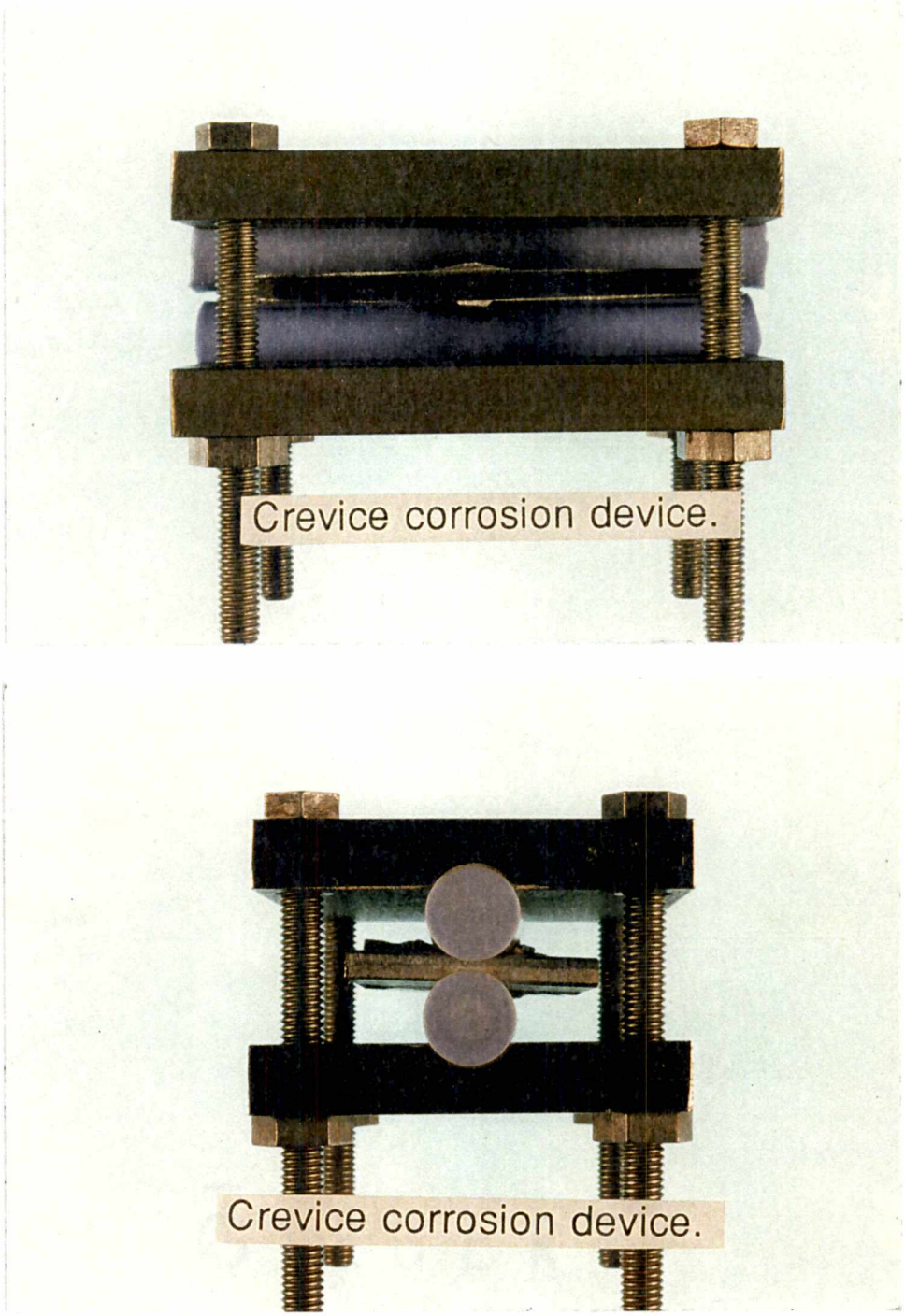


Figure 11. UT crevice corrosion device.

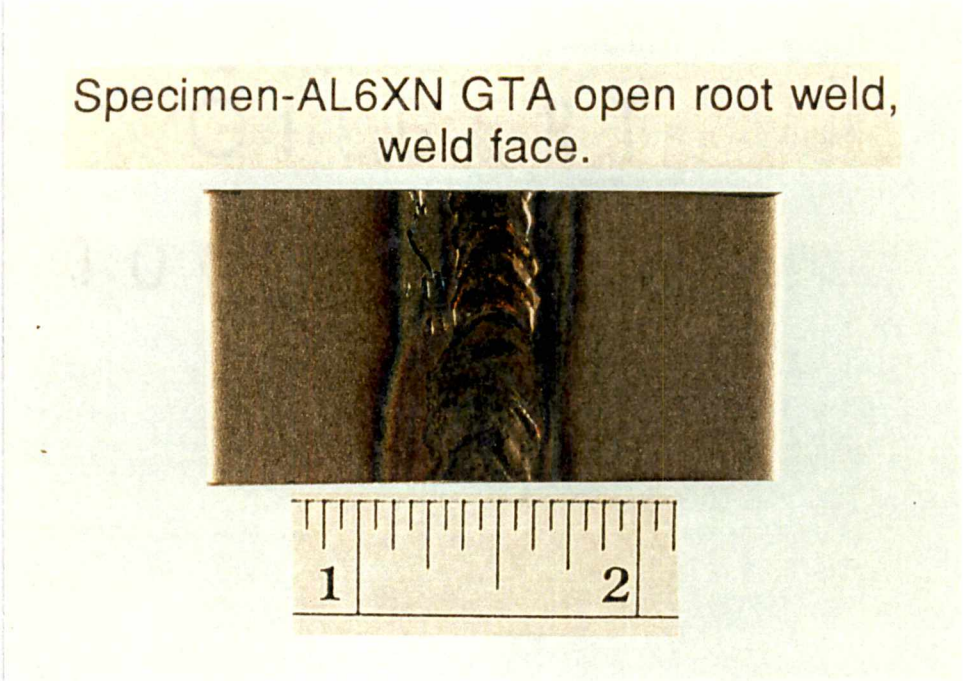


Figure 12. Crevice corrosion test specimen. (a) Weld face. (b) Weld root.

crevices across the various weld regions, including the weld fusion zone, the unmixed zone, the heat-affected zone and the unaffected base metal on both weld face and weld root are formed. The tests were conducted by submerging the specimen fixed in the UT crevice corrosion test device in 6% $FeCl_3$ for 72 hours at each desired temperature. The crevice corrosion behavior of the unmixed zone in the weld specimens was evaluated by measuring the extent of the corrosion in the unmixed zone.

3.3.3 Solution Heat Treatment

Solution heat treatment was conducted on weld coupons to study the effect of solution treatment on localized corrosion behavior in the unmixed zone by reducing alloy element segregation. The time for solution treatment was determined based on the calculation of alloy element (Mo) diffusion time for a given temperature and a measured diffusion distance using the following equations:

$$X = \sqrt{Dt} \qquad (3\text{-}1)$$

$$D = D_0 \exp(-Q/RT) \qquad (3\text{-}2)$$

From equations (3-1) and (3-2), we have

$$t = X^2/[D_0 \exp(-Q/RT)] \qquad (3\text{-}3)$$

where: $X = 0.003125$ mm, diffusion distance is measured as the average radius of cellular dendrites in the unmixed zone.

D_0 (Mo in austenite) = 4 [mm^2/sec]

Q (Mo in austenite) = 240,000 [J/mol]

R = 8.314 [J/mol•K]

The time for solution heat treatment (t) as a function of solution treatment temperature (T) is presented in Figure 13. Based on the calculated time-temperature curve, a time period of 30 min was selected for solution treatment at temperatures of 2100°F, 2150°F, and 2200°F followed by a water quench. Solution treatment was conducted by Haynes International Inc.

3.3.4 Microhardness Testing

Microhardness testing was used to evaluate the mechanical properties of the unmixed zone in super-austenitic stainless steel weldments. Specimens were polished and etched to reveal the unmixed zone before microhardness testing. A Leco M-400-G1 type microhardness tester was used for conducting hardness measurements. A knoop indentor was chosen with a 100 g load and 15 seconds loading time due to the narrow width of the unmixed zone. Hardness traverses were made across the various zones including the base metal, the unmixed zone and the composite fusion zone.

3.3.5 Bend Testing

Both longitudinal and transverse bend tests were employed with a face bend for autogenous welds and root bend for open root welds to determine the relative ductility of the unmixed zone in contrast to other regions in welds. Test specimens were extracted from the weldment made on 1/8" thick super-austenitic stainless steels. The specimens were bent (3 point bending) in a U-shaped die by means of a centrally applied force as shown in Figure 14. The

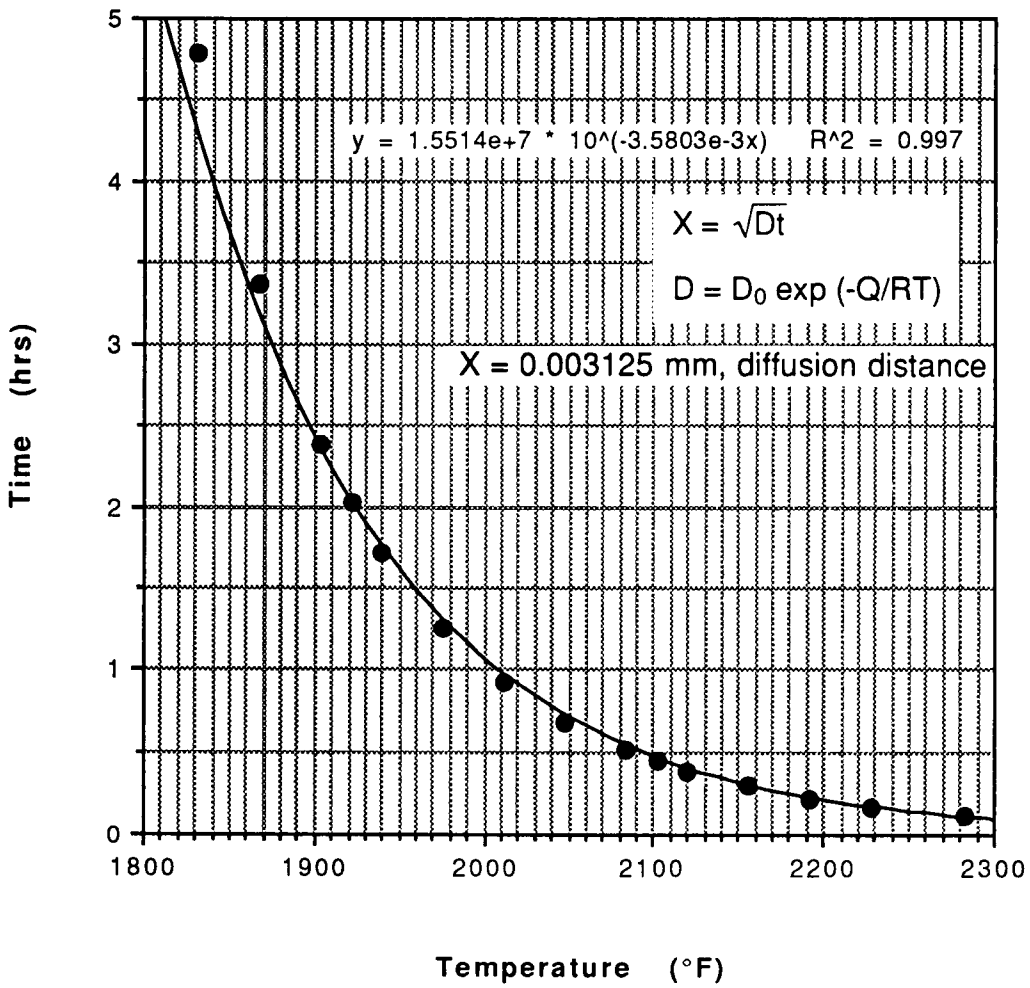
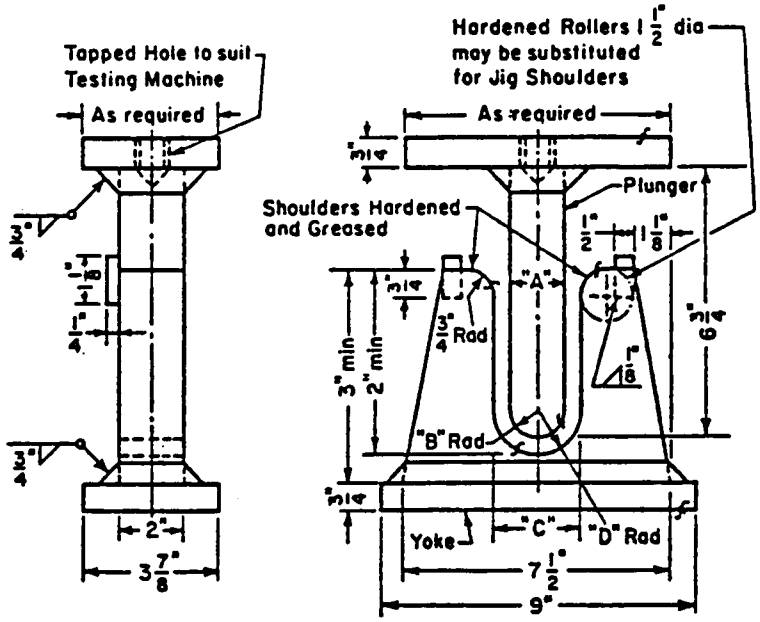


Figure 13. Calculation of solution heat treatment time as a function of temperature.



Thickness of Specimen in. (mm)	A, in. (mm)	B, in. (mm)	C, in. (mm)	D, in. (mm)
3/8 (9.5)	1 1/2 (38)	3/4 (19)	2 3/8 (60)	1 3/16 (30)
1/8 (3.2)	2 1/8 (54)	1 1/16 (27)	2 3/8 (60)	1 3/16 (30)
t	$4t$	$2t$	$6t + 1/8$ (+3.2)	$3t + 1/16$ (+1.6)

Figure 14. Bend Test Fixture.

specimen was forced into the die by a plunger with a radius of 1/4" which provides 22% surface strain. The convex surface of the bent specimens was examined for cracks or other open defects under a stereo macroscope at 70X. Bend tests were conducted according to ASTM E190-64, Standard Method for Guided Bend Test for Ductility of Welds [47].

CHAPTER IV

EXPERIMENTAL RESULTS AND DISCUSSION

4.1 Evaluation of Unmixed Zone

4.1.1 Metallographic Evaluation of Unmixed Zone

In general, conventional metallographic etching techniques do not satisfactorily reveal the unmixed zone since the unmixed zone is nominally of the same composition as the adjacent HAZ and the only difference in the appearance between the unmixed zone and the HAZ is the solidification substructure of the unmixed zone. The unmixed zone can be mistakenly identified as a part of the HAZ if improper etchants and etching techniques are used. Thus, selection of etchants and etching techniques is important for revealing the unmixed zone.

A proper identification and examination of the unmixed zone by metallographic techniques depends on utilization of specific solute sensitive etchants to reveal the segregation resulting from solidification in the unmixed zone. Also, these etchants should not be sensitive to transformation products which results from subsequent metallurgical changes. The development of these etchants is normally a trial and error process but potentiostatic electrolytic techniques are considered more appropriate to selectively reveal the segregation of certain elements and thus reveal the unmixed zone.

To reveal the unmixed zone in the super-austenitic stainless steel weldments, metallographic specimens were extracted from AL-6XN SMA bead-on-plate (BOP) weld coupons in three orientations (longitudinal cross-section,

transverse cross-section and a top view) as shown in Figures 15 through 17. In this study, two etching techniques and three etchants were selected to reveal the unmixed zone (Table 12). The unmixed zone appearance as revealed using the selected etchants are shown in Figures 18 through 20 for AL-6XN SMA BOP welds (C-22 and Inconel 625 filler metals). It is evident that glyceregia reveals the unmixed zone as a dark-etching region compared to the light-etching base metal and weld metal (see Figure 18). Oxalic acid etching results in light-etching in both the unmixed zone and the base metal (see Figure 19). Both glyceregia and oxalic acid etchants clearly show the solidification substructure in the unmixed zone. Aqua-regia also shows the solidification substructure in the unmixed zone (see Figure 20). However, since aqua-regia reveals both the unmixed zone and base metal as dark-etching regions, the unmixed zone may sometimes be mistakenly identified as a part of the un-melted base metal, especially when the unmixed zone is narrow. Therefore, glyceregia and oxalic acid provide better as-etched appearances of the unmixed zone compared to aqua regia. It was also found that electrochemical etching is easier to perform and provides a uniformly etched surface appearance in comparison to chemical etching.

4.1.2 Extent and Distribution of Unmixed Zone

The examination of the unmixed zone distribution was first conducted on AL-6XN SMA BOP welds (C-22 and Inconel 625 filler metals), AL-6XN GTA open root weld (C-22 filler metal) and 654SMO GTA open root weld (P16 filler metal). The specimens extracted from these welds were polished to 0.05 μm and etched with oxalic acid to reveal the unmixed zone. The transverse cross-

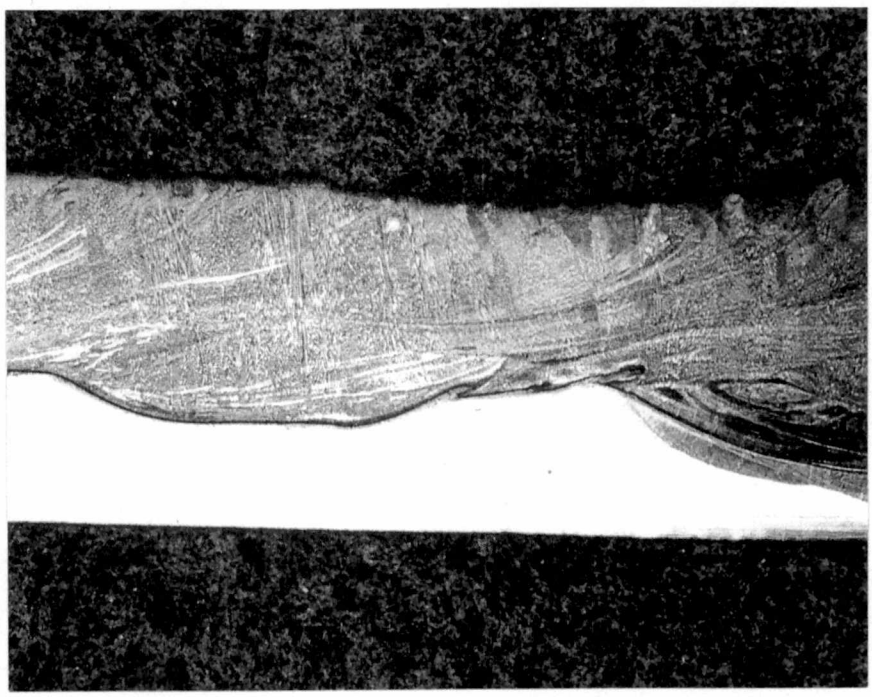


Figure 15. Longitudinal cross-section of AL-6XN SMA BOP weld, 15X.

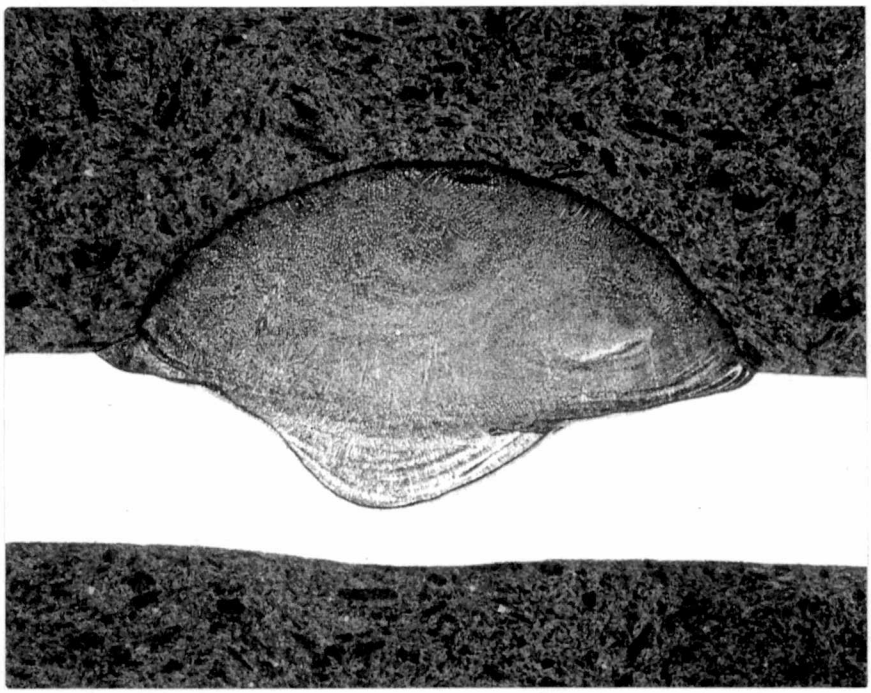


Figure 16. Transverse cross-section of AL-6XN SMA BOP weld, 15X.

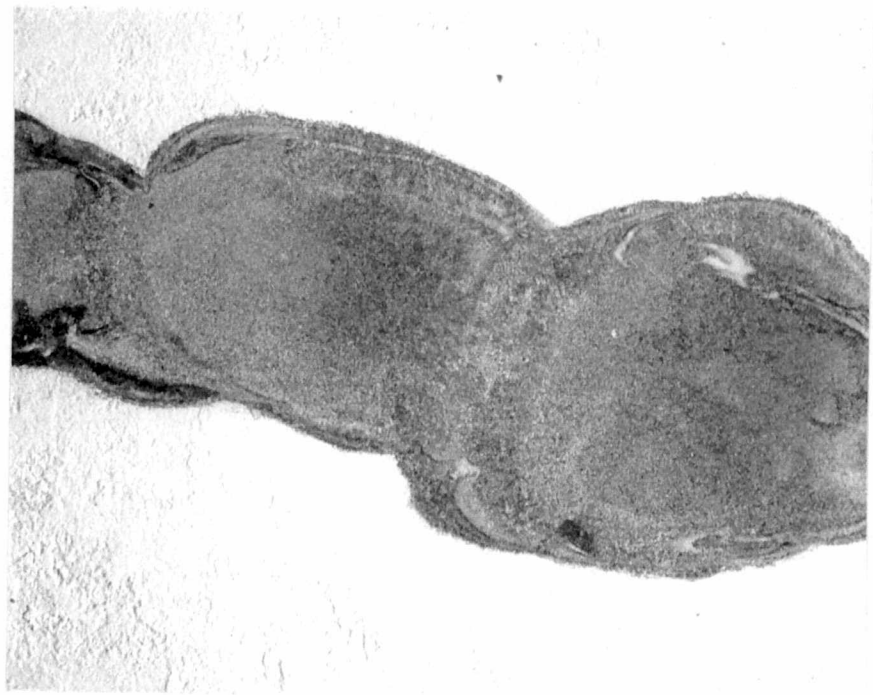


Figure 17. top-view of AL-6XN SMA BOP weld, 15X.

Table 12. Etchants and Etching Techniques

Etchants	Composition	Etching Method
Aqua regia	30 ml HCl 10 ml HNO_3 10 ml H_2O	Chemical
Oxalic Acid	10 g COOHCOOH 90 ml H_2O	Electrochemical*
Glyceregia	30 ml HCl 10 ml HNO_3 30 ml Glycerol	Electrochemical*

* Electrochemical etching parameters: 1.0 ampere, 10 volts, 15 seconds.

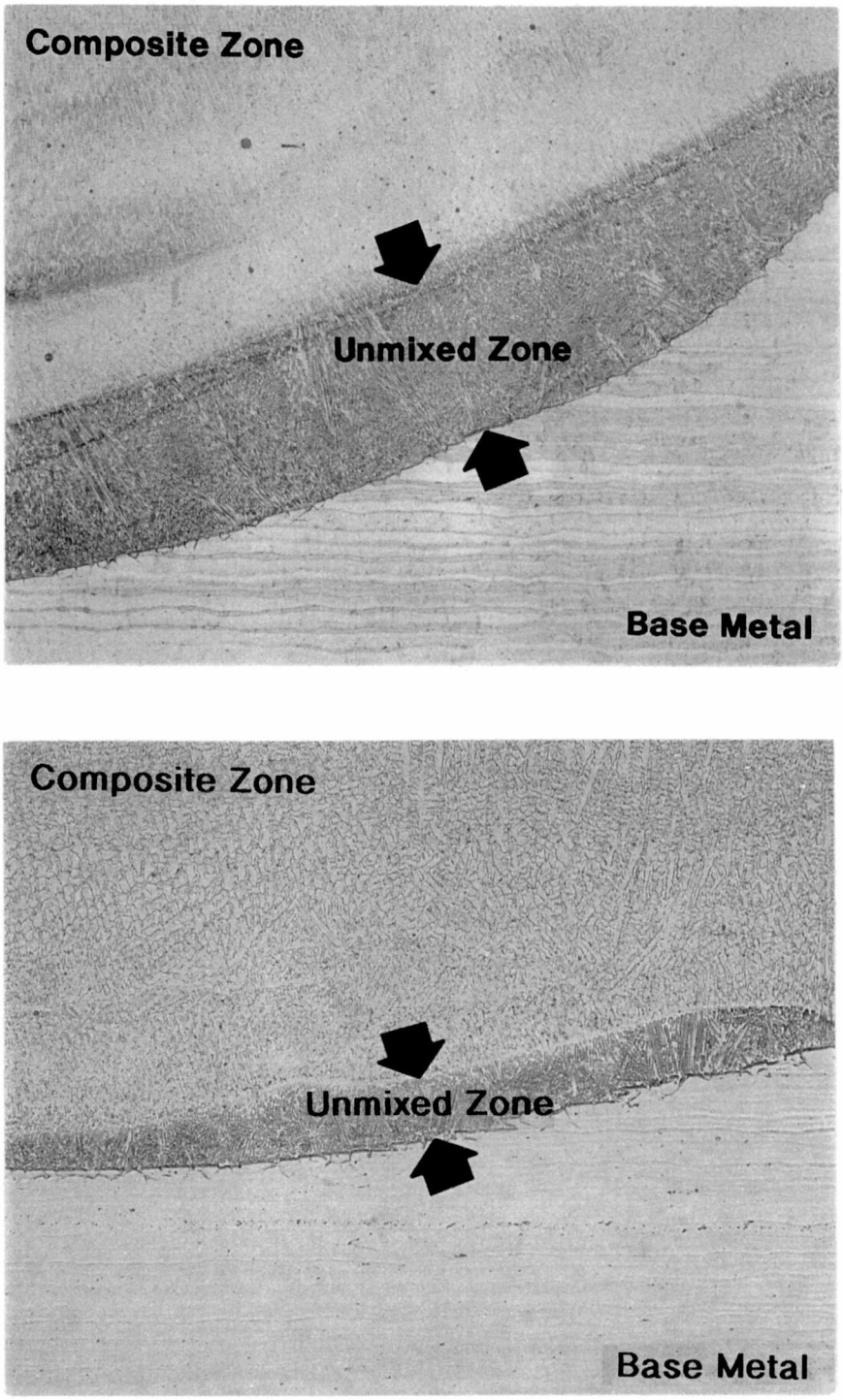


Figure 18. The unmixed zone revealed using electrolytic glyceregia, (a) weld with C-22 filler metal, (b) weld with Inconel 625 filler metal, 100X.

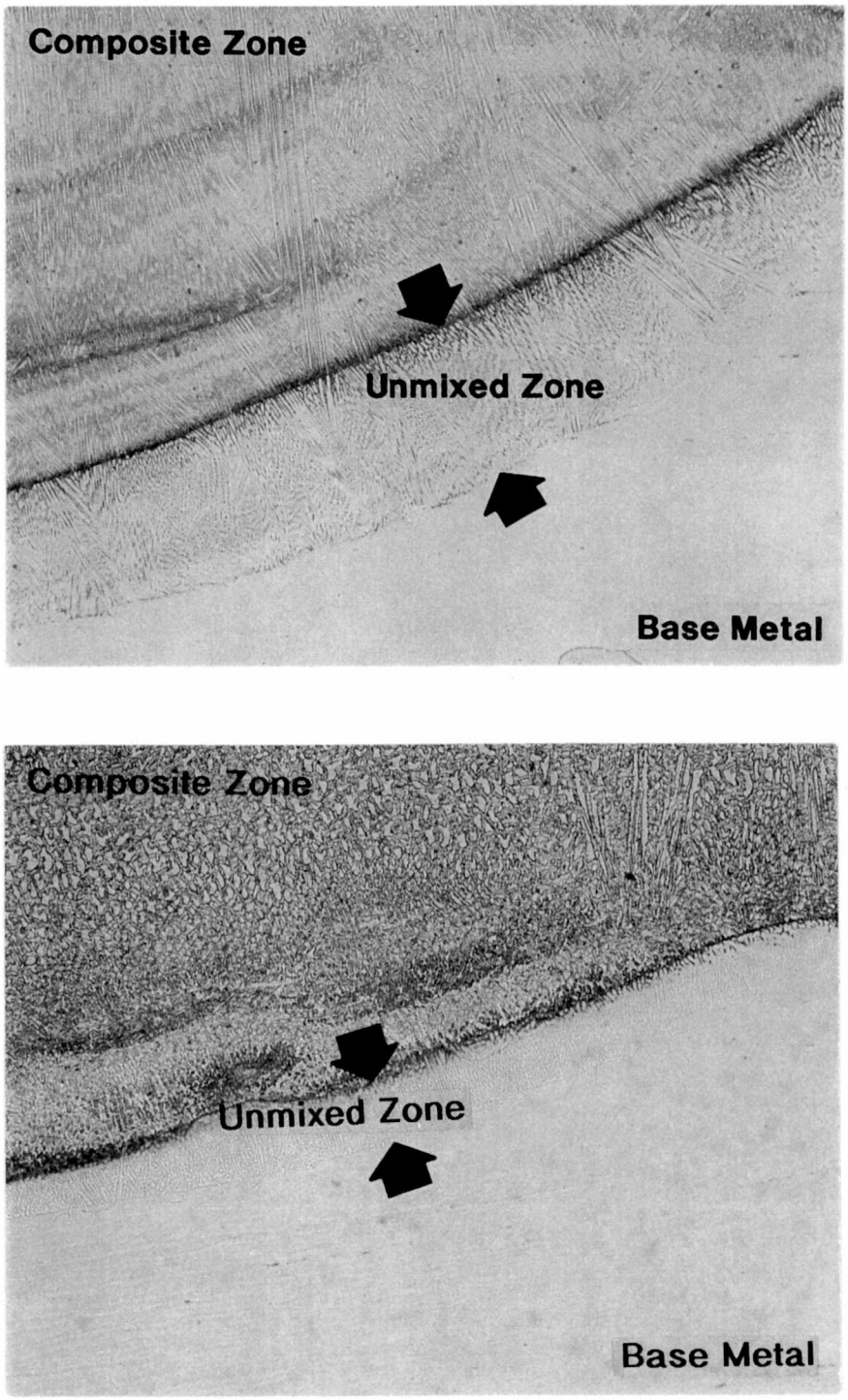


Figure 19. The unmixed zone revealed using electrolytic oxalic acid, (a) weld with C-22 filler metal, (b) weld with Inconel 625 filler metal, 100X.

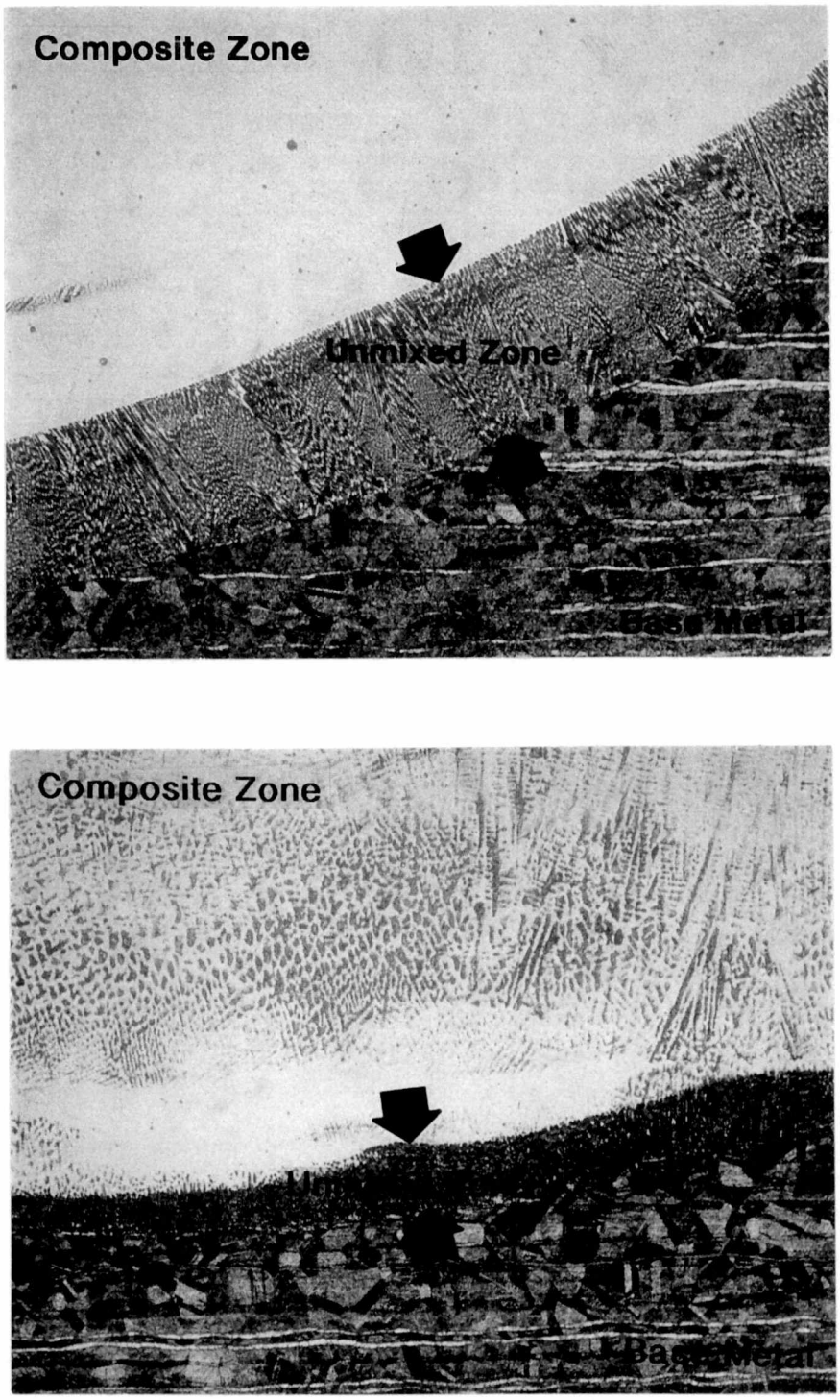


Figure 20. The unmixed zone revealed using chemical aqua-regia, (a) weld with C-22 filler metal, (b) weld with Inconel 625 filler metal, 100X.

sections of the typical AL-6XN SMA BOP welds and GTA open root welds are illustrated in Figures 21 and 22 respectively. The extent and distribution of the unmixed zone along the weld interface was examined using optical microscopy. The width of the unmixed zone was measured perpendicular to the weld interface on a transverse weld cross-section as a function of distance from the weld face toward the weld root. The variation in the width of the unmixed zone along the weld interface is shown in Figures 23 and 24 for SMA BOP welds (on AL-6XN with C-22 and Inconel 625 fillers) and for GTA open root welds (on AL-6XN and 654SMO), respectively.

For AL-6XN SMA BOP welds (as shown in Figure 23), it is evident that a minimum in the width of the unmixed zone occurs near the top surface of the weld and a maximum near the root of the weld. This is true for all SMA BOP dissimilar welds used in this study. The change in width of the unmixed zone as a function of location is due to the fact that the motion of the molten metal in upper part of the weld pool is significantly more turbulent resulting in a better mixing of the filler metal with the melted base metal. On the other hand, the motion of the molten metal in the lower part of the weld pool is laminar or less turbulent. Thus, the melted base metal freezes without significant mixing with the filler metal near the bottom of the weld. Thus, the unmixed zone is wider in the lower part of the weld than at the weld surface.

The width of the unmixed zone in AL-6XN SMA BOP welds made with C-22 filler metal is wider than with Inconel 625 filler metal (see Figure 23). This is because of the difference in the melting temperature range between the filler metals and the base metal. Matthews and Savage [13, 14] have suggested that an unmixed zone is easily created when the melting range of the filler metal is

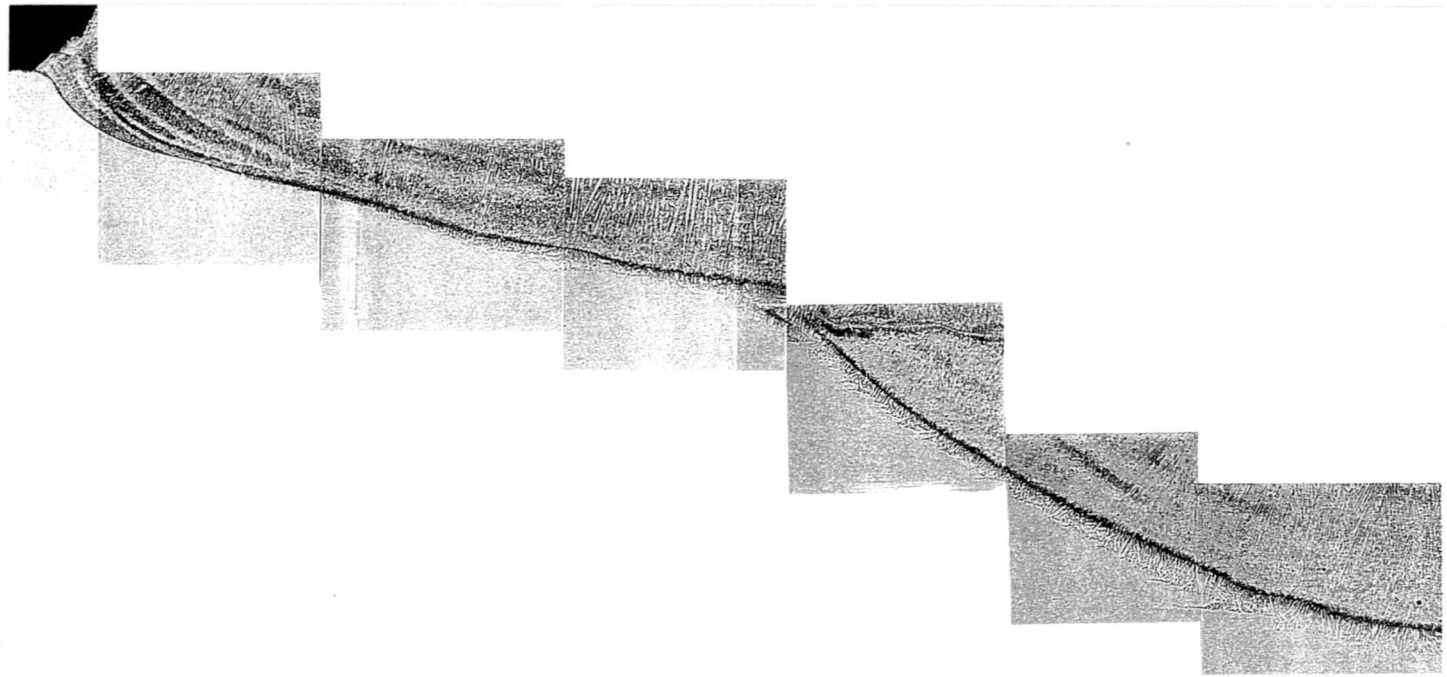


Figure 21. The area for measurement of distribution of the unmixed zone along welding interface on transverse cross-section of AL-6XN SMA BOP weld (C-22 filler metal), 80X.

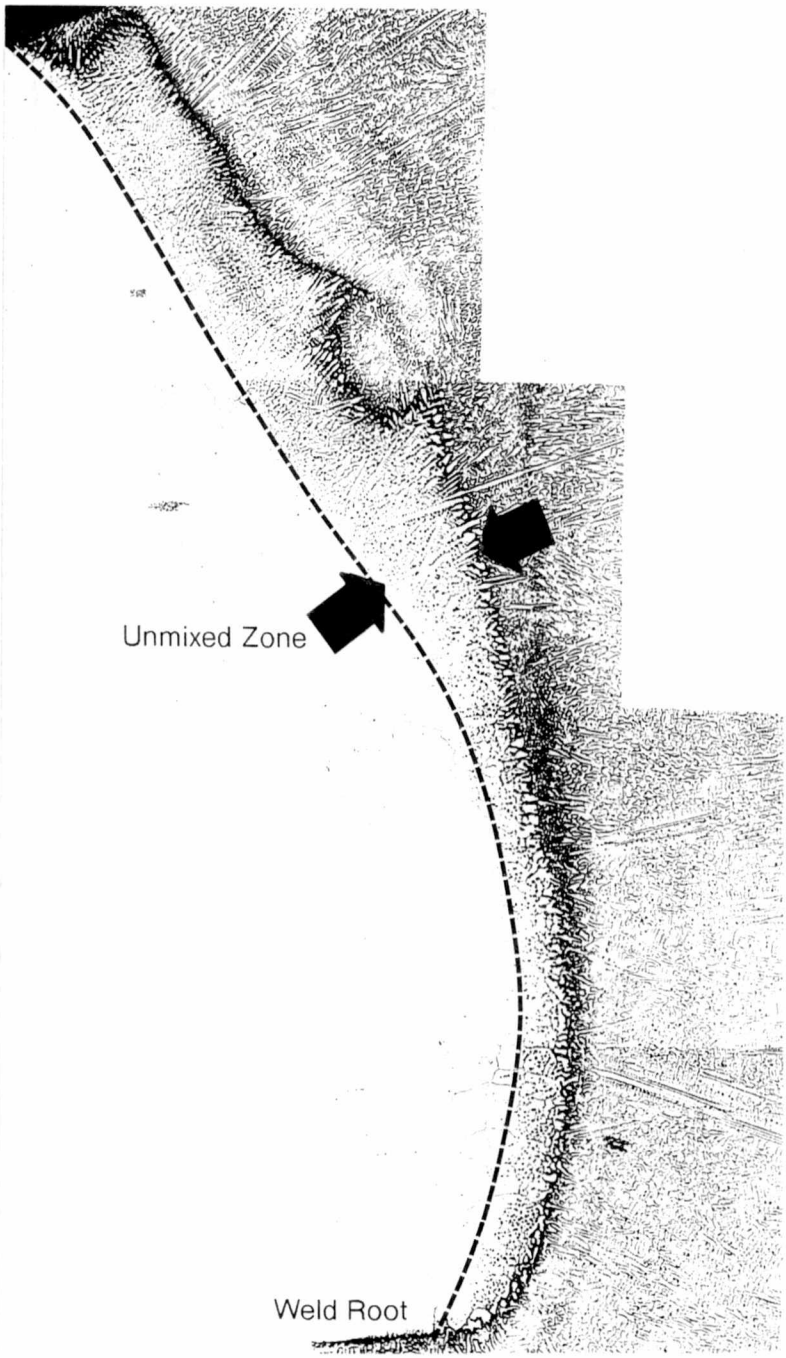


Figure 22. The area for measurement of distribution of the unmixed zone along welding interface on transverse cross-section of AL-6XN GTA open root weld (C-22 filler metal), 70X.

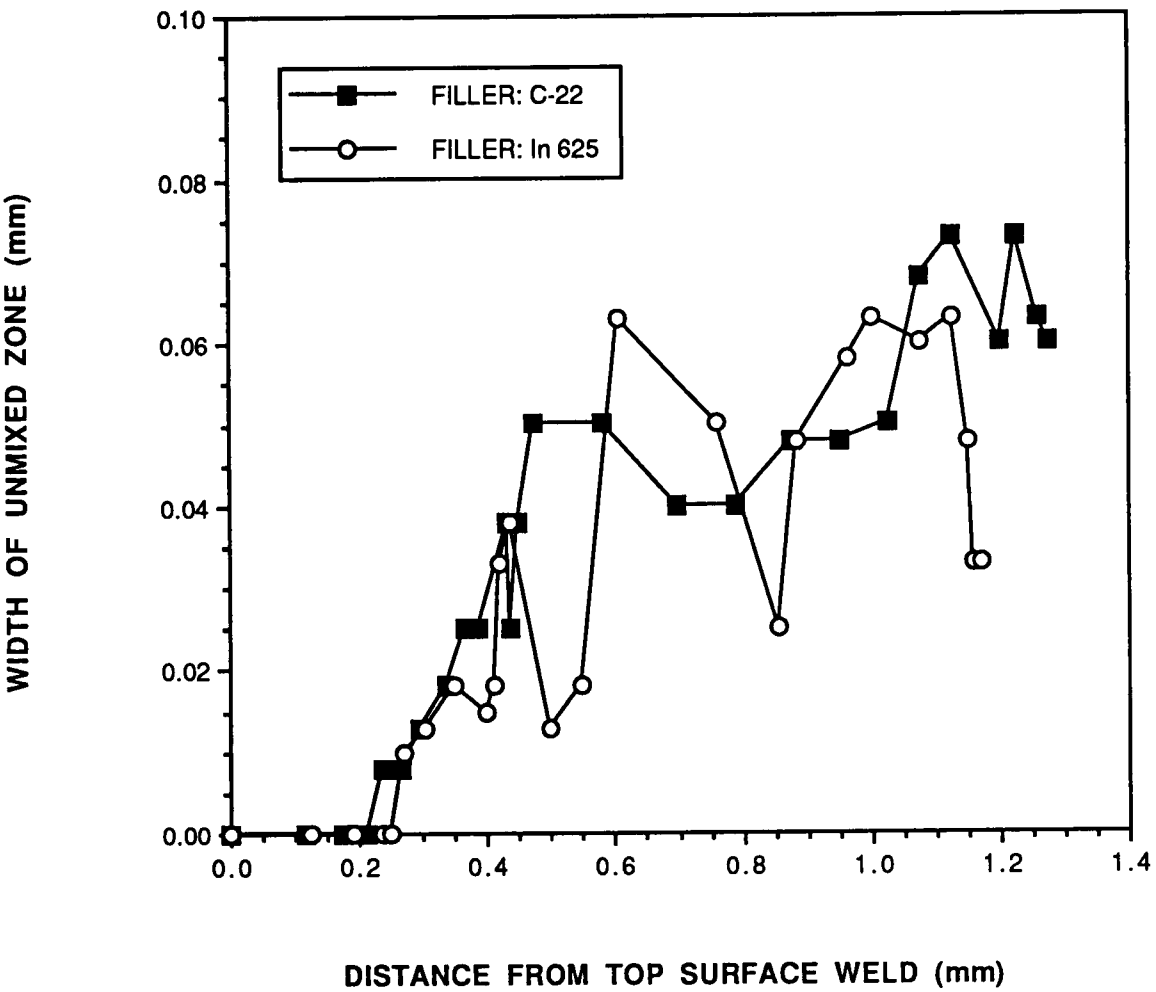


Figure 23. Width of the unmixed zone along welding interface on transverse cross-section of AL-6XN SMA BOP weld with C-22 and Inconel 625 filler metals.

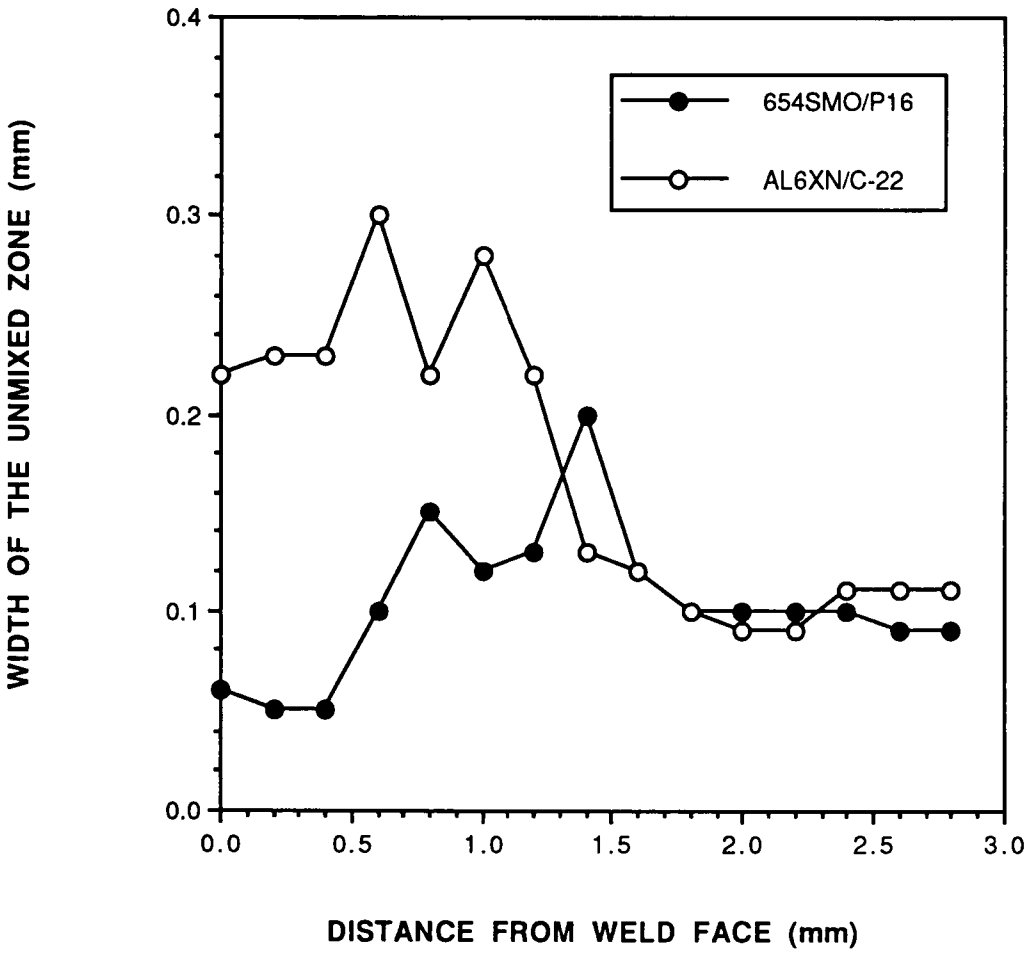


Figure 24. Width of the unmixed zone along welding interface on transverse cross-section of GTA open root welds on AL-6XN (C-22 filler) and 654SMO (P16 filler).

equal to or greater than that of the base metal. As shown in Table 10, C-22 filler metal has similar melting range (2475 -2550°F) to AL-6XN base metal (melting range: 2410 - 2550°F), in comparison with Inconel 625 filler metal (melting range: 2350 - 2460°F). Based on the knowledge of the viscosity of liquid metal as a function of temperature and melting point of the metal as shown in Figure 25 [48], it is to be noted that metal with a higher melting point has a higher viscosity. Thus, for a given welding condition, the filler metal with a higher melting range will be expected to provide better conditions for not mixing with the melted base metal. As a result, a wider unmixed zone will form for a filler metal with a higher melting range. This is consistent with the observation made in this study in terms of the weld with C-22 (melting range: 2475-2550°F) presenting a wider unmixed zone than with Inconel 625 (melting range: 2350-2460°F).

In the case of GTA open root welds, the widest unmixed zone is located near the sheet mid-plane and a relatively wide unmixed zone has also been observed at the weld face in some cases (see Figure 24). Unlike the unmixed zone distribution in SMA BOP weld, the unmixed zone in a GTA open root weld tends to extend to the weld face. The average width of the unmixed zone in 654SMO welds is less than that in AL-6XN welds. It is believed that the difference in the unmixed zone width is due to the fact that the liquidus temperature of the 654SMO (2417-2498°F) is about 50 F° lower than that of AL-6XN (2410-2550°F). As a result, a narrower unmixed zone is expected in 654SMO weldments than in AL-6XN.

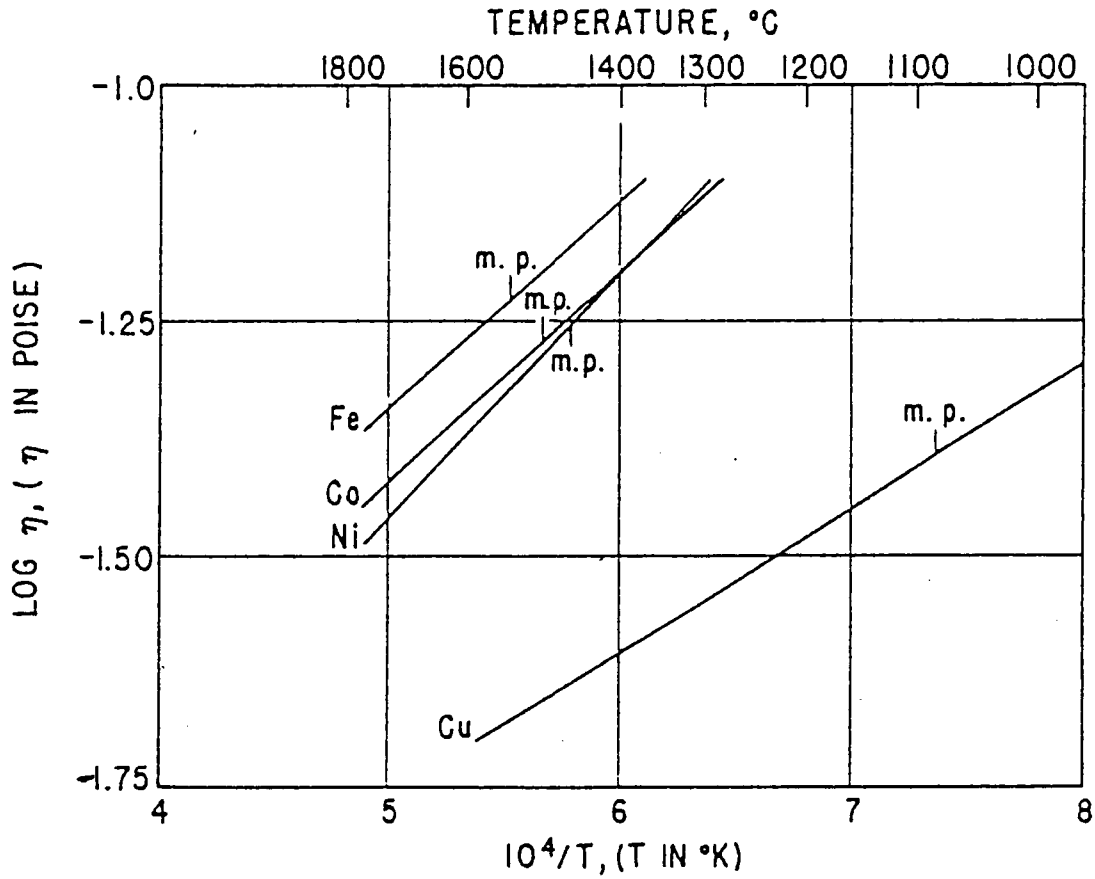


Figure 25. Variation of viscosity of some metals with temperature [48].

4.1.3 Evaluation of Unmixed Zone Using SEM with EDS Analysis

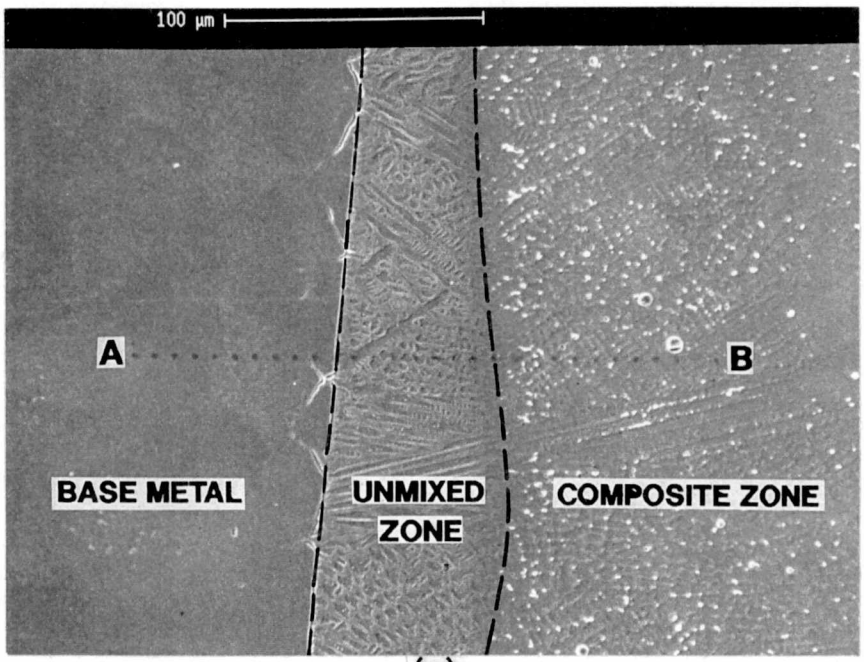
SMA BOP weldments on AL-6XN (C-22, Inconel 112 and 686CPT electrodes), 654SMO (P16 filler) and 254SMO (C-22 filler) were examined using the SEM with EDS on the face (top-view) section of the welds. The specimens were polished (0.05 μm) and etched to reveal the unmixed zone before SEM evaluation. A SEM with an automated EDS program was employed for quantitative analysis of the unmixed zone. The distribution of alloying elements across the unmixed zone was determined at 5.0 μm intervals for AL-6XN welds (C-22 and 686CPT filler metals) and 254SMO welds (C-22 filler), 2.5 μm for 654SMO weld (P16 filler) due to difference in width of the unmixed zones in these welds.

Figure 26 (a and b) shows one example of SEM micrographs of the weld interface (AL-6XN SMA BOP weld with 686CPT filler metal) and the chemical composition profiles of the elements Ni, Cr, Mo and Fe across the unmixed zone along the line AB. Based on the results of EDS analysis, it is evident that the unmixed zone in super-austenitic stainless steel dissimilar welds has the same chemical composition as that of the respective base metal. The alloying element, Fe, contained in the composite zone shown in the EDS analysis is lower than that of the filler metal composition due to the dilution effect of the base metal.

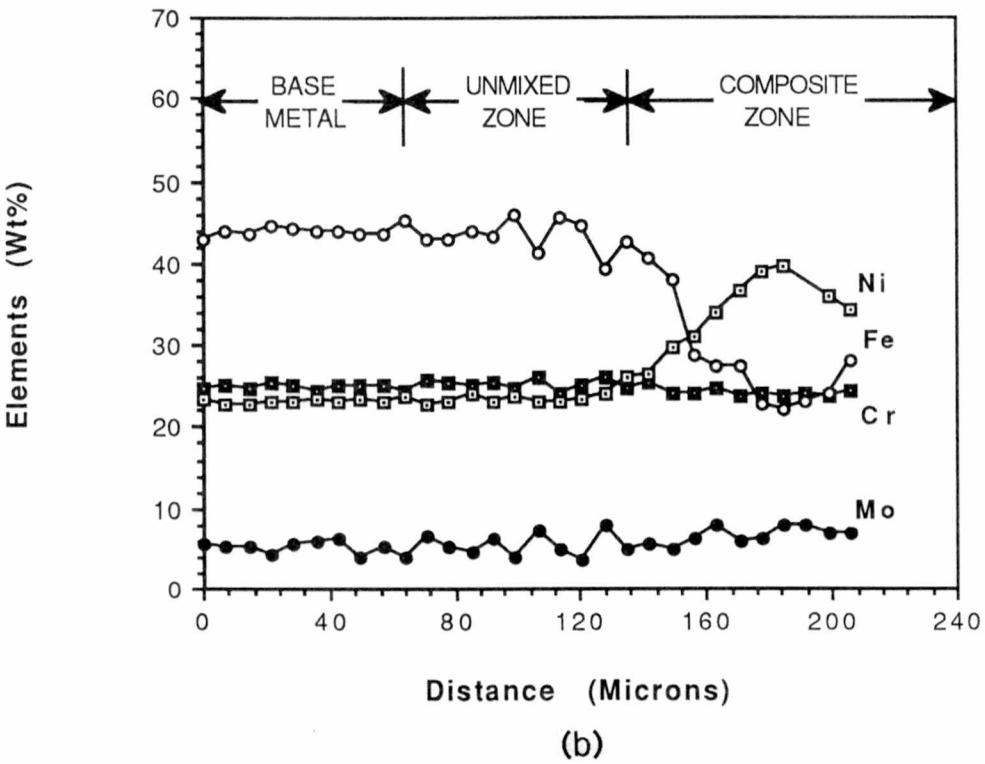
4.1.4 Solidification and Segregation in Unmixed Zone

• Solidification in Unmixed Zone

Evaluation of the solidification behavior in unmixed zone was conducted on AL-6XN (CN-3MN casting) SMA BOP weld (Inconel 112 filler) using optical



(a)



(b)

Figure 26. (a) SEM micrograph at weld interface of AL-6XN SMA BOP weld with 686CPT filler metal, (b) chemical profile of alloying elements along line AB in (a).

microscopy. Specimens were extracted from the weldment in a transverse weld cross-section. For evaluation of the unmixed zone solidification behavior, specimens were polished to 0.05 μm and etched electrolytically with Glyceregia to reveal the solidification substructure in both the unmixed zone and the base metal as presented in Figure 27 (a and b, bright and dark field images). A coarse dendritic solidification substructure is evident in the base metal. Comparing the solidification orientation of the casting base metal with the solidification substructure in the unmixed zone, it is evident that they have the same solidification orientation, and the unmixed zone grows directly from the unmelted base metal. This observation shows that the unmixed zone solidifies epitaxially.

• Segregation in Unmixed Zone

Variation in element distribution shown in Figure 26 (b) indicates that segregation occurs in the unmixed zone during re-solidification. It is well known that molybdenum is a primary element necessary to provide high pitting and crevice corrosion resistance. Thus, the content and distribution of Mo plays an important role in determining the localized corrosion behavior of super-austenitic stainless steel. If Mo segregation occurs in the unmixed zone, the localized corrosion behavior of the unmixed zone will be different from that of the base metal. Therefore, segregation behavior in the unmixed zone is important and a better understanding of the unmixed zone corrosion behavior can be obtained from a knowledge of solidification segregation.

To determine Mo segregation in the unmixed zone, quantitative EDS at 4 μm intervals was conducted on a polished and etched specimen extracted from

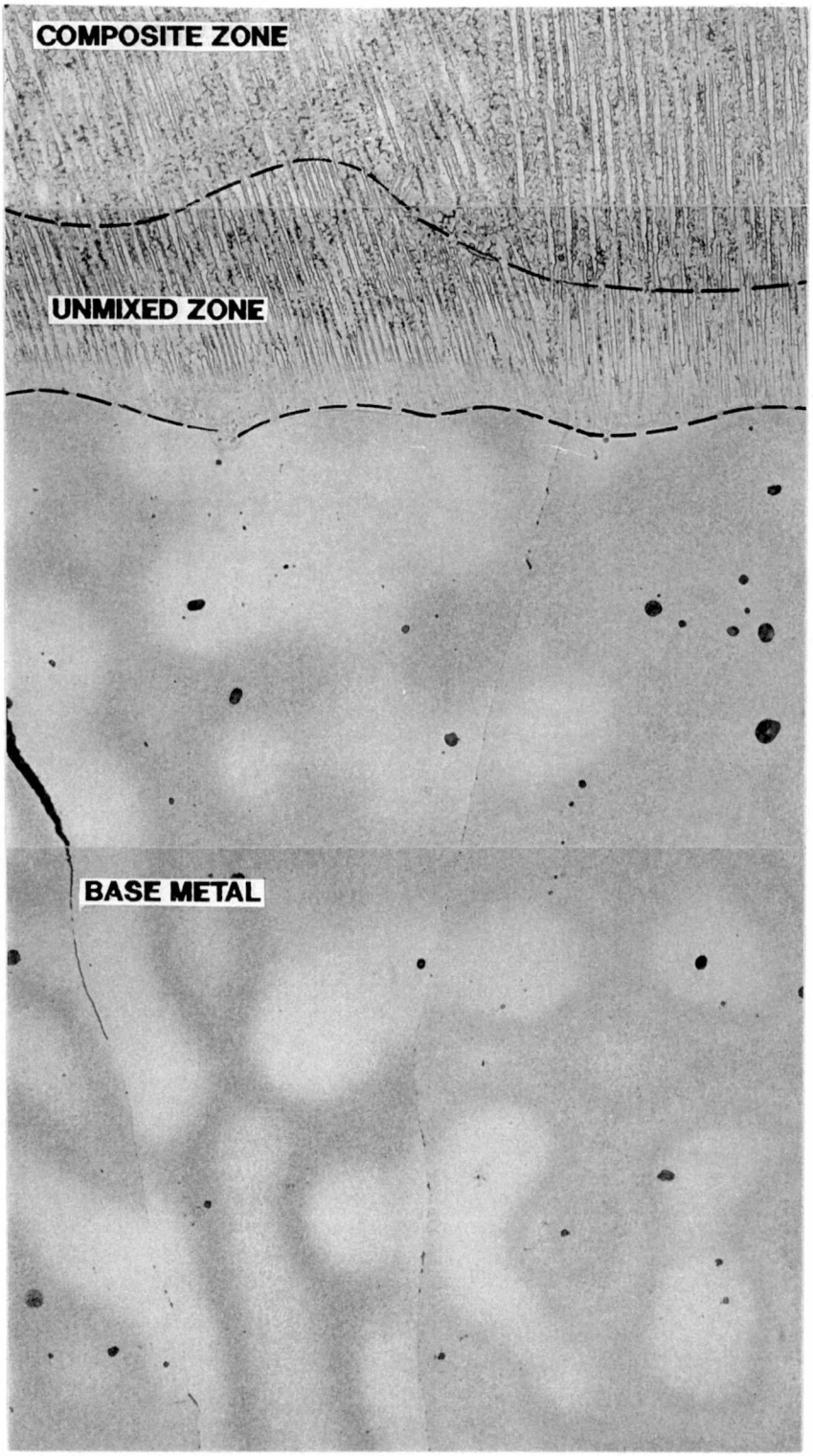


Figure 27a. Solidification morphology in CN-3MN SMA BOP (casting) weld with 112 electrode, transverse cross-section, bright field image, 200X.

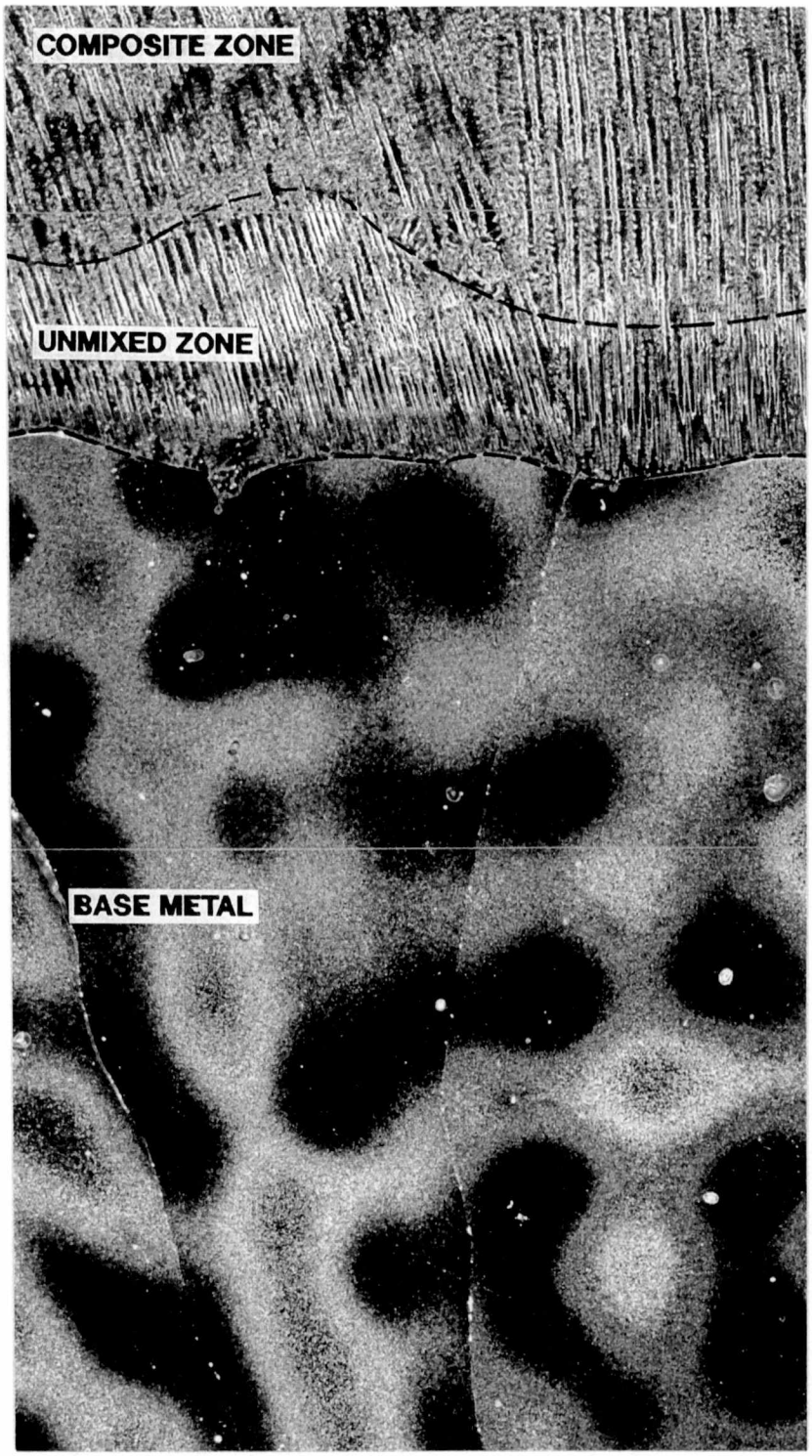


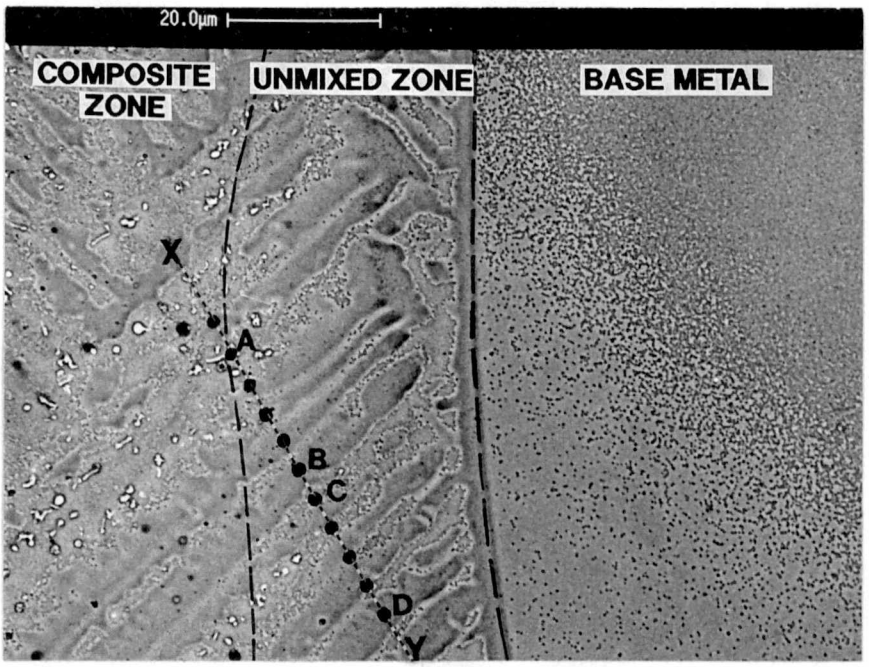
Figure 27b. Solidification morphology in CN-3MN SMA BOP (casting) weld with 112 electrode, transverse cross-section, dark field image, 200X.

AL-6XN (CN-3MN casting) SMA BOP weld {Inconel 112 (625) filler}. The unmixed zone area where EDS was conducted is shown in Figure 28a. The Mo content across several cellular dendrites in the unmixed zone was determined along line XY for each marked location shown in Figure 28a. The variation in the Mo content along line XY for each location in the unmixed zone is presented in Figure 28b, and also the average Mo content of the base metal (6.3 wt%) is plotted in Figure 28b for comparison.

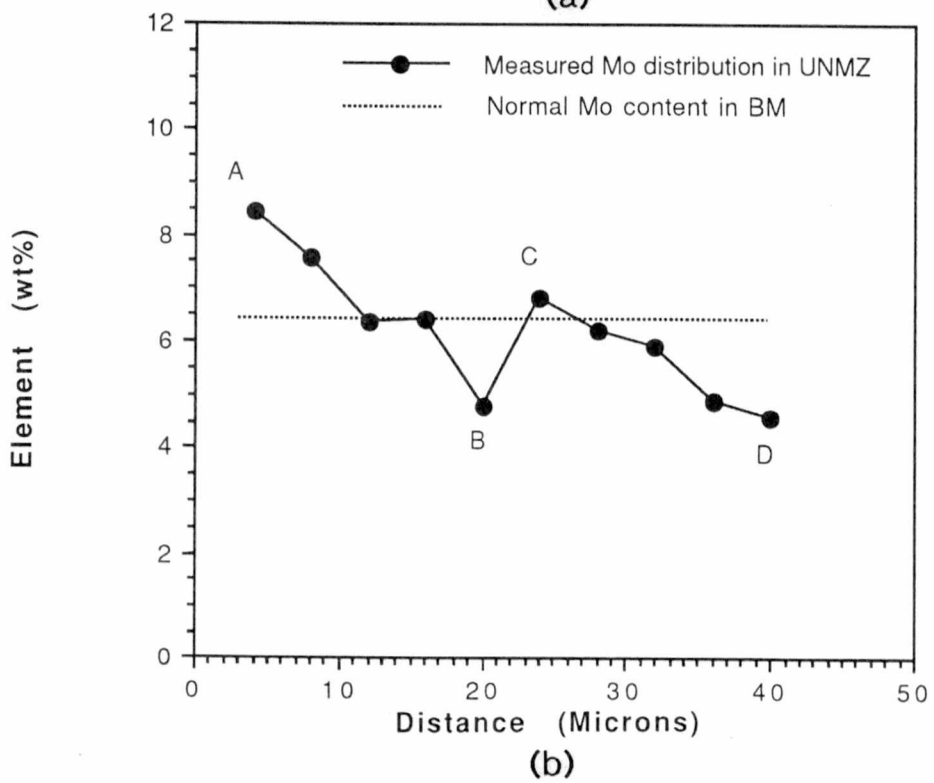
As a result of Mo segregation, the cellular dendrite boundaries (shown by points A and C in Figure 28b) have higher Mo content than the average Mo content in the base metal. On the other hand, the lowest Mo content is found in the core of cellular dendrites as shown by points B and D in Figure 28b. It is to be noted that Mo content in the core of cellular dendrites is approximately 4.7 wt%, which is lower than the average Mo content in the base metal (6.3 wt%). Based on these data, it is evident that Mo segregation occurred during in-situ resolidification of the unmixed zone and this will dominate the localized corrosion behavior of the unmixed zone.

4.1.5 Effect of Solution Heat Treatment on Unmixed Zone

As discussed above, it is believed that Mo segregation is the main reason for reduced localized corrosion resistance in the unmixed zone. To minimize the extent of Mo segregation and subsequently improve the localized corrosion resistance of the unmixed zone, 30 minute solution heat treatments were conducted on AL-6XN, 254SMO and 654SMO SMA BOP welds, GTA open root dissimilar welds as well as AL-6XN GTA autogenous welds at 2100°F, 2150°F and 2200°F respectively. Extensive oxidation was



(a)



(b)

Figure 28. (a). Micrograph at weld interface of CN-3MN SMA BOP weld (Inconel 112 electrode), (b). Molybdenum profile along line XY in the unmixed zone in (a).

observed on the surface of the solution treated welds at all three temperatures of 2100°F, 2150°F, and 2200°F for 30 min and an extremely rough surface condition was created mostly on the AL-6XN welds during solution heat treatment. These conditions were corrected by using a 600 grit finish on corrosion coupons extracted from these welds.

To investigate the effect of solution heat treatment on Mo segregation in the unmixed zone, metallographic evaluation of the unmixed zone was performed using optical microscopy. The specimens were extracted from the AL-6XN GTA open root welds (C-22 filler) in both the as-welded and solution heat treated conditions. Electrolytic oxalic acid was chosen for revealing the unmixed zone. The typical appearances of the unmixed zone in AL-6XN GTA open root welds (C-22 filler) for the as-welded and solution heat treated (2100°F, 30 min) condition are presented in Figures 29a and b respectively. The comparison of the unmixed zone features in AL-6XN GTA open root welds (C-22 filler) with and without solution heat treatment is shown in Figure 30 (a and b) at 100X. It is to be recognized that, after solution heat treatment , the solidification substructure in the unmixed zone is more difficult to define as compared to the unmixed zone before solution treatment. The solidification substructure is virtually "invisible" in some areas of the unmixed zone after solution treatment (2100°F for 30 min). This indicates that segregation in the unmixed zone is significantly reduced by solution heat treatment. In addition, grain growth associated with solution heat treatment is evident.

The effect of solution heat treatment on alloying element distribution in the unmixed zone was evaluated using SEM with an EDS analysis. Transverse cross-section specimens from AL-6XN, 254SMO and 654SMO (P16 filler) GTA

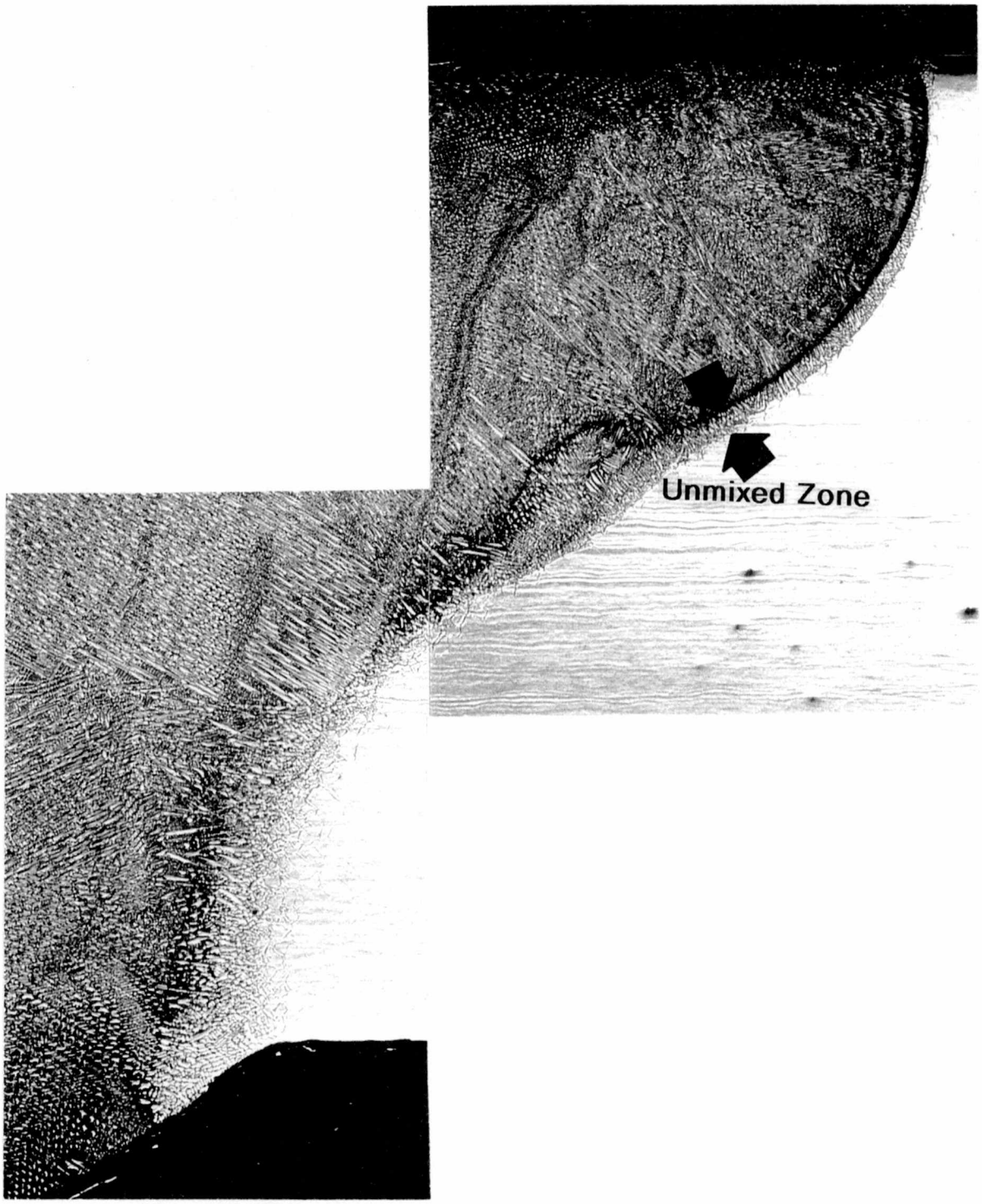


Figure 29. (a) The unmixed zone distributed along weld interface - AL-6XN GTA open root weld (C-22 filler) in the as-welded condition, transverse cross-section, 50X.

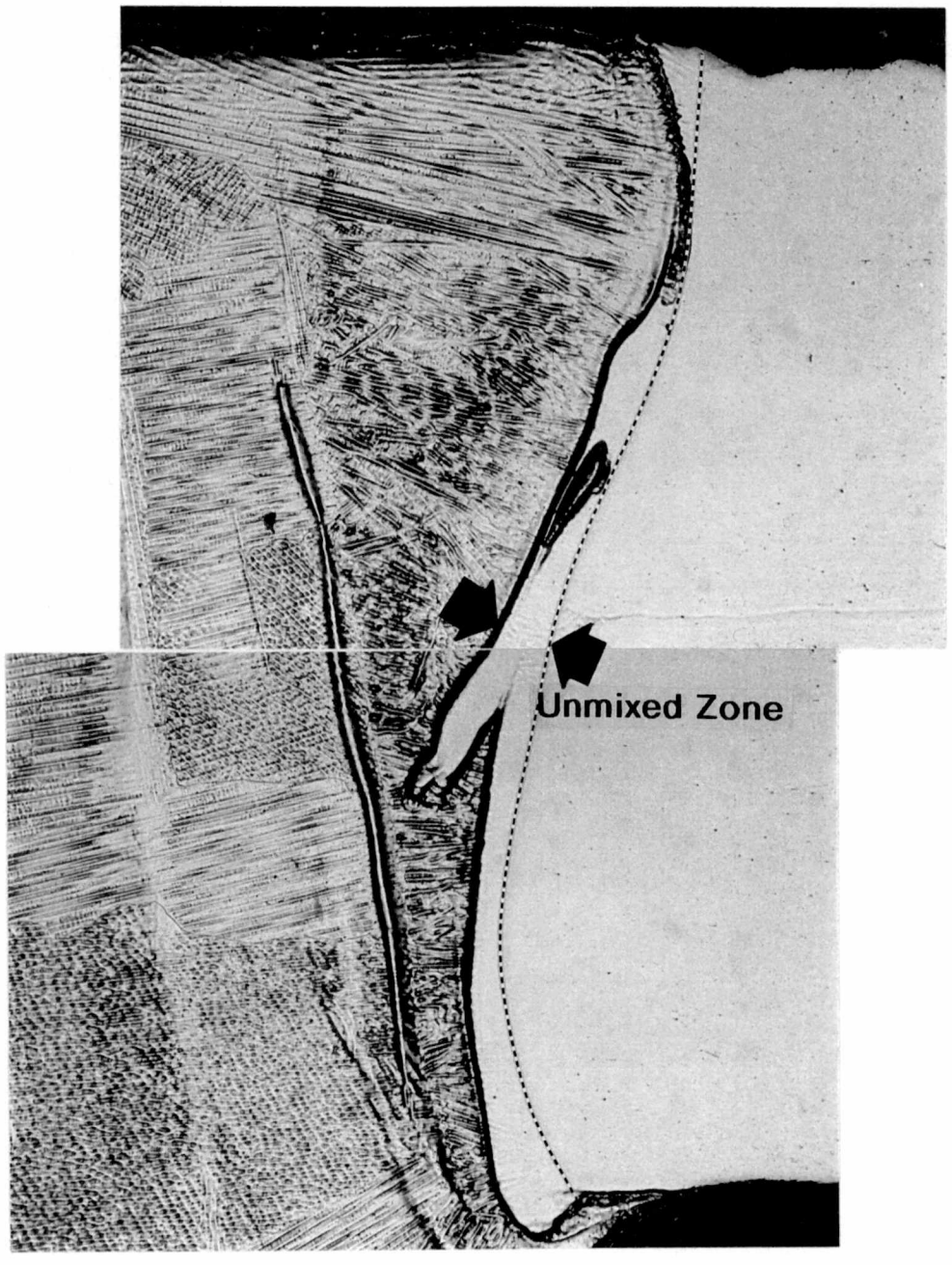


Figure 29 (cont'd). (b) AL-6XN GTA open root weld (C-22 filler) in solution heat treated condition (2100°F for 30 min), transverse cross-section, 50X.

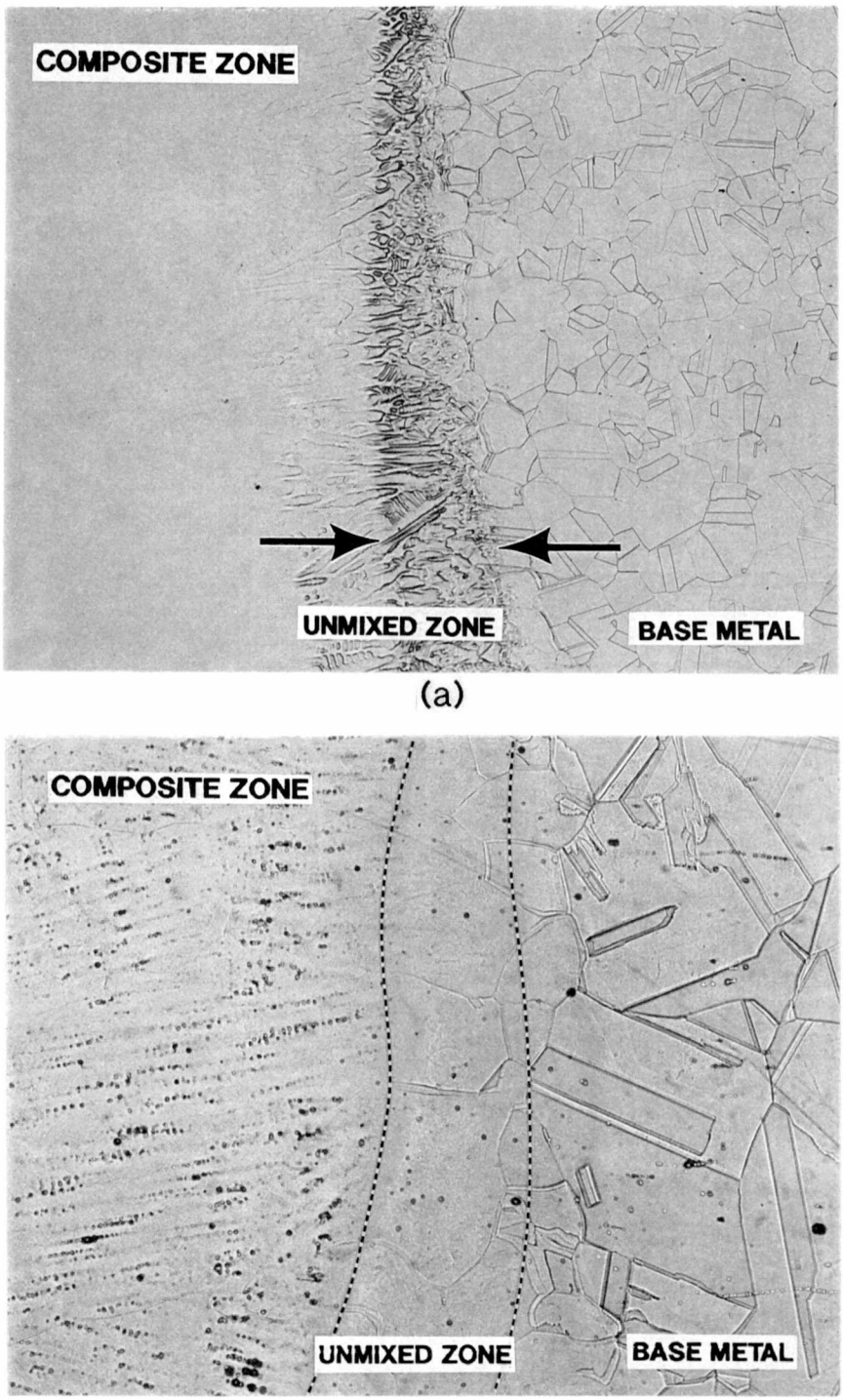
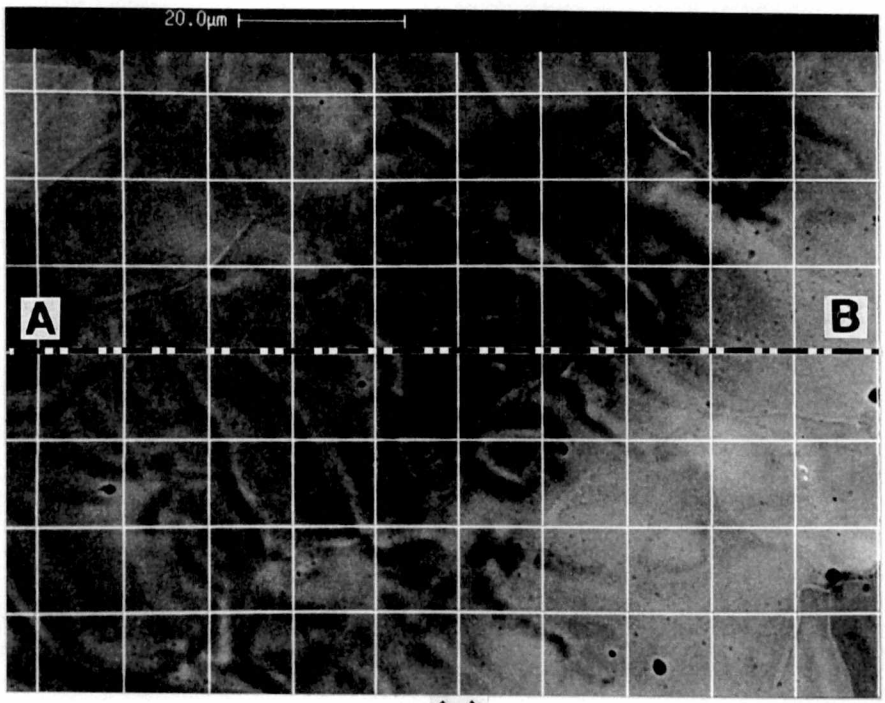


Figure 30. The unmixed zone along weld interface - AL-6XN GTA open root weld (C-22 filler) on transverse cross-section, (a) as-welded condition, (b) solution heat treated at 2100°F for 30 min, 100X.

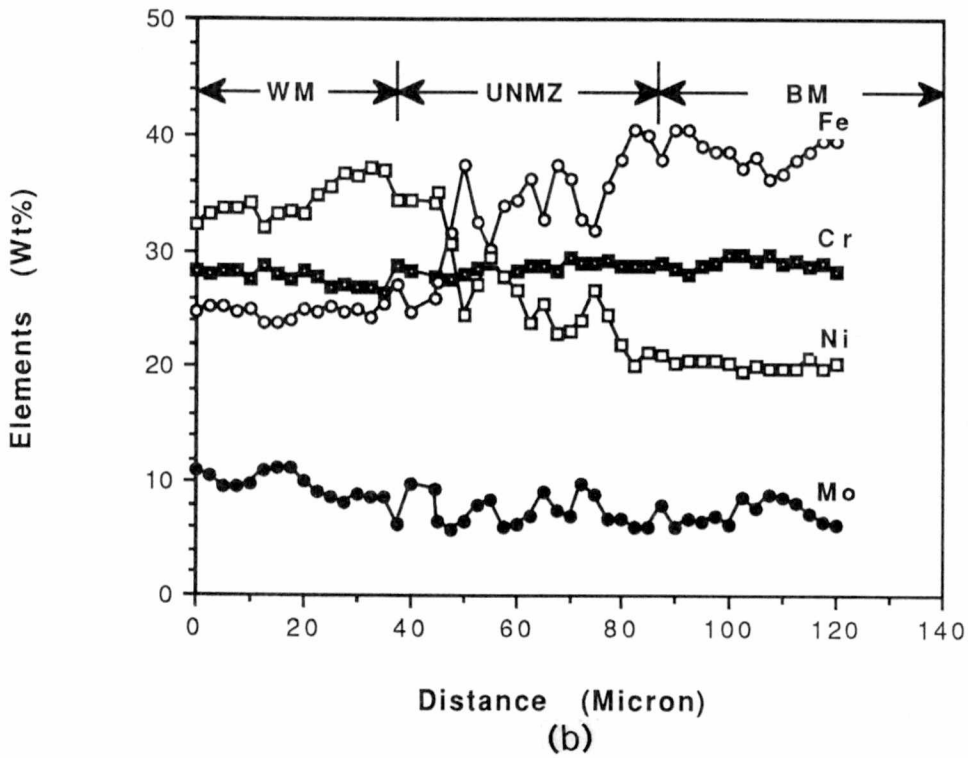
open root welds were used for EDS analysis in both the as-welded and solution heat treated (2100°F, 30 min) condition. EDS analysis on 654SMO weld gives the best example for comparison under these two conditions. SEM micrographs, at the 654SMO weld interface, are presented in Figures 31a and 32a for these two conditions. The distribution of the alloying elements across the unmixed zone was determined at 2.5 μm intervals using EDS. Figures 31b and 32b show the chemical composition profile for Ni, Cr, Mo and Fe across the unmixed zone in 654SMO weld along line AB in Figures 31a and 32a for the specimens in the as-welded and solution heat treated condition, respectively. It is evident that a 30-minute solution treatment at 2100°F for 654SMO (P16 filler) welds provides a significant homogenization of the alloying elements in the unmixed zone by diffusion. This is expected to result in a significant improvement in the localized corrosion resistance of the unmixed zone. This improvement as will be discussed in subsequent sections did indeed occur for all weldments (AL-6XN, 254SMO and 654SMO) solution treated.

4.1.6 Effect of Welding Technique on Unmixed Zone Occurrence

To investigate the influence of welding technique on the unmixed zone formation, the width of the unmixed zone for both the GMA and GTA (manual) open root welds (C-22 filler with a same heat input of 10KJ/in) was measured along weld interface on transverse cross-sections. The width distribution for the unmixed zone in the GMA and GTA welds (10 KJ/in heat input) are presented in Figure 33. It is clear that the width of the unmixed zone is greater in the GTA weld than in the GMA weld at locations near the weld face and root. In contrast, near the sheet mid-plane, the unmixed zone width in the GTA weld is less than



(a)



(b)

Figure 31. (a) SEM micrograph at weld interface of 654SMO GTA open root weld (P16 filler metal) in as-welded condition, (b) chemical profile of alloying elements along line AB in (a).

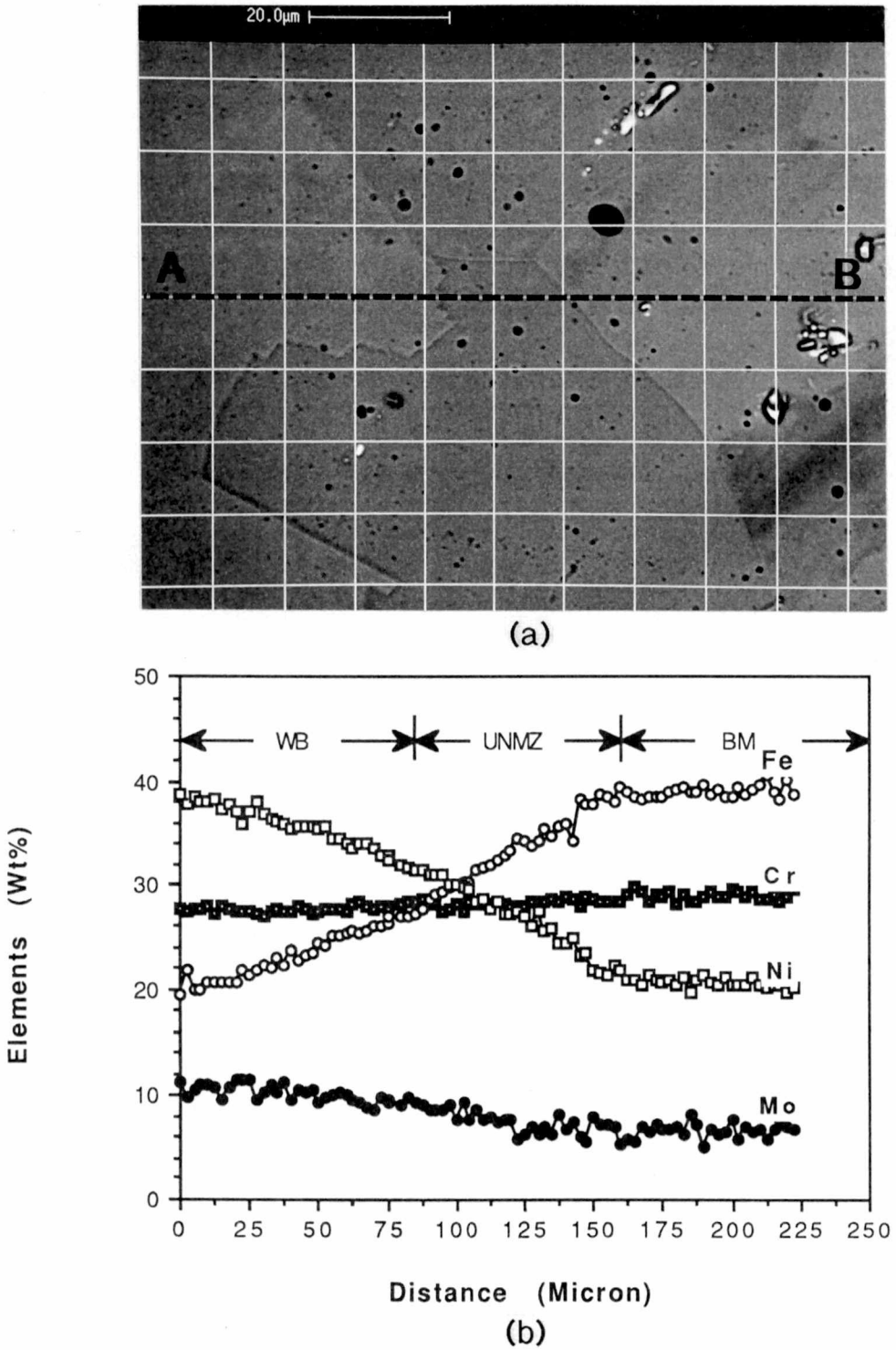


Figure 32. (a) SEM micrograph at weld interface of 654SMO GTA open root weld (P16 filler metal) after solution treatment at 2100°F for 30 min, (b) chemical profile of alloying elements along line AB in (a).

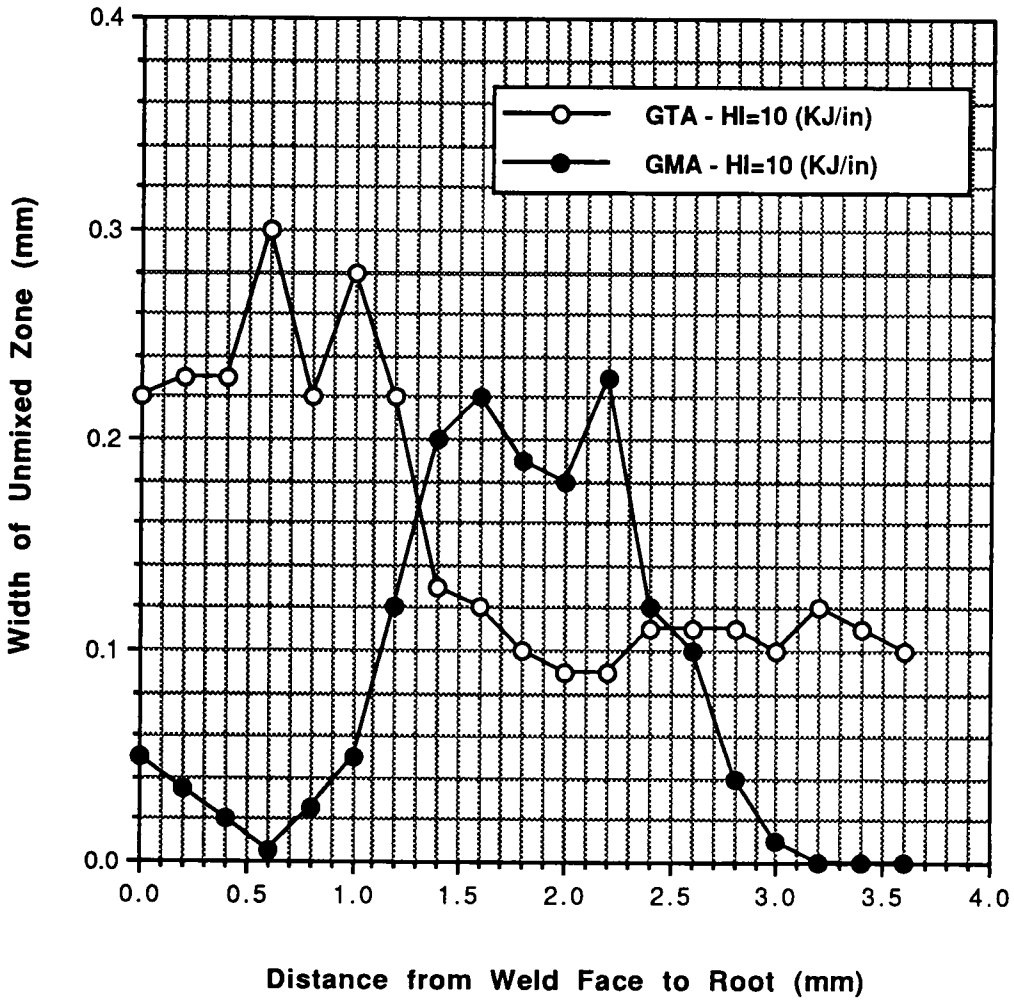


Figure 33. Width of the unmixed zone along weld interface on transverse cross-section - AL-6XN GMA open root weld (C-22 filler) and AL-6XN manual GTA open root weld (C-22 filler).

that in the GMA weld. However, the average width of the unmixed zone is greater for the GTA weld (0.17 mm) than for the GMA weld (0.09 mm) with the same heat input.

4.1.7 Summary of Evaluation of Unmixed Zone

Based on the evaluation of the unmixed zone in this study, it is evident that the unmixed zone which exists in fusion welds can be revealed using a solute sensitive etchant with proper etching techniques.

The unmixed zone formation and its distribution can be influenced by a number of factors, such as welding technique and physical properties of filler metals (melting range). The distribution of the unmixed zone along the weld interface significantly depends on these factors. For SMA BOP welds, the widest unmixed zone region was determined to be near the root of the weld and the unmixed zone barely reaches the weld face. However, in both GTA and GMA open root welds, the widest unmixed zone was observed near the sheet mid-plane. In contrast to the unmixed zone in SMA BOP welds, the unmixed zone in GTA and GMA open root welds extends to the weld face in most cases. It has also been found that the average width of the unmixed zone is greater for GTAW than for GMAW. In addition, the wider unmixed zone is created when a filler metal with melting range higher than that of the base metal is used in welding.

Depletion of Mo in the core of the cellular dendrites in the unmixed zone were found by EDS analysis. It is believed that the depletion of Mo in the unmixed zone is caused by Mo segregation during resolidification. Since Mo is the major alloying element responsible for localized corrosion resistance, Mo

segregation in the unmixed zone can result in differences in localized corrosion behavior between the unmixed zone and base metal. However, through a proper solution heat treatment, Mo segregation can be reduced, which is an effective way to improve the localized corrosion behavior of the unmixed zone.

4.2 Pitting Corrosion Behavior of Unmixed Zone

4.2.1 Critical Pitting Temperature of Unmixed Zone

• Immersion Corrosion Testing

Pitting corrosion tests were aimed at determining the critical pitting temperature of the unmixed zone in super-austenitic stainless steel weldments. Immersion corrosion tests were performed on 1" square specimens extracted from SMA BOP welded coupons (AL-6XN - C-22, Inconel 112 and 686CPT filler metals), (254SMO - C-22 filler metal) and (654SMO - P16 filler metal). Specimens from AL-6XN, 254SMO and 654SMO GTA autogenous welds and the respective base metals were tested for comparison. All corrosion specimens were polished (0.05 μm) and etched to reveal the unmixed zone before corrosion testing. Immersion corrosion tests were conducted in a 10% (dry) ferric chloride solution (pH = 1.0 at 23°C) for 24 hours at an initial test temperature of 50°C for the dissimilar welds and 40°C for the autogenous welds, respectively. Pitting tests were run with a 2 C° temperature increment from starting temperature until pits were observed under optical microscopy at 100X.

The test results are shown in Table 13. The CPTs of the unmixed zone, the autogenous fusion zone and the base metal are shown in Figure 34 as a

Table 13. The Critical Pitting Temperatures (CPT) of The Unmixed Zone, The Autogenous Fusion Zone and The Base Metals

Material	CPT (°C)			PRE_N
	UNMZ Dissimilar Weld	FZ Autogenous Weld	Base Metal	
254SMO	64	56	80	46
AL-6XN	80	60	90	48
654SMO	>101	101	>101	63

$PRE_N = [Cr\%] + 3.3*[Mo\%] + 30*[N\%]$

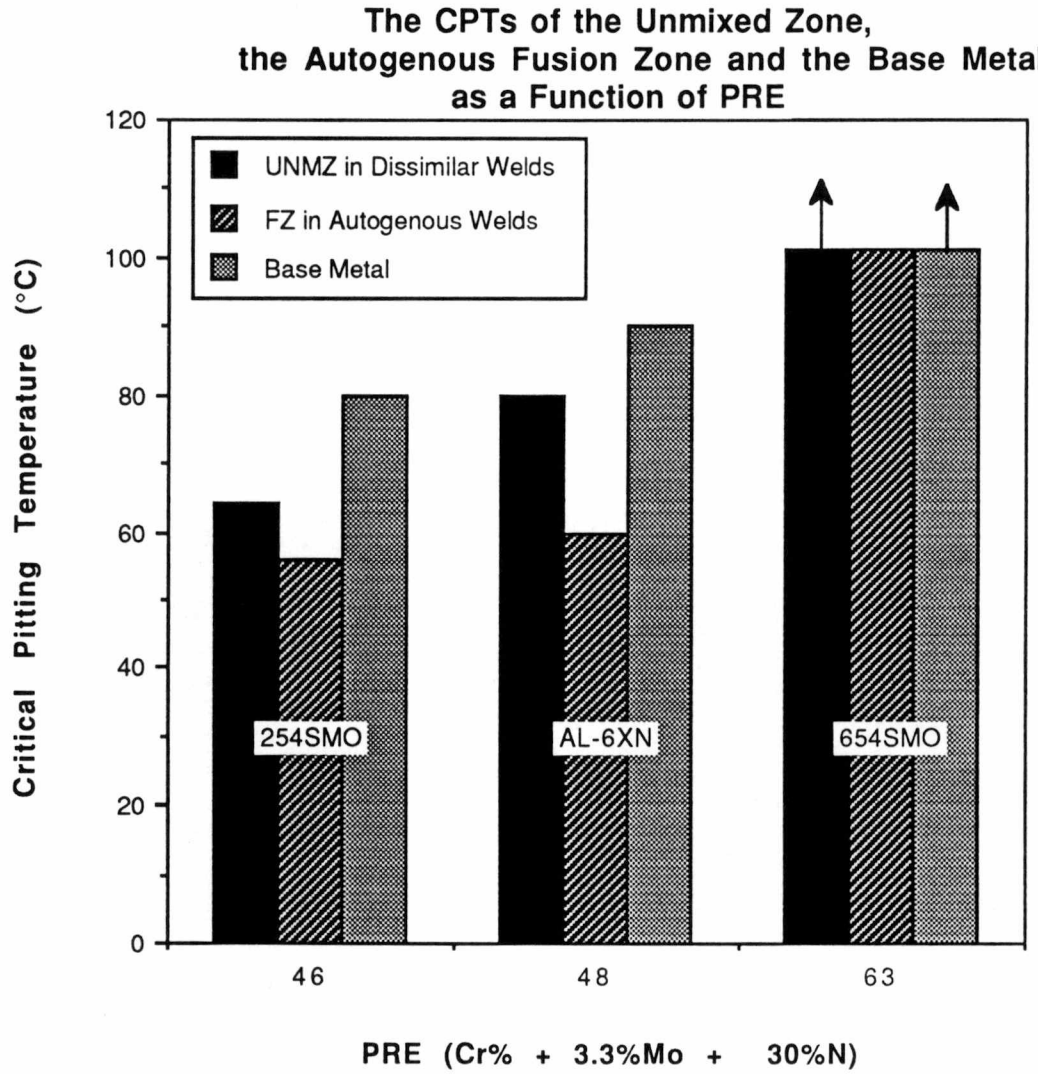


Figure 34. Critical pitting temperature of the unmixed zone as a function of pitting resistance equivalent of the base metals. (Test solution: 10% $FeCl_3$, Test time: 24 hours and surface condition: 0.05 μm).

function of the pitting resistance equivalent (PRE_N) of the respective base metals. From the CPTs vs. pitting resistance equivalent (PRE_N) in Figure 34, it is evident that the CPT of the unmixed zone increases with increasing in PRE_N of the base metals for the same type weld (dissimilar or autogenous). With the same PRE_N, the CPTs of the unmixed zone {80°C for AL-6XN, 64°C for 254SMO, >101°C (the boiling temperature of 10% $FeCl_3$ solution) for 654SMO} are lower than that of the base metal (90°C for AL-6XN, 80°C for 254SMO, >101°C for 654SMO). This indicates that the pitting corrosion resistance of the unmixed zone is inferior to that of the base metal.

However, the CPTs of the autogenous fusion zone in GTA BOP welds (60°C for AL-6XN, 56°C for 254SMO and 101°C for 654SMO) are lower than that of unmixed zone in SMA BOP dissimilar welds (80°C for AL-6XN, 64°C for 254SMO, >100°C for 654SMO). For example, the CPT of the AL-6XN autogenous fusion zone is 60°C, which is 20C° lower than the CPT of the unmixed zone in its SMA dissimilar welds. This indicates that the pitting resistance of the fusion zone in autogenous welds is not only inferior to that of the base metal but also inferior to that of the unmixed zone in dissimilar welds. (It is to be noted that the entire fusion zone of autogenous welds essentially is an unmixed zone). The diameter of cellular dendrites in the autogenous fusion zone (0.0193 mm average diameter) is larger than that in the unmixed zone (0.00625 mm average diameter). It is believed that alloying element segregation in an autogenous fusion zone is greater than that in an unmixed zone of a dissimilar weld and this may be one reason for the inferior pitting resistance in the fusion zone in autogenous welds. This significant difference in the CPT of the unmixed zone between GTA autogenous welds and SMA

dissimilar welds (C-22 and Inconel 625 filler metals) is considered important in corrosion application. This is consistent with the results obtained by Flasche and Ahluwalia for Nickel-base alloy weldments with matching composition and overalloyed filler metals [10]. However, an extensive investigation is needed to further understand the apparent differences in CPT of the unmixed zone between GTA autogenous welds and SMA dissimilar welds.

The pitting appearance of the autogenous welds tested at 60°C (CPT of AL-6XN autogenous fusion zone) is shown in Figure 35, while the pitting appearance of the AL-6XN dissimilar welds tested at 80°C (CPT of the unmixed zone in AL-6XN dissimilar weld) is shown in Figure 36. It is evident that pitting occurs at the core of the cellular dendrites in the unmixed zone, as well as in the autogenous fusion zone. It was determined, by EDS analysis, that the core of a cellular dendrite has the lowest Mo content in the unmixed zone. Thus, the core of the cellular dendrite in the unmixed zone has a lower pitting resistance than the other unmixed zone microstructural locations. The further investigation of pit initiation and propagation behavior in the unmixed zone will be discussed in the section 4.2.2.

• Electrochemical Corrosion Testing

In addition to determining the CPT of the unmixed zone by immersion corrosion testing, a cyclic polarization scanning technique was utilized to confirm the pitting corrosion resistance of the unmixed zone. For cyclic polarization scanning tests, specimens, 1" square, were extracted from an AL-6XN SMA BOP weld with C-22 filler and an AL-6XN autogenous GTA weld. Before testing, the specimens were polished to 0.05 μm and etched

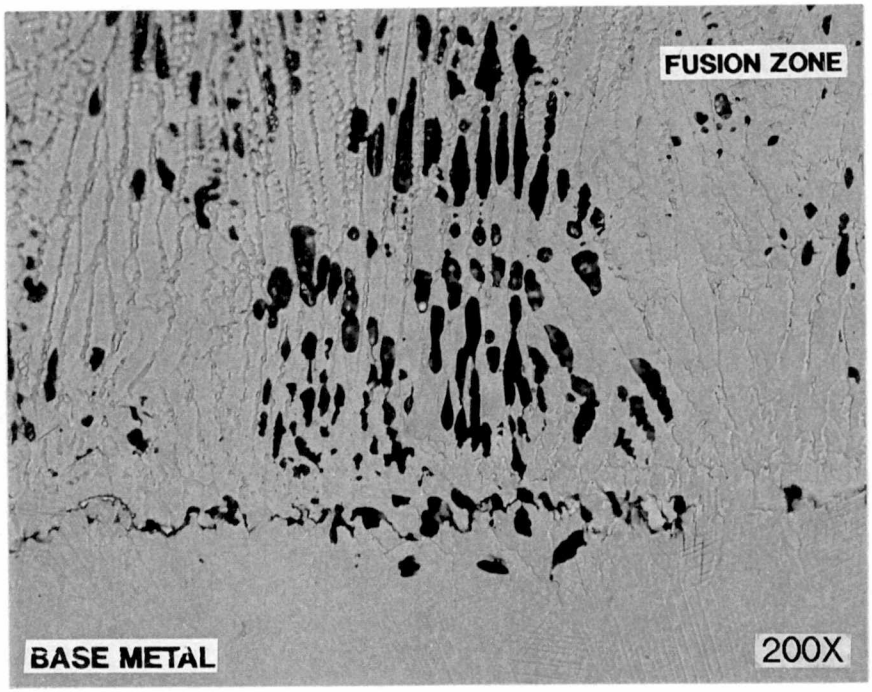


Figure 35. Pitted sample surface of AL-6XN SMA BOP autogenous weld - Test solution: 10% $FeCl_3$, test time: 24 hours, test temperature: 60°C.

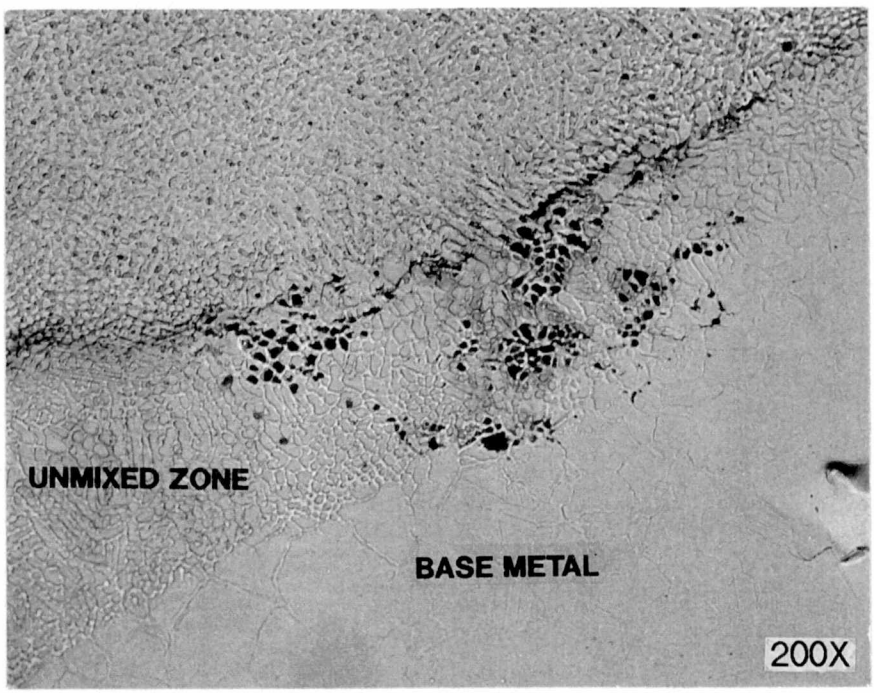


Figure 36. Pitted sample surface of AL-6XN SMA BOP weld (C-22 filler metal) - Test solution: 10% $FeCl_3$, test time: 24 hours, test temperature: 80°C.

electrolytically with oxalic acid to determine the extent of the unmixed zone. The specimen surface, except for a 1cm^2 test region, was covered with amercoat epoxy prior to testing. The selected area for cyclic polarization analysis was prepared with the following surface conditions:

1) dissimilar weld without unmixed zone on the surface

2) dissimilar weld with unmixed zone on the surface

3) autogenous weld fusion zone on the surface only

4) base metal

Cyclic polarization data were measured using a computer controlled EG & G model 273 potentiostat. The test cell was used with a saturated (KCl) silver/silver-chloride reference electrode and a electrolyte test solution (6% $FeCl_3$, 2 liters) which was kept aerated. All electrochemical measurements were made at 23°C (room temperature). Test parameters were as follows:

Initial potential E = -35 mv (vs E_{corr}).

Vertex potential E = 800 mv (vs E_{corr}).

Final potential E = E_{corr} -20 mv (vs R).

Scan rate 0.17 mv/s.

Cyclic polarization curves for the specimens with above four selected conditions are presented in Figures 37 through 39. The values of E_{corr} (mV), apparent E_B (mV) (since O_2 may evolution at the same time), E_p (mV), i_p ($\mu A/cm^2$), and hysteresis loop area ($mV \cdot \mu A/cm^2$) are listed in Table 14.

The cyclic polarization curve of the AL-6XN dissimilar weld with the unmixed zone exposed on the surface is shown in Figure 37 in comparison to the AL-6XN base metal. Since the corrosion potential of both specimens ($E_{corr,BM}$ = 480 mv, $E_{corr\ UNMZ}$ = 460 mv) are lower than their protection potential

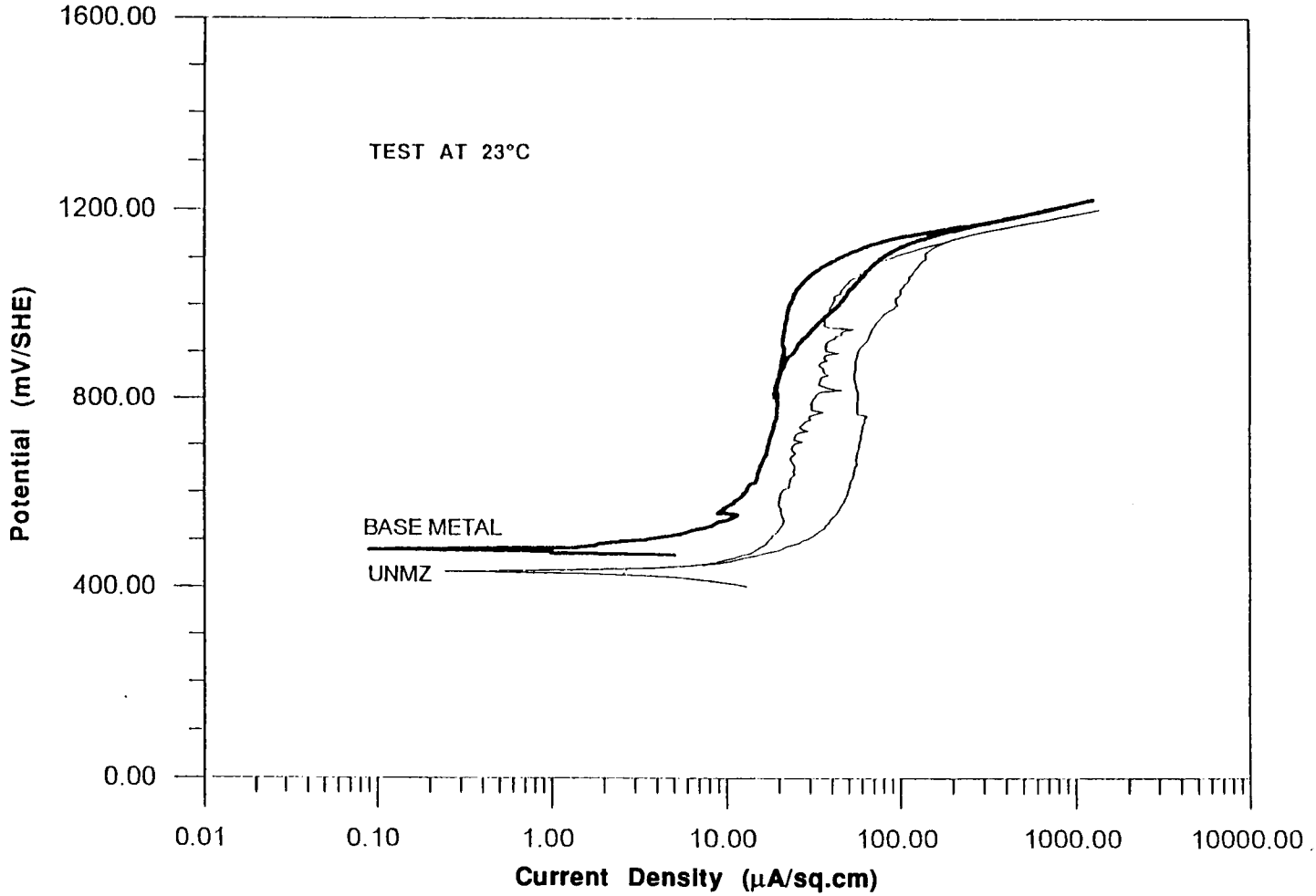


Figure 37. Cyclic polarization curve of AL-6XN dissimilar welded specimen with the unmixed zone on surface in comparison with that of AL-6XN un-welded base metal.

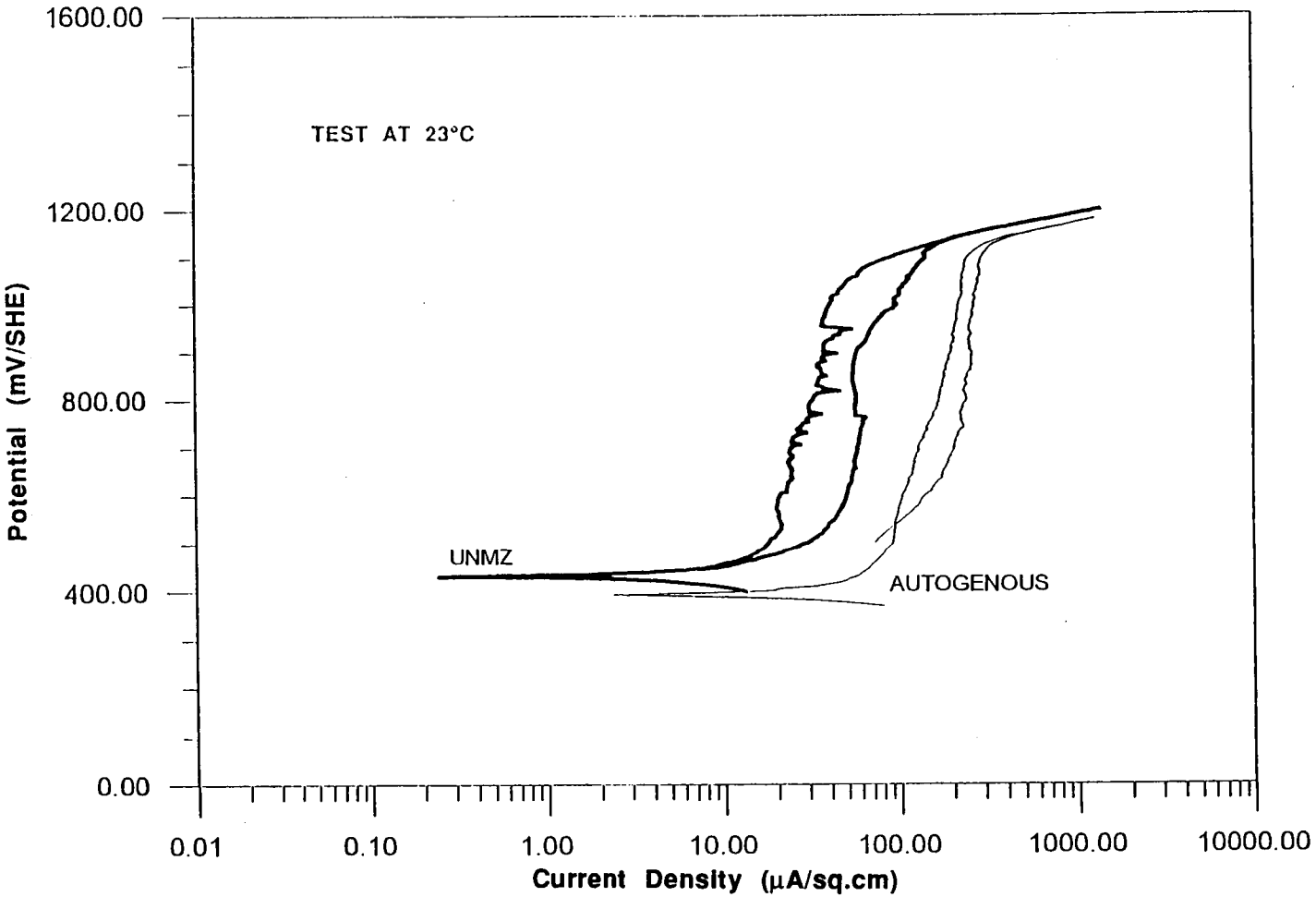


Figure 38. Cyclic polarization curve of AL-6XN autogenous fusion zone in comparison with that of the dissimilar welded specimen with the unmixed zone on the surface.

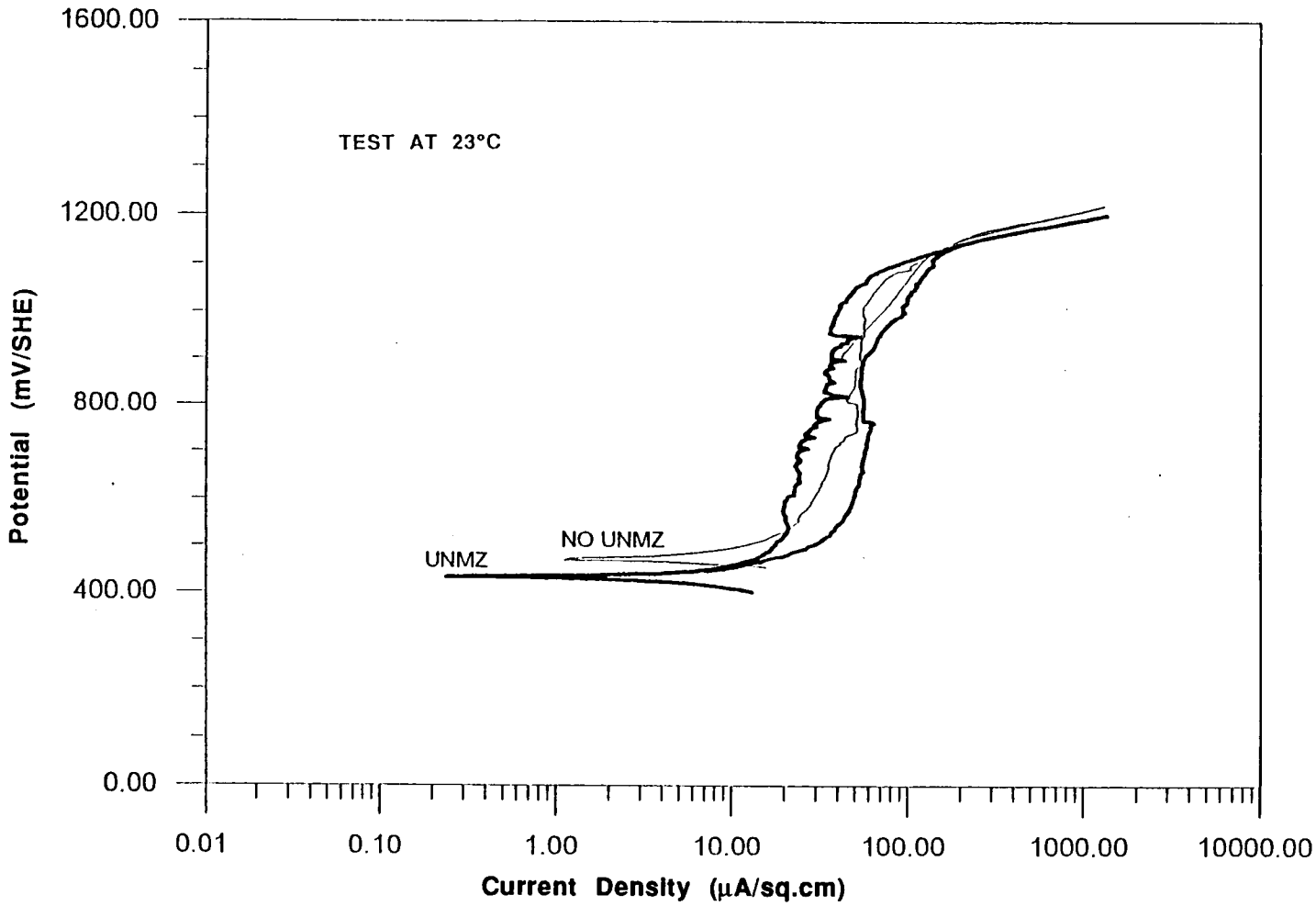


Figure 39. Cyclic polarization curve of AL-6XN dissimilar welded specimen with the unmixed zone on surface in comparison with that of AL-6XN dissimilar welded specimen without the unmixed zone on surface.

Table 14. The Results of Polarization Scanning Test

Specimens	E_{corr} (mv)	(apparent) E_B (mv)	E_p (mv)	i_p ($\mu A/cm^2$)	Loop Area ($mV \cdot \mu A/cm^2$)
Base Metal	480	≈ 1100	900	15	129
Dissimilar Weld Without UNMZ	460	≈ 1100	950	25	26
Dissimilar Weld With UNMZ	430	≈ 1100	450	20	414
Autogenous Fusion Zone	400	≈ 1100	550	90	159

($E_{p,BM}$ = 900 mv, $E_{p\ UNMZ}$ = 450 mv), no pitting initiated on the samples under the test conditions (23°C, 6% $FeCl_3$ solution). With an increase in potential as shown in Figure 37, however, it is evident that the two specimens exhibit a different localized corrosion tendency. The cyclic polarization curve of the AL-6XN dissimilar weld with the unmixed zone exposed on the surface generates a larger hysteresis loop (Loop area $_{UNMZ}$ = 414 mV•μA/cm^2) and higher passive current density ($i_{p\ UNMZ}$ = 20 μA/cm^2) compared to the AL-6XN base metal (Loop area $_{BM}$ = 129 mV•μA/cm^2, $i_{p\ BM}$ = 15 μA/cm^2). This behavior implies that the specimen with the unmixed zone exposed on the surface shows a greater susceptibility to pitting corrosion and is more difficult to re-passivate than the base metal. Thus, the unmixed zone again has been shown to induce a lower pitting corrosion resistance compared to the base metal.

In the case of the autogenous weld fusion zone, the cyclic polarization curve is presented in Figure 38 compared with that of the AL-6XN dissimilar weld with the unmixed zone exposed on the surface. The cyclic polarization curve of the autogenous fusion zone shows a higher passive current density ($i_{p,\ auto}$ = 90 μA/cm$_2$ > $i_{p\ UNMZ}$ = 20 μA/cm^2) in addition to a hysteresis loop area of 159 mV•μA/cm^2, which indicates that the passive film on the autogenous fusion zone is less stable than that on the specimen with the unmixed zone exposed on the surface, thus, resulting in the greater susceptibility of the autogenous fusion zone to pitting corrosion and greater difficulty in re-passivation than that of the dissimilar metal weld unmixed zone.

Compared to the dissimilar welds with the unmixed zone exposed on the surface, the cyclic polarization curve of the dissimilar weld without an unmixed zone on the surface presents a much smaller hysteresis loop (loop area $_{No\text{-}UNMZ}$

= 26 mV•μA/cm^2 < Loop area $_{UNMZ}$ = 414 mV•μA/cm^2), in addition to a similar passive current density ($i_{p\ NO\text{-}UNMZ}$ = 25 μA/cm^2) as shown in Figure 39. This behavior implies that pits can be more easily re-passivated on a surface without the existence of a unmixed zone than on the surface with the unmixed zone exposed.

In summary, the cyclic polarization test results show that the unmixed zone in an AL-6XN dissimilar weld has a inferior pitting resistance compared to that of respective base metal. However, the pitting resistance of the autogenous fusion zone is worse than that of the dissimilar weld unmixed zone. These results are consistent with the previous immersion pitting corrosion test results .

4.2.2 Pit Initiation and Propagation Behavior in Unmixed Zone

Pit initiation and propagation behavior was investigated on AL-6XN SMA BOP welds (C-22 filler) in 10% $FeCl_3$ solution at 80°C as a function of test time. It is to be noted that a CPT of 80°C was determined for the unmixed zone in AL-6XN welds with 0.05 μm polished surface. 1" square specimens extracted from AL-6XN SMA BOP welds (C-22 filler) were used for this study. Specimens were polished to 0.05 μm and etched electrolytically with oxalic acid to reveal the unmixed zone in the face orientation before pitting tests. During the test, the specimens were vertically oriented in the test solution with the weld horizontal. Test temperature was maintained at 80°C. Pit initiation and propagation behavior was examined using optical microscopy. Figures 40 through 44 show pit morphology for test times of 2, 4, 30, 60 and 720 minutes. It is clear that only 2 minutes are needed for pits to initiate in the core of the cellular dendrites in the unmixed zone. At this stage, the intercellular dendritic regions remain un-

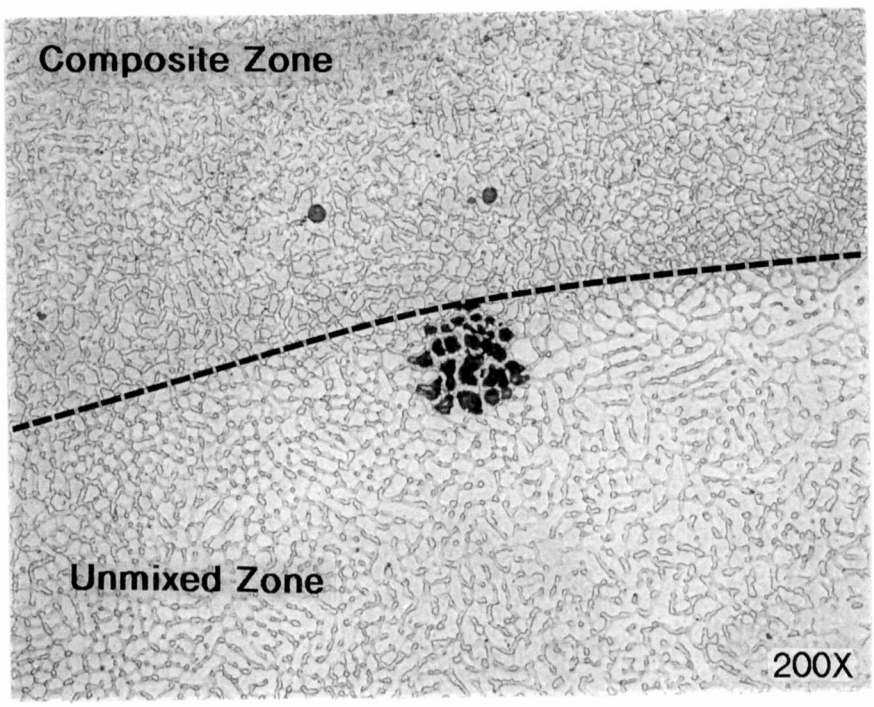


Figure 40. Pit initiation in the core of the cellular dendrite in the unmixed zone after 2 minutes in 10% $FeCl_3$ solution, 200X.

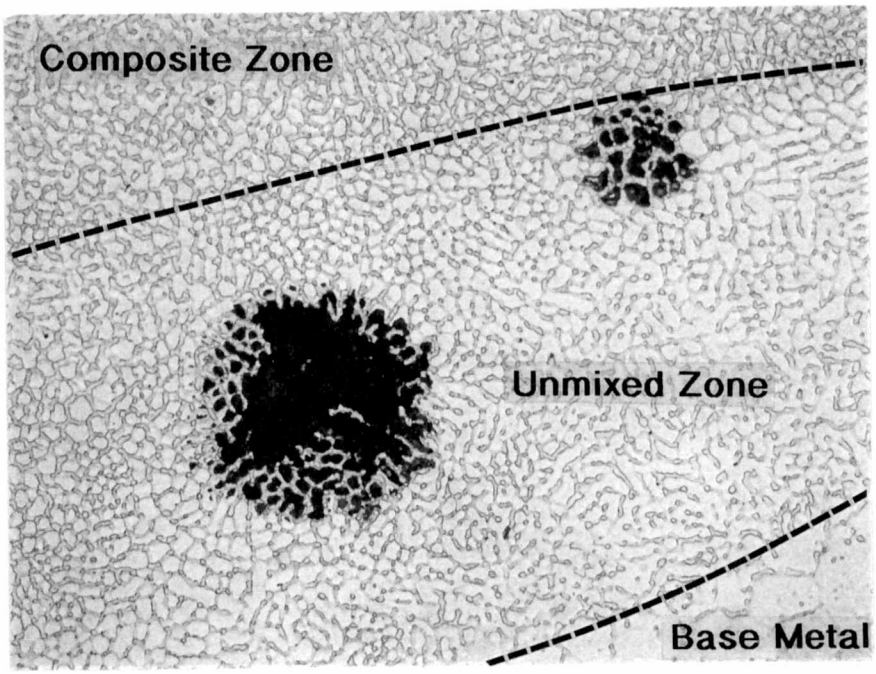


Figure 41. Pit propagation in the unmixed zone after 4 minutes in 10% $FeCl_3$ solution, 200X.

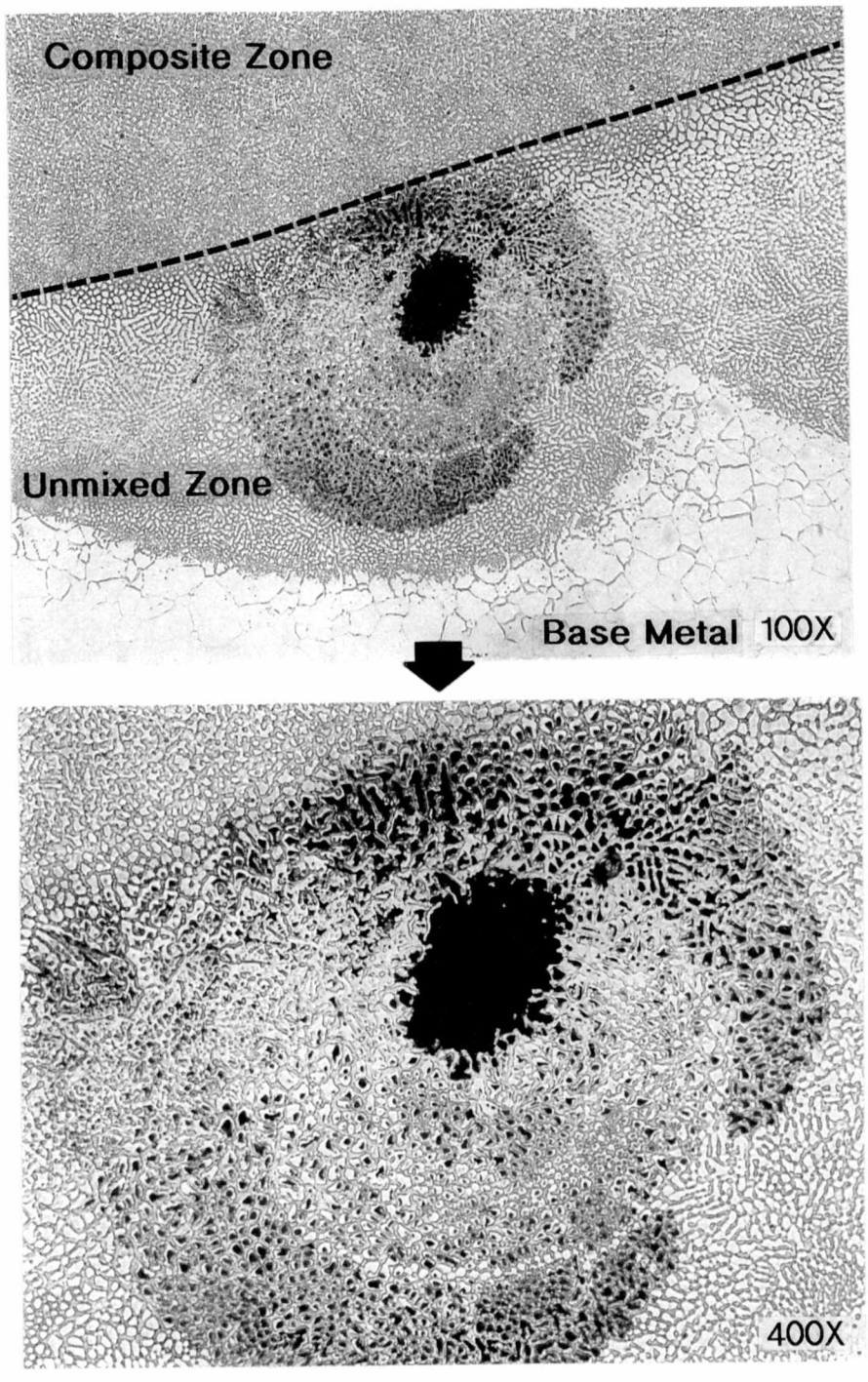


Figure 42. (a) Pit propagation in the unmixed zone after 30 minutes in 10% $FeCl_3$ solution, top view.

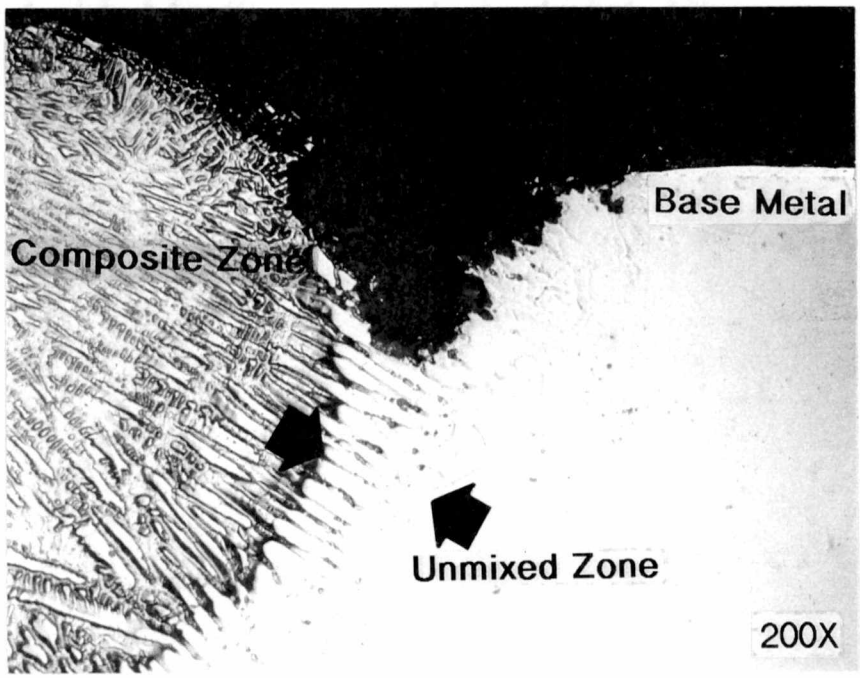


Figure 42. (b) Pit propagation in the unmixed zone, transverse cross-section, 80°C after 30 minutes in 10% $FeCl_3$ solution, 200X.

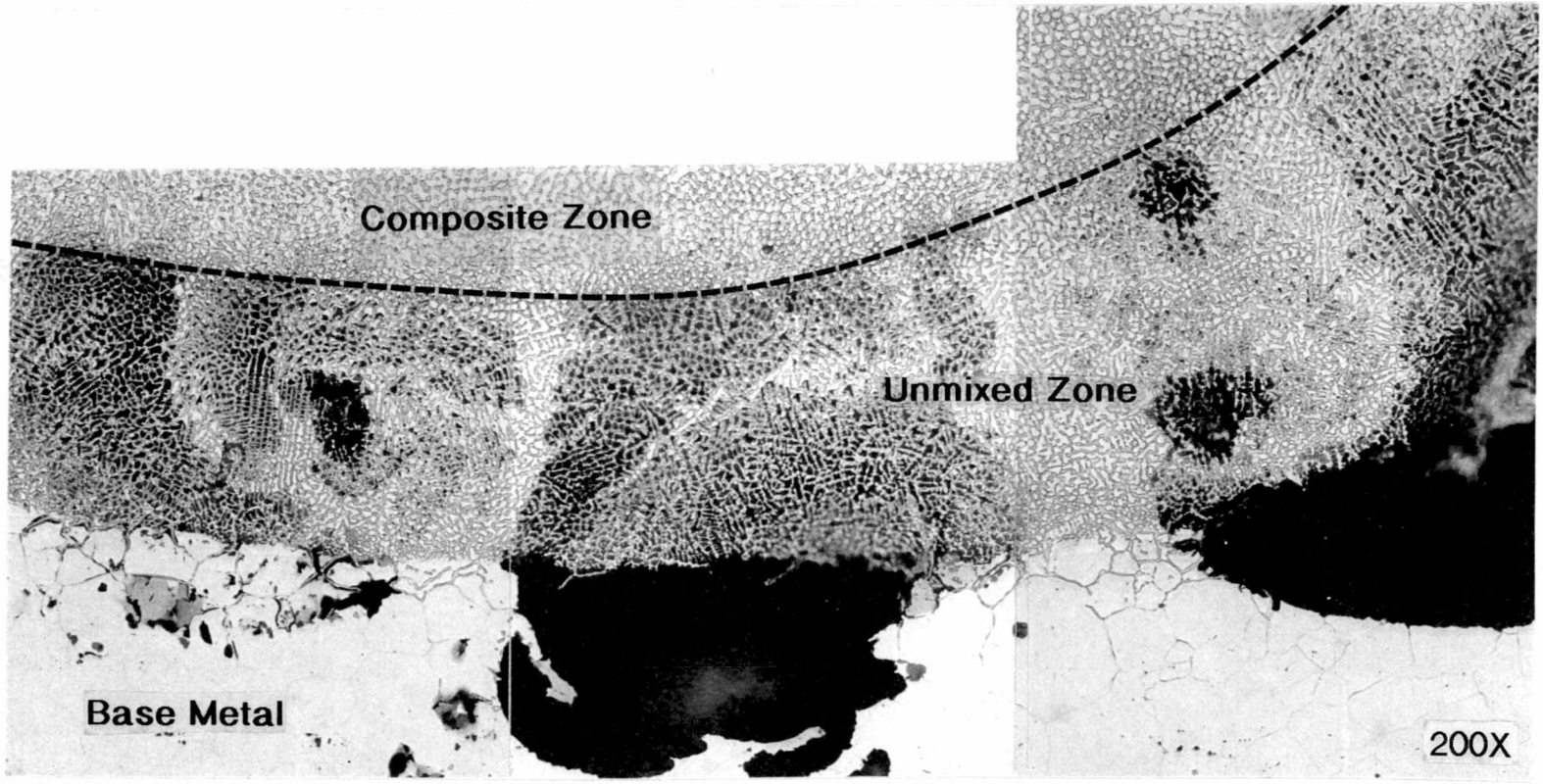


Figure 43. Pit propagation in the unmixed zone after 60 minutes in 10% $FeCl_3$ solution, top view.

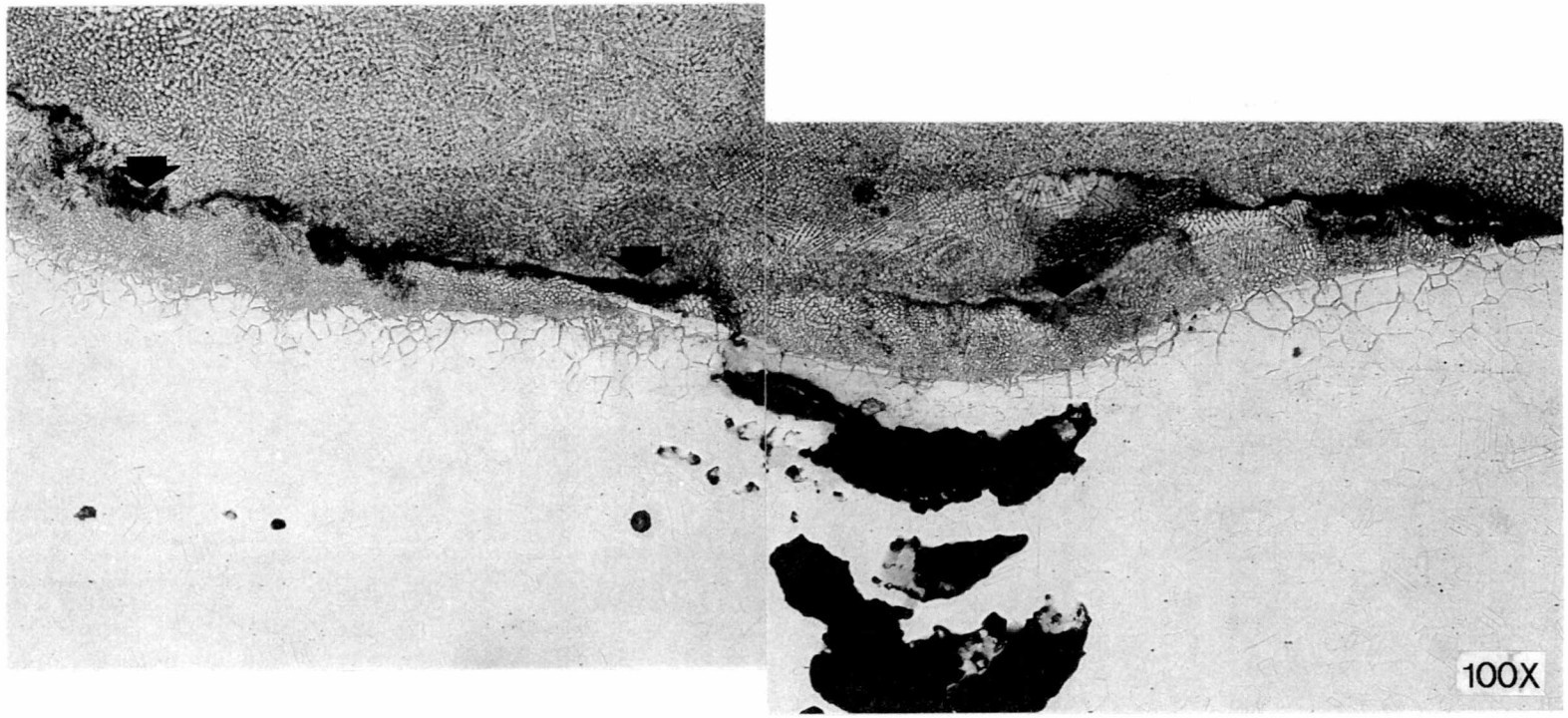


Figure 44. Pit propagation in the unmixed zone after 720 minutes in 10% $FeCl_3$ solution, top view.

corroded (see Figure 40). After 4 minutes, the intercellular dendritic regions begin to corrode with some additional pit initiation in the adjacent regions (see Figure 41). When the cellular dendrite boundaries corrode, a major pit is formed by connecting several adjacent pits. Then the major pit acts as a main channel for further corrosion.

After 30 minutes, the number of the pits in the core of the cellular dendrites surrounding the major pit is significantly increased (see Figure 42a) in comparison with the 4 minute test. Through the major pit, extensive corrosion under the sample surface is evident. It is believed that pit propagation mainly occurs underneath the sample surface through the major pit. For further evaluation of the pit propagation behavior, the tested specimen (at 80°C for 30 minutes) was transversely sectioned across the center of the corroded area to study the morphology beneath the surface. The pit propagation appearance beneath the surface on a transverse cross-section is shown in Figure 42b. It is evident that after the major pit was formed, pit propagation was concentrated underneath the surface. A typical "cave" propagation behavior is characterized by pit propagation in the unmixed zone. It is believed that this cave propagation behavior is related to the fact that the rough corroded metal surfaces in the "cave" enhance the corrosion rate. Thus, a significant fraction amount of pits observed on the surface surrounding the major pit were not initiated from the 0.05 μm finished outside surface but were formed by corrosion from underneath surface.

With an increase in test time to 60 minutes, several major pits were formed in the unmixed zone and a significant increase in the number of pits was observed as shown in Figure 43. At the same time, corrosion propagated into

the base metal. After 720 minutes, almost the entire unmixed zone was corroded as illustrated in Figure 44. Also, further propagation in the base metal is evident.

Based on the evaluation results above, pit initiation and propagation behavior can be modeled in the following steps:

Step. 1: Pits initiate at the core of the cellular dendrites in the unmixed zone. The boundaries of the cellular dendrites remained un-corroded.

Step. 2: With increasing time, the cellular dendrite boundaries in the corroded area are attacked and a major pit forms (which will act as a channel for further corrosion).

Step. 3: After the major pit is formed, pit propagation is concentrated beneath the surface with a typical "cave propagation" behavior.

Step 4: After a certain extent of "cave propagation" beneath the surface, corrosion breaks the surface through additional corrosion paths in the core of the cellular dendrites.

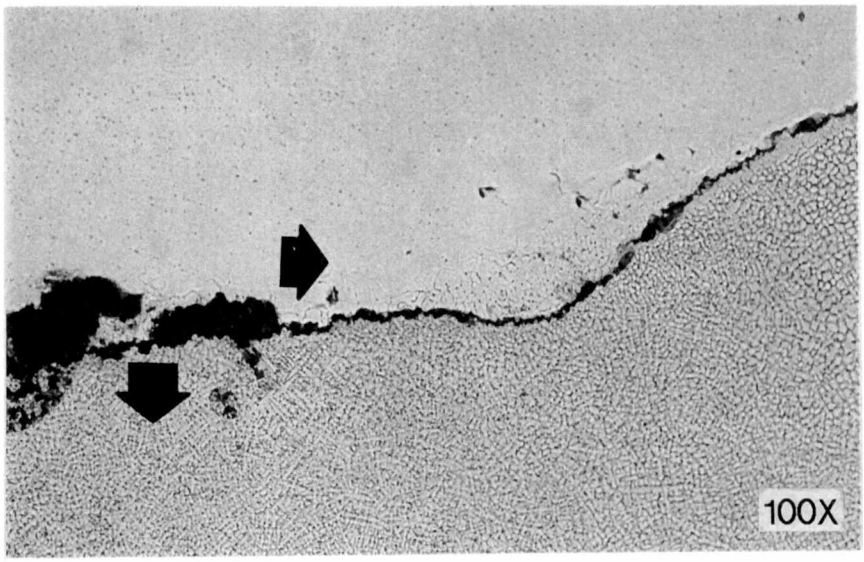
Pit propagation orientation was investigated using 1" square specimens extracted from the AL-6XN SMA BOP weld (C-22 electrodes) with a 0.05 μm surface finish. Prior to pitting tests, specimens were electrolytically etched with oxalic acid to reveal the unmixed zone in the face orientation. The specimens were placed vertically in the solution. The weld was oriented both horizontally and vertically to study the relationship between the specimen orientation and pit propagation direction. After 60 minutes in 10% $FeCl_3$ at 80°C, the specimens were metallographically examined using optical microscopy.

Figure 45a and b show pit propagation in the unmixed zone for the specimen with weld horizontal and vertical, respectively. With the weld horizontal, it is evident that pits initiated in the unmixed zone and then propagated downward vertically into the base metal. No upward propagation into the weld metal was observed (see Figure 45a). With the weld vertical, pits initiated in the unmixed zone and then propagated vertically downward along the entire unmixed zone (see Figure 45b). Thus, in terms of pit propagation orientation, it can be concluded that pits are always oriented vertically downward, independent of the weld or base metal orientation.

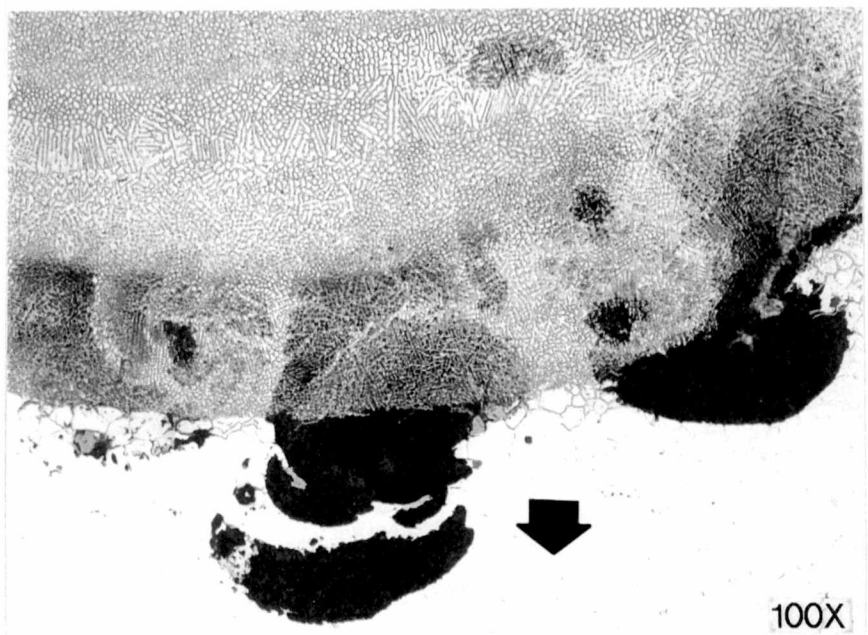
4.2.3 Effect of Solution Heat Treatment on Pitting Behavior of Unmixed Zone

It is believed that Mo segregation, during solidification of the unmixed zone, is the main reason for reduced localized corrosion resistance of this region. In order to reduce the extent of Mo segregation (and other elements), solution treatment was conducted on SMA BOP welds {AL-6XN (C-22 filler), 254SMO (C-22 filler), 654SMO (P16)} and GTA BOP AL-6XN autogenous welds. Based on the calculated time-temperature curve (see Figure 13), 30 min was selected for solution treatment at temperatures of 2100°F, 2150°F and 2200°F. Solution heat treatments were conducted in air and followed by water quenching.

Pitting tests were conducted in 10% $FeCl_3$ for 24 hours on 1" square specimens extracted from the solution treated (2100°F, 2150°F and 2200°F, 30 min) AL-6XN (C-22 filler), 254SMO (C-22 filler), 654SMO (P16 filler) SMA BOP dissimilar welds and AL-6XN GTA BOP autogenous welds. To eliminate the



(a)



(b)

Figure 45. AL-6XN SMA BOP welded specimen after 60 minutes in 10% $FeCl_3$ solution at 80°C with the weld oriented horizontally. (a). Pit propagation in upper unmixed zone. (b). Pit propagation in lower unmixed zone.

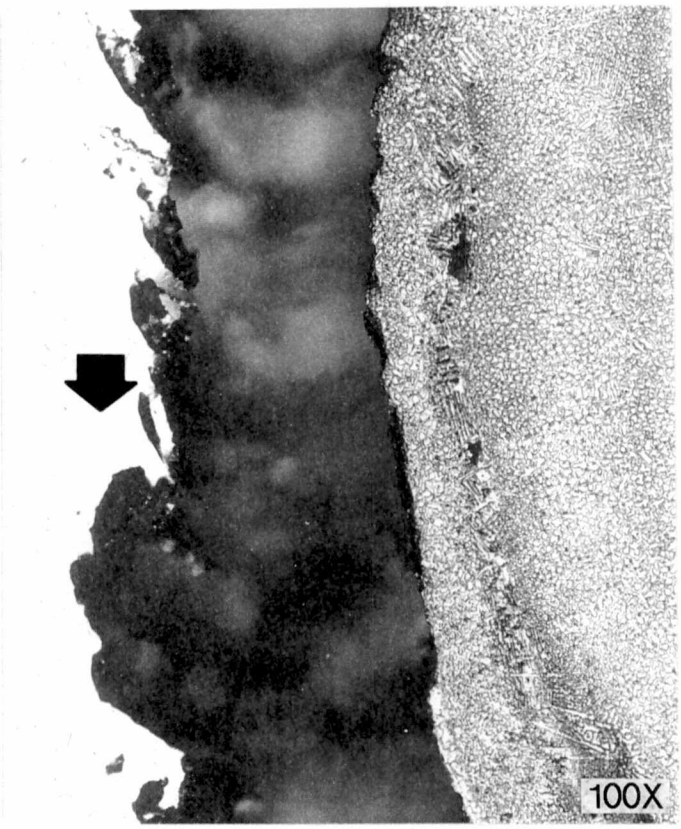


Figure 45 (cont'd). (c). AL-6XN SMA BOP welded specimen after 60 minutes in 10% $FeCl_3$ solution at 80°C with the weld oriented vertically.

influence of surface oxidation, a 600 grit surface was used in testing. For comparison of the pitting corrosion behavior of the unmixed zone between the as-welded and solution treated conditions, specimens in the as-welded condition were also tested. Pitting tests were conducted at the unmixed zone CPT (measured on 0.05 μm surface for as-welded condition) for each weld (80°C for the unmixed zone in AL-6XN SMA BOP dissimilar welds, 64°C for the unmixed zone in 254SMO SMA BOP dissimilar welds, >101°C for 654SMO SMA BOP dissimilar welds and 60°C for the fusion zone in AL-6XN GTA BOP autogenous welds).

The pitting test results for AL-6XN GTA BOP autogenous welds are shown in Figures 46 (a and b) and 47 (a, b and c) for the as-welded specimens and the solution heat treated specimen (at 2100°F, 2150°F, and 2200°F for 30 min), respectively. For the specimens in the as-welded condition, pitting occurred over the entire fusion zone of the autogenous weld, and no pitting was observed in the base metal (see Figure 46a and b). In contrast, for the specimens in solution treated condition (2100°F, 2150°F, and 2200°F for 30 min), no pitting corrosion occurred in either the fusion zone or the base metal (see Figure 47a, b and c). It is evident that after solution treatments, pitting corrosion resistance of the fusion zone in AL-6XN autogenous welds is significantly improved. For further evaluation, the CPTs were determined using specimens with 600 grit surface finish (in 10% $FeCl_3$ for 24 hours) for the AL-6XN autogenous fusion zone in both the as-welded and solution treated conditions (2100°F and 2200°F, 30 min) and for AL-6XN base metal. A CPT of 50°C was determined for the AL-6XN autogenous fusion zone in the as-welded condition, 82°C for the AL-6XN autogenous fusion zone in the solution treated

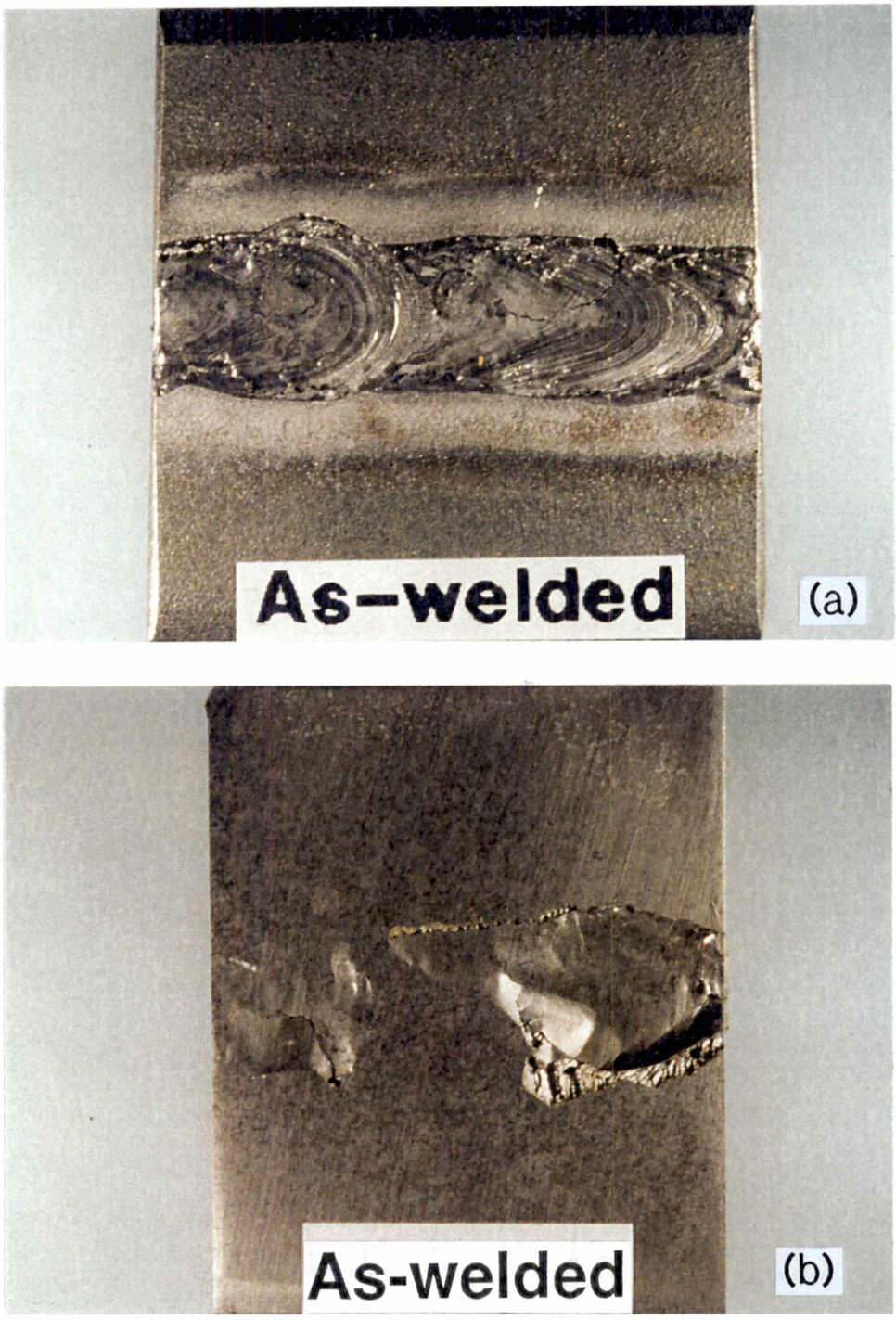


Figure 46. Pitting corrosion tested specimen - AL-6XN autogenous GTA BOP weld without solution heat treated, test at 60 °C for 24 hours in 10% $FeCl_3$ solution. (a). as-welded surface, (b). 600 grit surface.

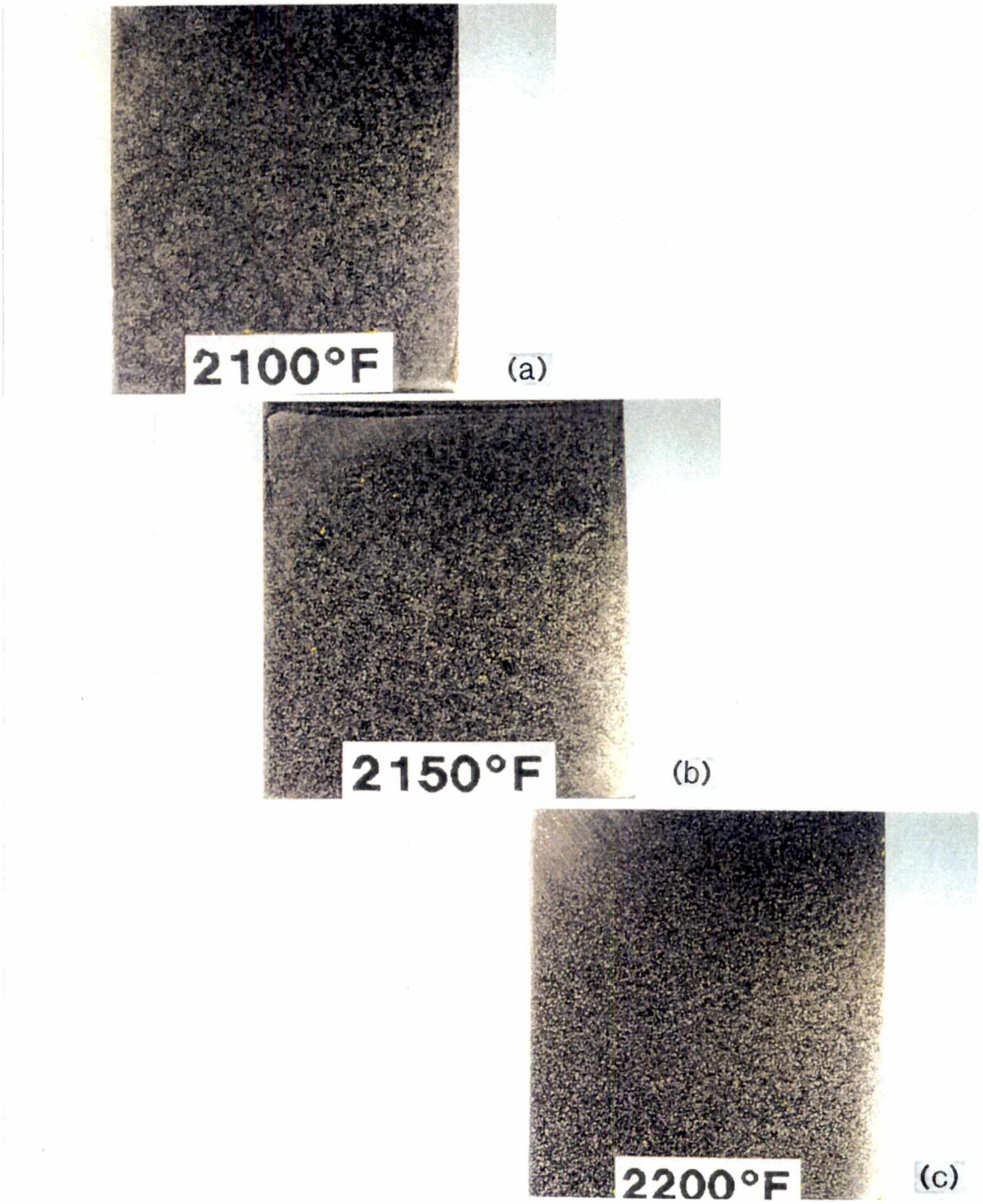


Figure 47. Pitting corrosion tested specimen - AL-6XN autogenous GTA BOP weld with 600 grit surface, solution heat treated at (a). 2100°F, (b). 2150 °F and (c). 2200°F, test at 60 °C for 24 hours in 10% $FeCl_3$ solution.

condition and 88°C for the AL-6XN base metal. It is evident that solution treatment at both 2100°F and 2200°F for 30 min. increases the CPT of the fusion zone is 32 C° over that of the fusion zone in the as-welded condition. Note that the CPT (82°C) of the fusion zone in the solution treated condition is only 6C° lower than that of the base metal. Thus, it is concluded that solution treatment significantly improves the pitting corrosion resistance of the fusion zone in autogenous welds.

Since the autogenous fusion zone has characteristics similar to the unmixed zone in dissimilar welds, it is expected that solution treatment can also affect in improving pitting corrosion resistance of the unmixed zone in dissimilar welds. As an example, pitting corrosion test results for the unmixed zone in solution treated AL-6XN SMA BOP dissimilar welds are discussed below.

Figures 48 (a and b) and 49 (a, b and c) show the pitting test results for AL-6XN SMA BOP welds (C-22 filler) in the as-welded and solution treated condition respectively. It is evident that, without solution treatment, the entire unmixed zone was pitted (as-welded and 600 grit surface, see Figure 48a and b). However, after solution treatment at 2100°F, 2150°F and 2200°F, no pitting was found in any weldment region (600 grit, see Figure 49a, b and c). Comparing the pitting behavior of the unmixed zone in AL-6XN SMA BOP welds (C-22 filler) before and after solution treatment, it is evident that the pitting resistance of the unmixed zone, as expected, is substantially improved by solution treatment (through the reduction in segregation extent of alloying elements by diffusion). CPTs for the unmixed zone in AL-6XN dissimilar welds in both the as-welded and solution treated conditions (2100°F and 2200°F, 30 min) were determined in 10% $FeCl_3$ (24 hours, 600 grit surface finish). A CPT of 60°C was determined for the

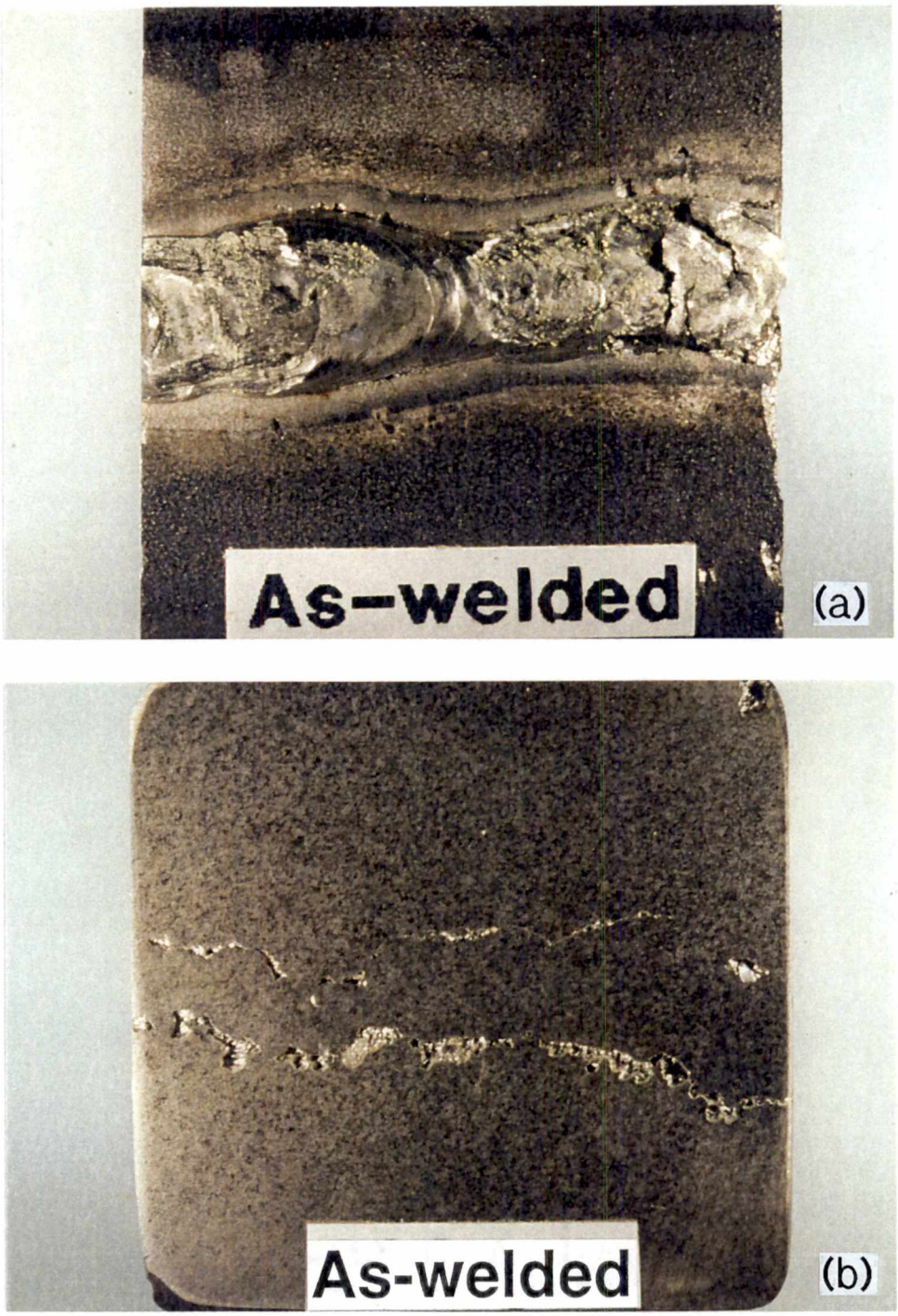


Figure 48. Pitting corrosion tested specimen - AL-6XN GTA BOP weld (C-22 filler) without solution heat treated, test at 80 °C for 24 hours in 10% $FeCl_3$ solution. (a). as-welded surface, (b). 600 grit surface.

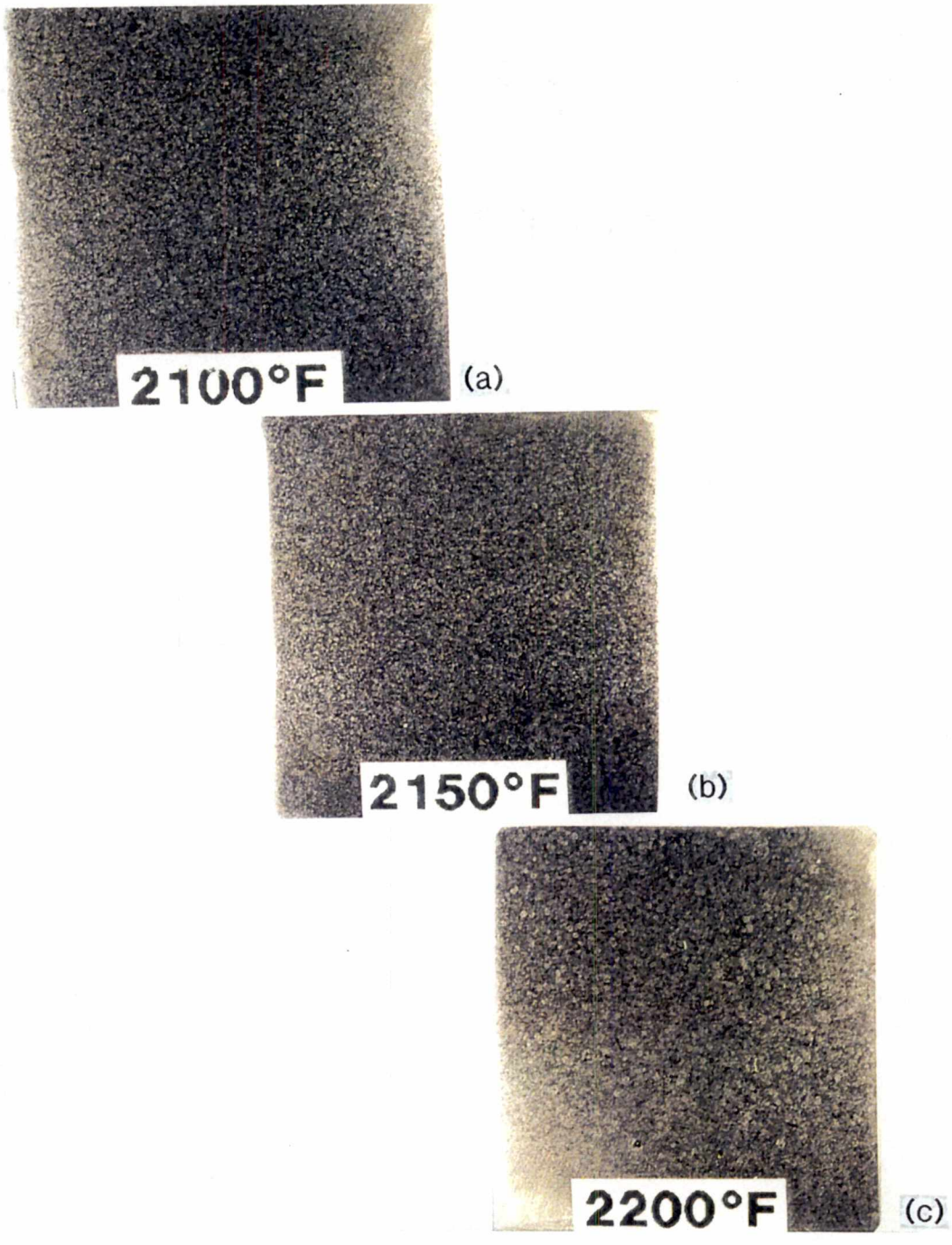


Figure 49. Pitting corrosion tested specimen - AL-6XN GTA BOP weld (C-22 filler) with 600 grit surface, solution heat treated at (a). 2100°F, (b). 2150 °F and (c). 2200°F, test at 80 °C for 24 hours in 10% $FeCl_3$ solution.

unmixed zone in the as-welded condition, and 88°C for the solution treated conditions (2100°F and 2200°F, 30 min). Note that a CPT of 88°C is equivalent to that of the base metal and 28C° higher than that of the unmixed zone (60°C) without solution treatment. It is concluded that after solution treatment at 2100°F or 2200°F for 30 min, the pitting resistance of the unmixed zone is equivalent to that of the base metal.

Similar comparison pitting tests (64°C, 10% $FeCl_3$, 24 hours) were conducted on 254SMO SMA BOP welds (C-22 filler) in both the as-welded and solution treated (2100°F, 2150°F, and 2200°F for 30 min) conditions. The test results are presented in Figures 50 (a and b) and 51 (a, b and c). Similar to AL-6XN SMA BOP dissimilar welds (C-22 filler), pitting occurred in the unmixed zone of the non-solution treated 254SMO (C-22) specimens (as-welded and 600 grit surface conditions, see Figure 50a and b). No pits were found on solution treated (2100°F, 2150°F, and 2200°F) specimens except a few pits on the edge of the specimens (edge effect) (600 grit surface, see Figure 51a, b and c). These observations again confirm that solution treatment is an effective way to improve pitting resistance of the unmixed zone.

4.2.4 Effect of Surface Finish on Pitting Behavior of Unmixed Zone

The effect of surface finish on the pitting behavior of the unmixed zone was evaluated using 1" square specimens (extracted from an AL-6XN SMA BOP weld) with surface finish of 0.05 μm (Al_2O_3 power), 6 μm (diamond), 600 grit (emery) and 240 grit (emery). Based on the unmixed zone CPT data determined in 10% $FeCl_3$, (24 hours), 80°C for a 0.05 μm surface finish and 60°C for a 600 grit surface finish, it is evident that the surface finish has a

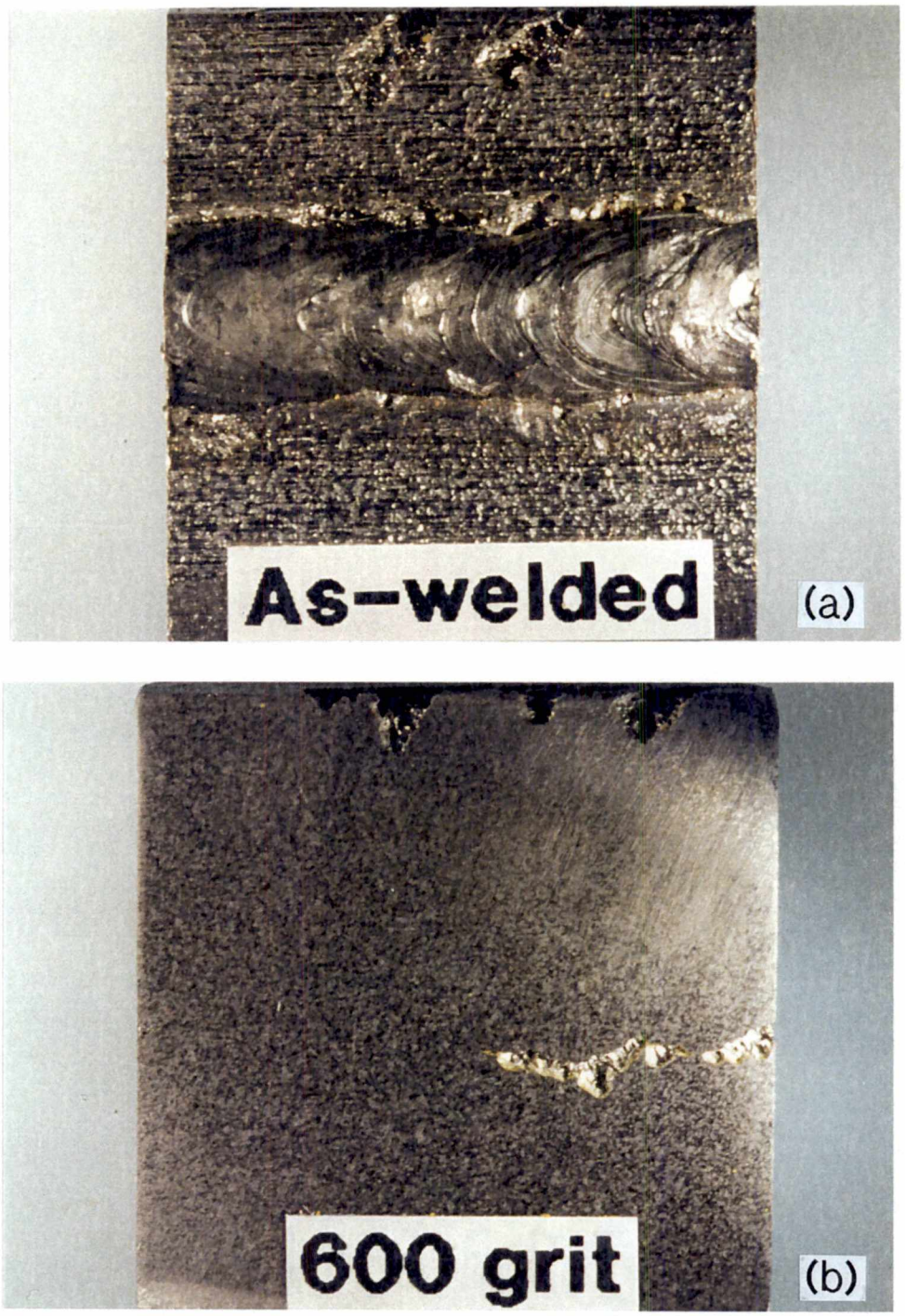


Figure 50. Pitting corrosion tested specimen - 254SMO GTA BOP weld (C-22 filler) without solution heat treated, test at 46 °C for 24 hours in 10% $FeCl_3$ solution. (a). as-welded surface, (b). 600 grit surface.

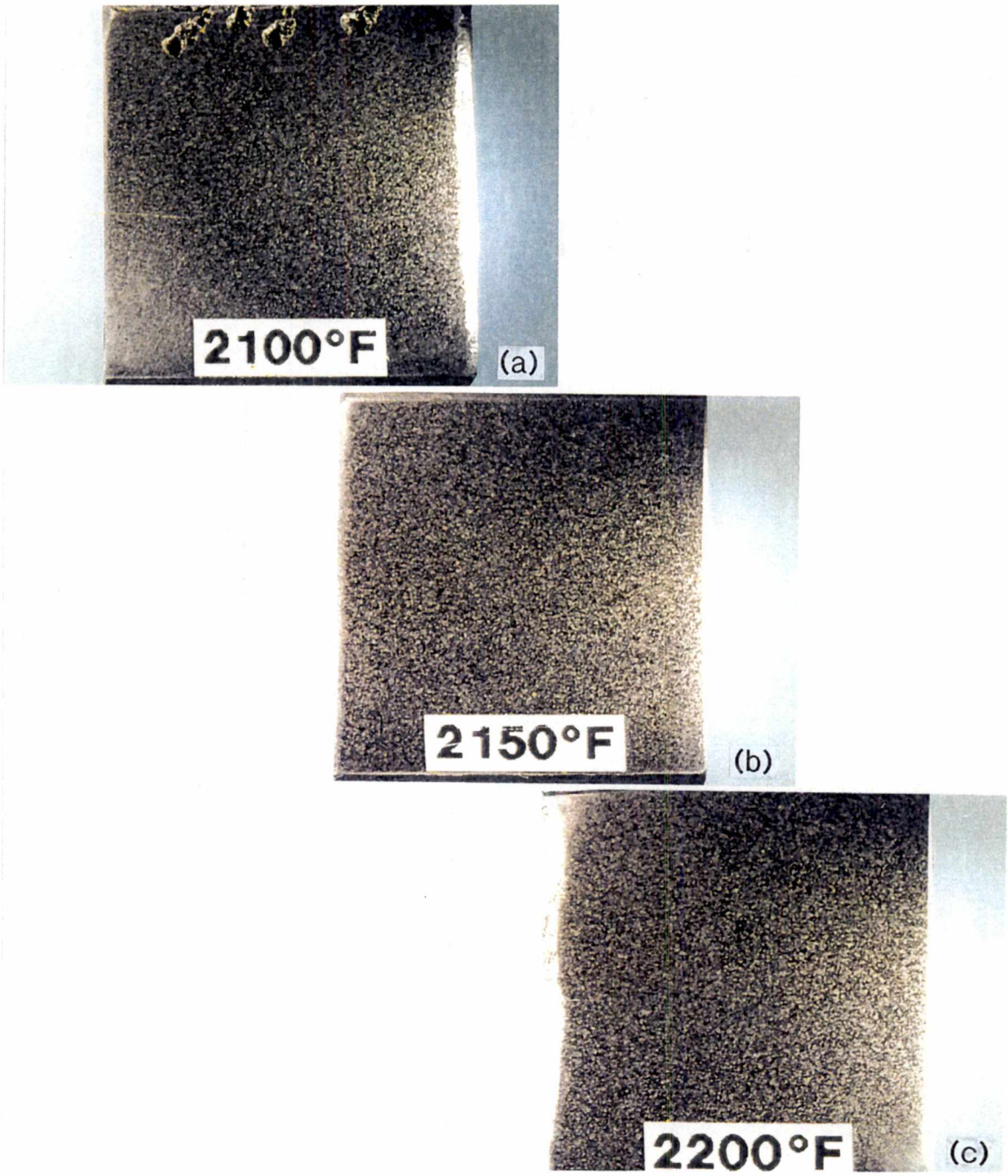


Figure 51. Pitting corrosion tested specimen - 254SMO GTA BOP weld (C-22 filler) with 600 grit surface, solution heat treated at (a). 2100°F, (b). 2150 °F and (c). 2200°F, test at 64 °C for 24 hours in 10% $FeCl_3$ solution.

significant influence in pitting behavior of the unmixed zone. For further confirmation of surface effects, extensive pitting tests were conducted at the CPT of the unmixed zone (80°C) in 10% $FeCl_3$ for 24 hours with 0.05 μm, 6 μm, 600 grit and 240 grit surface conditions. The pitting ratio of the unmixed zone (Pitted Unmixed Zone Length / Total Unmixed Zone Length) for each surface condition was measured after a 24-hour exposure. Test results for each surface condition are shown in Table 15. Based on the pitting ratio in the unmixed zone for specimens with different surface finishes, it is evident that the extent of pitting corrosion in the unmixed zone increases with increasing surface roughness.

4.2.5 Summary of Unmixed Zone Pitting Corrosion Behavior:

The CPT of the unmixed zone in SMA BOP dissimilar welds was determined to be 80°C for AL-6XN, 64°C for 254SMO and >101°C (boiling temperature of 10% $FeCl_3$ solution) for 654SMO, while the CPT of the base metals was determined to be 90°C for AL-6XN, 80°C for 254SMO and >101°C for 654SMO under the same test conditions (10% $FeCl_3$, 24 hours, 0.05μm specimen surface). Thus, the pitting resistance of the unmixed zone is inferior to that of base metal. However, the CPT of the fusion zone in GTA BOP autogenous welds was determined to be 60°C for AL-6XN, 56°C for 254SMO and 101°C for 654SMO. Compared to the CPT of the unmixed zone for filler added welds (80°C for AL-6XN, 64°C for 254SMO and >101°C for 654SMO) under the same test conditions (10% $FeCl_3$, 24 hours, 0.05μm specimen surface), the pitting corrosion resistance of the fusion zone in GTA BOP autogenous welds is lower than that of unmixed zone in SMA BOP dissimilar welds.

Table 15. Corrosion Test Results for Different Surface Condition

Specimen	Surface Finish	Pitting Location	Pitting Ratio* (%)
AL-6XN/Inconel 112	6 micron diamond	Initiation in UNMZ	~0
AL-6XN/Inconel 112	600 grit emery	Extend along UNMZ	8
AL-6XN/Inconel 112	240 grit emery	Extend along UNMZ	18

* Pitting Ratio = Pitted UNMZ Length / Total UNMZ Length

Pitting corrosion resistance of the unmixed zone was evaluated using cyclic polarization tests based on the measurement of hysteresis loop area and passive current density in comparison with the respective base metal. The cyclic polarization test results show that the pitting corrosion resistance of the unmixed zone is inferior to that of the respective base metal, while the pitting corrosion resistance of the fusion zone in the autogenous welds is lower than that of the unmixed zone in the dissimilar welds. These test results are consistent with the immersion pitting test results.

Pit initiation and propagation behavior in the unmixed zone is characterized in four major steps:

Step. 1: Pits initiate at the core of the cellular dendrites in the unmixed zone. The boundaries of the cellular dendrites remain un-corroded.

Step. 2: With increasing time, the cellular dendrite boundaries in the corroded area are attacked and a major pit is formed (which acts as a channel for further corrosion).

Step. 3: After the major pit is formed, pit propagation occurs beneath the surface with a typical "cave propagation" behavior.

Step 4: After a certain extent of "cave propagation" beneath the surface, corrosion breaks the surface through additional corrosion paths in the core of the cellular dendrites.

In addition, pit propagation orientation is always oriented downward regardless of the sample placement in the solution.

The surface roughness has a significant effect on pitting behavior of the unmixed zone. A rougher surface exacerbates pitting corrosion in the unmixed zone.

A proper solution heat treatment is remarkably effective in improving the pitting corrosion resistance of the unmixed zone. A thirty minute solution heat treatment at 2100°F can improve the pitting corrosion resistance of the unmixed zone in AL-6XN dissimilar welds equivalent to that of the base metal. The same solution heat treatment (2100°F, 30 min) can improve the pitting resistance of AL-6XN GTA autogenous fusion zone slightly lower than that of the respective base metal. It is believed that the improvement of pitting resistance in the unmixed zone and autogenous fusion zone results from the reduction of Mo segregation.

4.3 Crevice Corrosion Behavior of Unmixed Zone

In this section, discussions focus on crevice corrosion behavior of the unmixed zone. The influence of surface condition and solution heat treatment on crevice corrosion behavior of the unmixed zone is also investigated.

4.3.1 Evaluation of Crevice Corrosion Behavior of Unmixed Zone

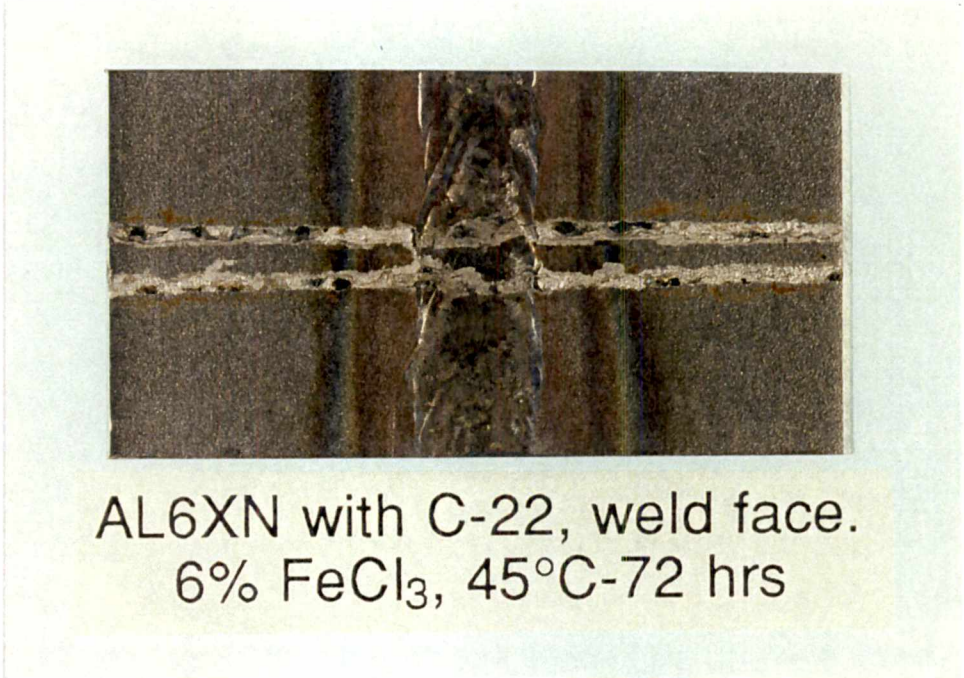
Crevice corrosion tests were performed on AL-6XN GTA open root welds (C-22, Inco-Weld 686CPT and Inconel 625 fillers), 254SMO GTA open root welds (C-22, Inco-Weld 686CPT, Inconel 625 and C-276 fillers) and 654SMO GTA open root welds (P16 filler) using the UT crevice corrosion fixture (see Figure 11). Specimens extracted from open root welds, 2"X1"X0.125", were

assembled in the UT Crevice Corrosion Device at a torque of 32 in-oz and immersed in 6% $FeCl_3$ for 72 hours at each temperature. The test results for each weld are discussed below.

i) AL-6XN GTA filler added open root welds

Based on a CCCT of 43°C determined by LaQue crevice corrosion testing for AL-6XN base metal (72 hours, 6% $FeCl_3$ solution) [5], the initial crevice corrosion test temperature was chosen as 45°C for AL-6XN welded specimens (filler added and autogenous weldments). After 72 hours at 45°C in 6% $FeCl_3$, crevice corrosion occurred over the entire specimen length along the crevice across the base metal, the HAZ, the unmixed zone and the weld metal. Figure 52, as an example, shows the corroded surface of the tested specimen (AL-6XN open root weld - Inconel 625 filler). Further crevice corrosion tests were performed at temperatures of 23°C (room temperature) and 0°C in 6% $FeCl_3$ for 72 hours. Surface appearance of the specimens tested at temperatures of 23°C and 0°C are shown in Figures 53 and 54. At 23°C, crevice corrosion occurred in the unmixed zone, the HAZ and the base metal, no corrosion was observed in the weld metal. For the crevice test at 0°C, crevice corrosion was restricted to the unmixed zone and the HAZ (heat tinted zone) as presented in Figure 54. Weight loss measurements are given in Table 16 for specimens at these test temperatures. Since the CCCT of both the unmixed zone and the heat tinted zone are below 0°C, the corrosion initiation behavior in the unmixed zone and heat tinted zone can not be distinguished under the crevice corrosion conditions.

However, as shown in Figure 52, it is evident that the unmixed zone



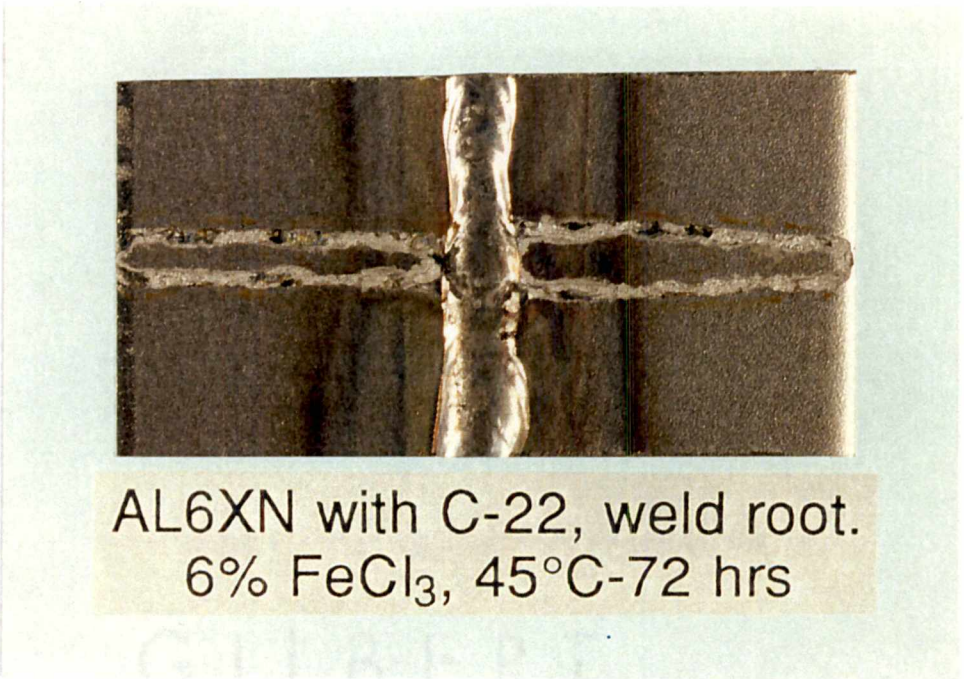
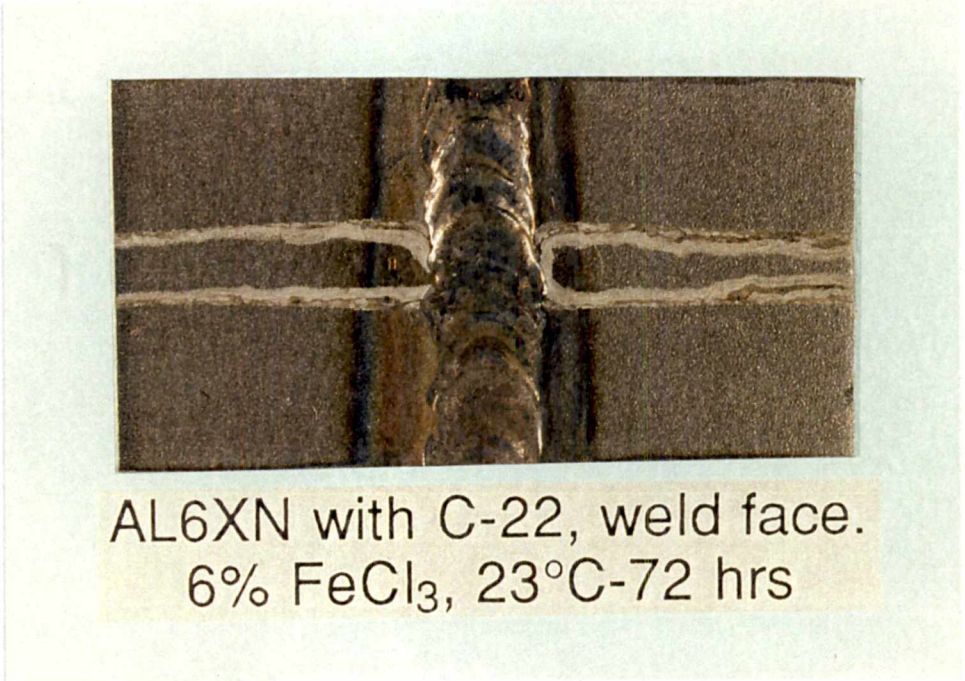


Figure 52. (Crevice corrosion tested specimen - AL-6XN GTA open root welds (Inconel 112 filler), as-welded surface, tested at 45°C for 72 hours in 6% $FeCl_3$ solution.



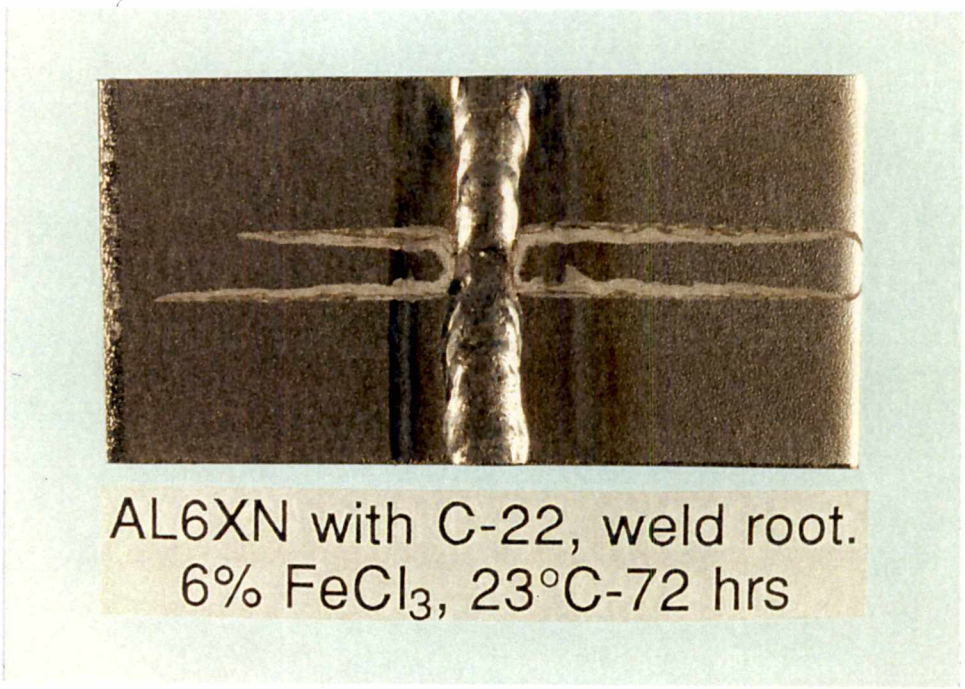
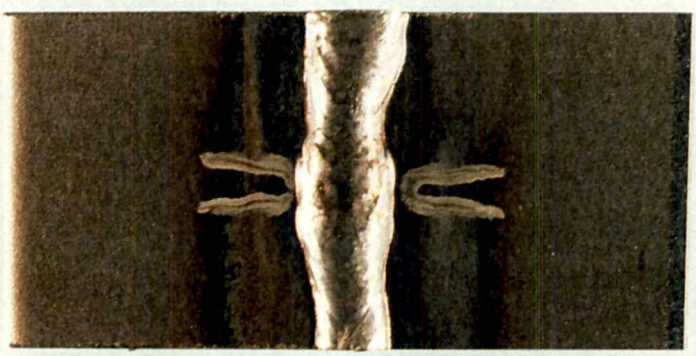


Figure 53. Crevice corrosion tested specimen - AL-6XN GTA open root welds (Inconel 112 filler), as-welded surface, tested at 23°C for 72 hours in 6% $FeCl_3$ solution.



AL6XN with C-22, weld face.
6% $FeCl_3$, 0°C-72 hrs



AL6XN with C-22, weld root.
6% $FeCl_3$, 0°C-72 hrs

Figure 54. Crevice corrosion tested specimen - AL-6XN GTA open root welds (Inconel 112 filler), as-welded surface, tested at 0°C for 72 hours in 6% $FeCl_3$ solution.

Table 16. Weight Loss after Crevice Corrosion Testing

Specimen		Weight Loss at 60°C [g]	Weight Loss at 45°C [g]	Weight Loss at 23°C [g]	Weight Loss at 0°C [g]
BM	Filler				
	C-22	1.922	0.224	0.021	0.002
AL-6XN	686CPT	-	0.217	0.018	0.002
	Inconel625	-	1.294	0.015	0.003
	C-22	3.030	0.912	0.006	0.002
254SMO	686CPT	-	1.686	0.009	0.004
	Inconel625	-	1.239	0.008	0.004
	C-276	-	1.228	0.007	0.004
654SMO	P16	0.408	0.010	0.000	0.000

corrodes more severely than other regions at 45°C after 72 hours in 6% $FeCl_3$ solution in terms of the width and the depth of corroded area. For further investigation of crevice corrosion behavior of the unmixed zone, a specimen (tested at 45°C for 72 hours) was sectioned across the weld through a corroded area. Corrosion morphology at the weld face and weld root on this cross-section is presented in Figure 55. The corroded unmixed zone area at weld face and weld root is shown in Figure 56 (a and b) at 200X in comparison to the corresponding before-test area. Measurements of depth and width of corroded areas were performed on both the cross-section (along line AB in Figure 57a) and a weld root surface (along line AB in Figure 58a). The distributions of the depth and width of the corroded area are illustrated in Figures. 57b and 58b, respectively. It is evident that the deepest and widest corroded area is in the unmixed zone. Therefore, the unmixed zone has a lower resistance to crevice corrosion in comparison to the other regions.

ii) 254SMO and 654SMO GTA filler added open root weldments

Crevice corrosion behavior of the unmixed zone in 254SMO (C-22, C-276, Inconel 625, and 686CPT fillers) and 654SMO (P16 filler) GTA open root welds was investigated using the same test procedure as used for the AL-6XN weldments. The results on the unmixed zone in 254SMO weldments are generally consistent with that of AL-6XN weldments. Again, the unmixed zone has the lowest crevice corrosion resistance compared to the other regions. However, compared to AL-6XN under the same test conditions (45°C, 72 hours, 6% $FeCl_3$), the extent of crevice corrosion in 254SMO is deeper and wider. A comparison of the depth and width of the corroded unmixed zone between

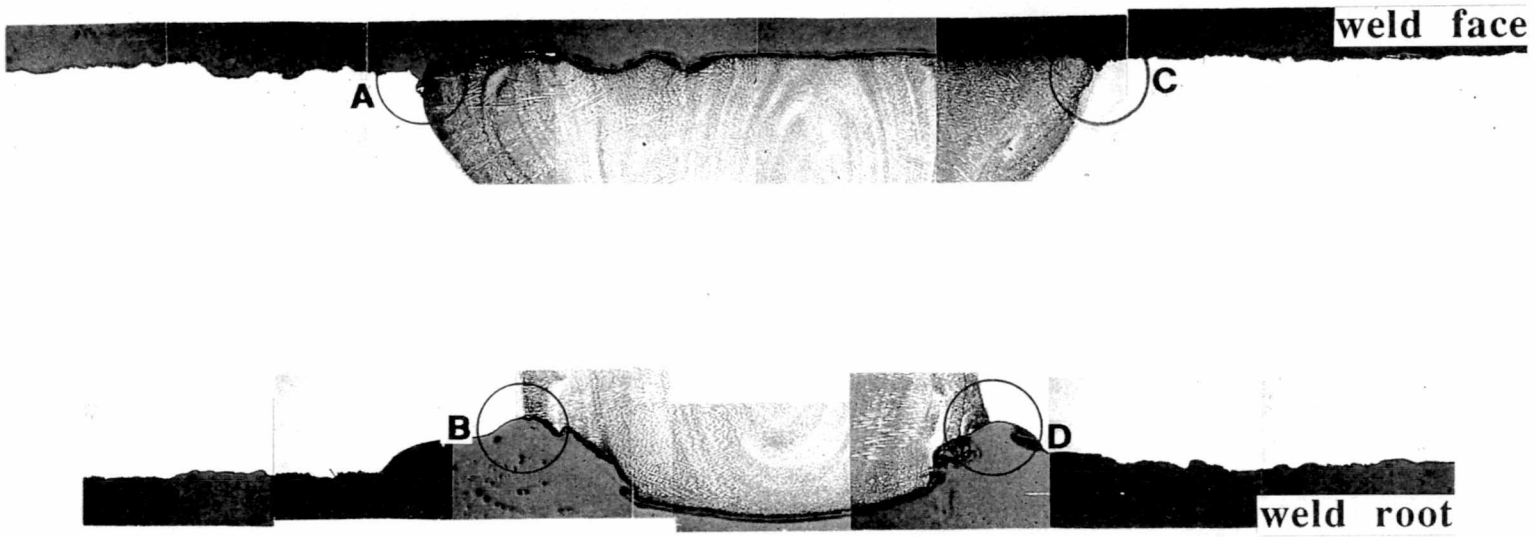


Figure 55. Crevice corrosion tested specimen - AL-6XN GTA open root welds (Inconel 112 filler), transverse cross-section, tested at 45°C for 72 hours in 6% $FeCl_3$ solution, 12X.

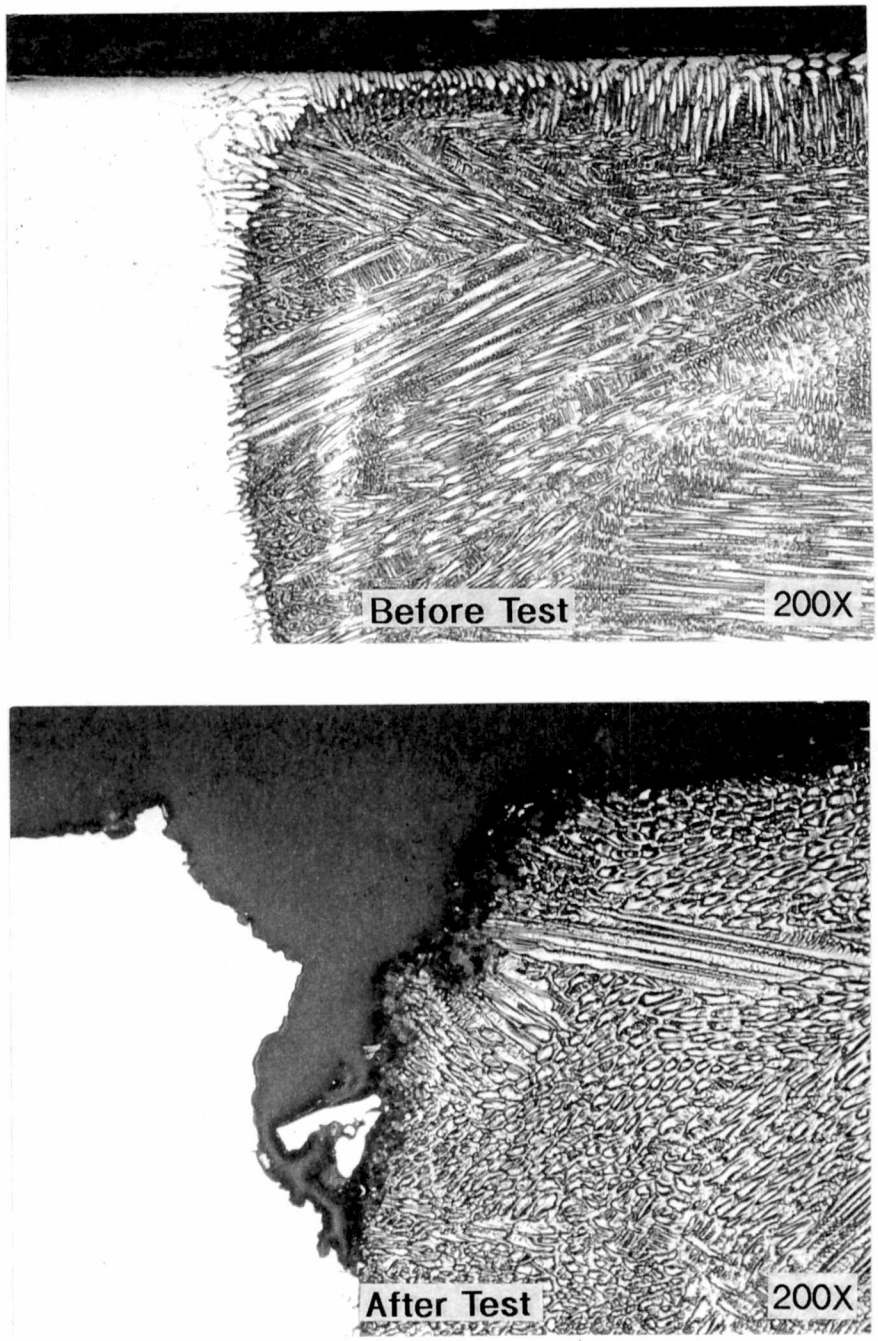


Figure 56. Comparison of the unmixed zone appearances before and after crevice corrosion test at 45°C in 6% $FeCl_3$ for 72 hours, AL-6XN GTA open root welds (Inconel 112 filler), transverse cross-section, (a) location A in Figure 63, 200X.

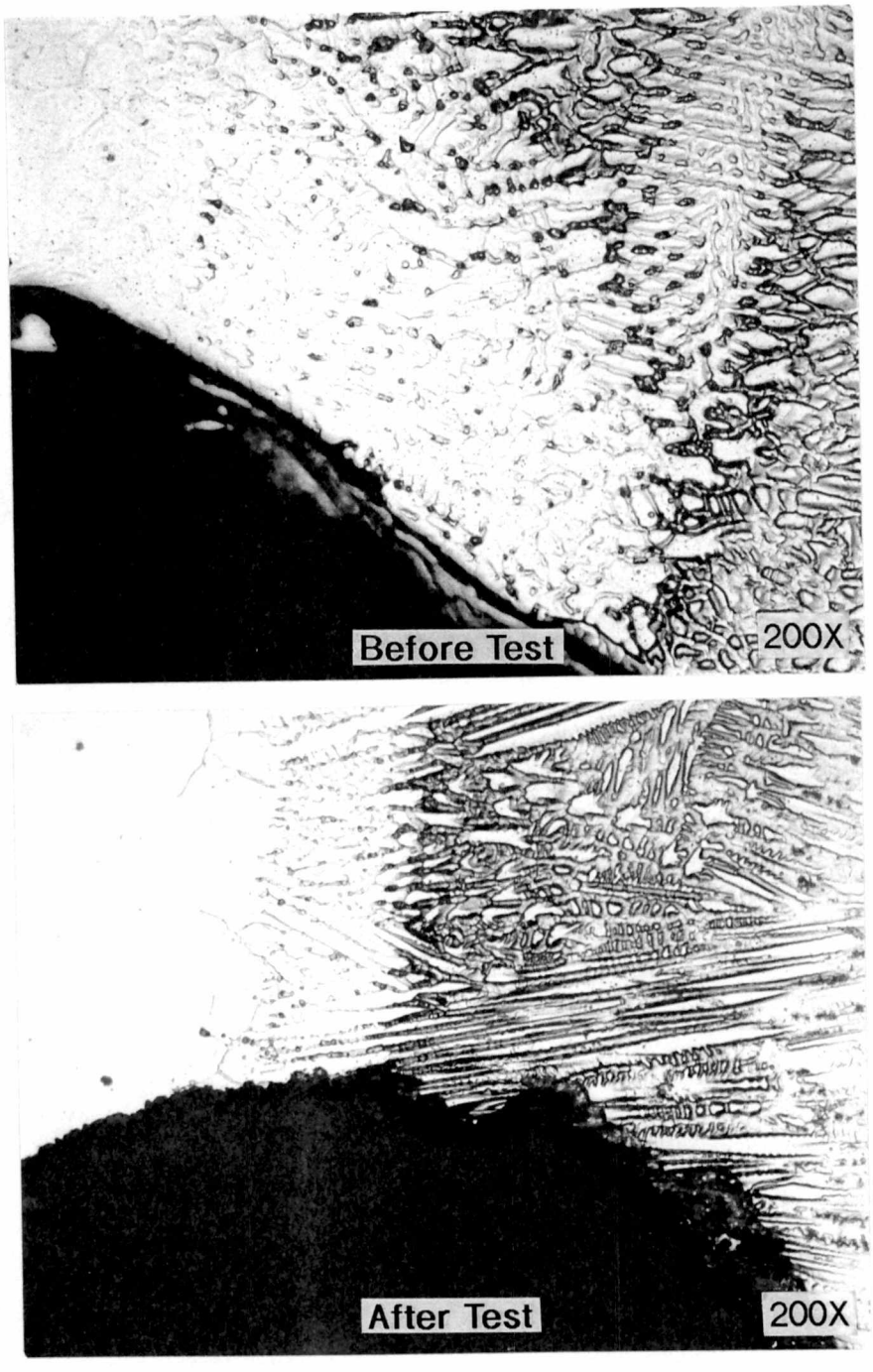
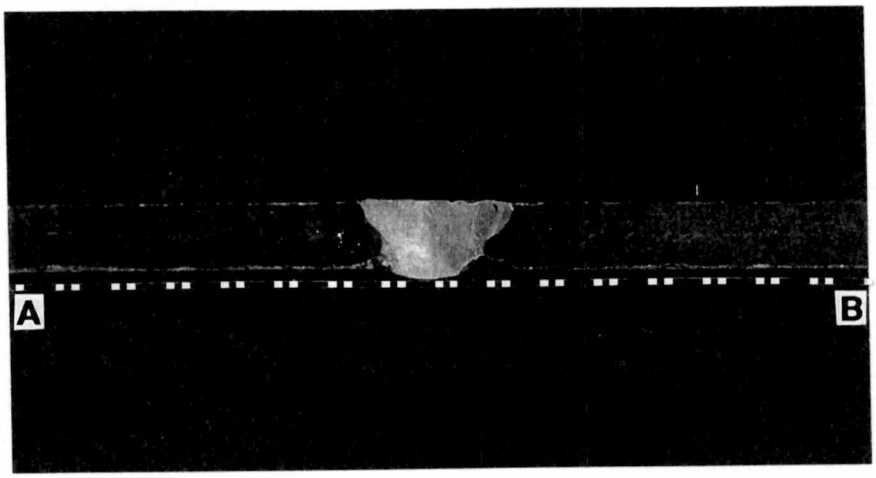
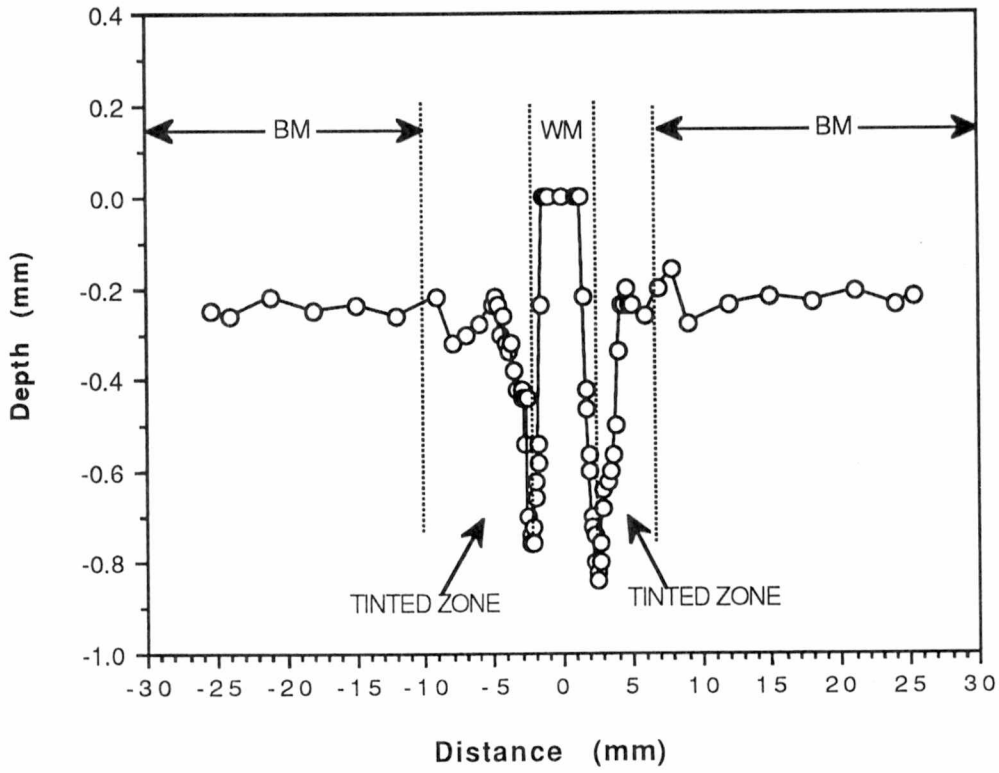


Figure 56 (cont'd). Comparison of the unmixed zone appearances before and after crevice corrosion test at 45°C in 6% $FeCl_3$ for 72 hours, AL-6XN GTA open root welds (Inconel 112 filler), transverse cross-section, (b) location C in Figure 63, 200X.

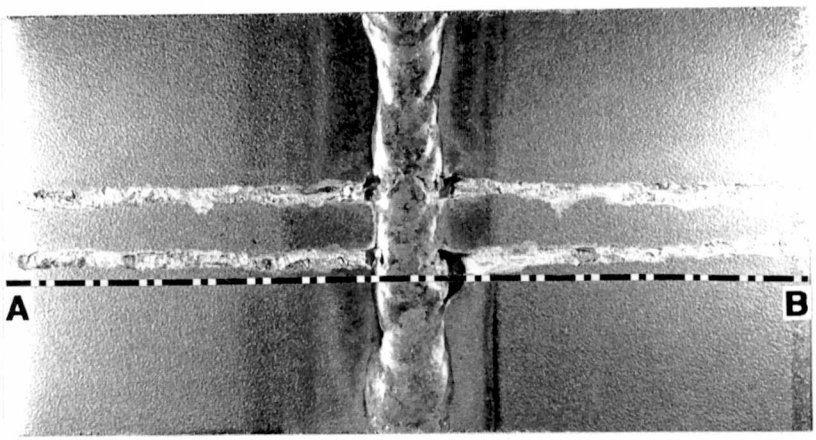


(a)

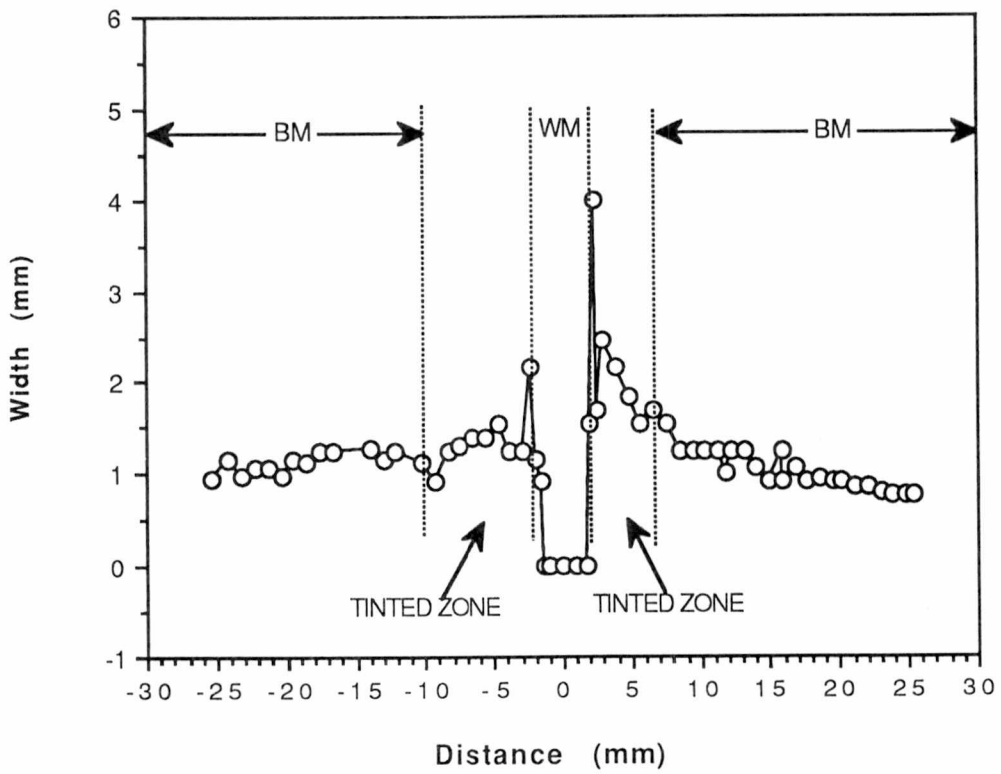


(b)

Figure 57. AL-6XN GTA open root welds (686CPT filler), test at 45°C in 6% $FeCl_3$ for 72 hours, (a). transverse cross-section of tested specimen, (b). crevice corrosion depth distribution.



(a)



(b)

Figure 58. AL-6XN GTA open root welds (686CPT filler), test at 45°C in 6% $FeCl_3$ for 72 hours, (a). weld root surface of tested specimen, (b). crevice corrosion width distribution.

254SMO and AL-6XN weldments is shown in Figures 59 and 60, respectively. Note that Mo, Cr and N content of 254SMO (6.1%Mo, 19.9%Cr & 0.20%N) is lower than that of AL-6XN (6.3%Mo, 20.5%Cr & 0.22%N). In addition, the weight loss of each specimen tested at 60°C, 45°C, 23°C and 0°C was determined and is presented in Table 16.

For 654SMO welded specimens, crevice corrosion occurs in the unmixed zone and the heat tinted zone at temperatures above 23°C (room temperature) Thus, the CCCT of the unmixed zone for 654SMO welds is significantly higher than that of either AL-6XN or 254SMO weldments (below 0°C for both AL-6XN and 254SMO). This indicates that the unmixed zone in 654SMO weldments has higher crevice corrosion resistance than that in AL-6XN and 254SMO weldments. This is due to higher Mo, N, and Cr content (Mo: 7.3%, N: 0.487%, and Cr: 24.6%) of the 654SMO base metal. By comparing the extent of the crevice corrosion between the unmixed zone and other weld regions, it was again found that the unmixed zone corrodes more severely than the other weld regions (tests performed at 60°C). The weight losses for 654SMO welds for 60°C, 45°C, 23°C, and 0°C test temperatures are listed in Table 16 for comparison with AL-6XN and 254SMO.

Based on the crevice corrosion test results, it is evident that the unmixed zone in all three super-austenitic stainless steel weldments (AL-6XN, 254SMO and 654SMO) has lower crevice corrosion resistance compared to other weld regions. The unmixed zone in 654SMO welds has a better crevice corrosion resistance than either the AL-6XN and 254SMO welds.

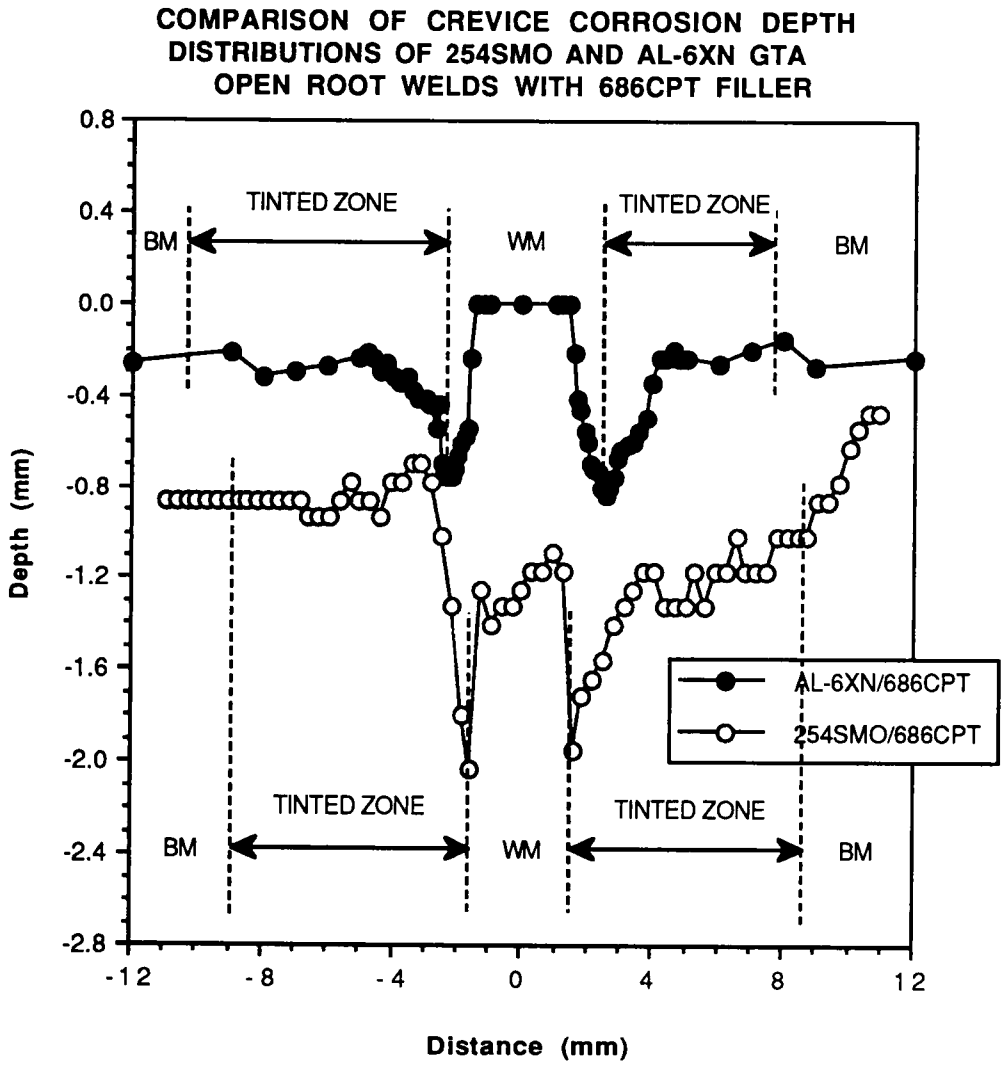


Figure 59. Comparison of crevice corrosion depth distribution of 254SMO and AL-6XN GTA open root welds (686CPT filler), test at 45°C in 6% $FeCl_3$ for 72 hours.

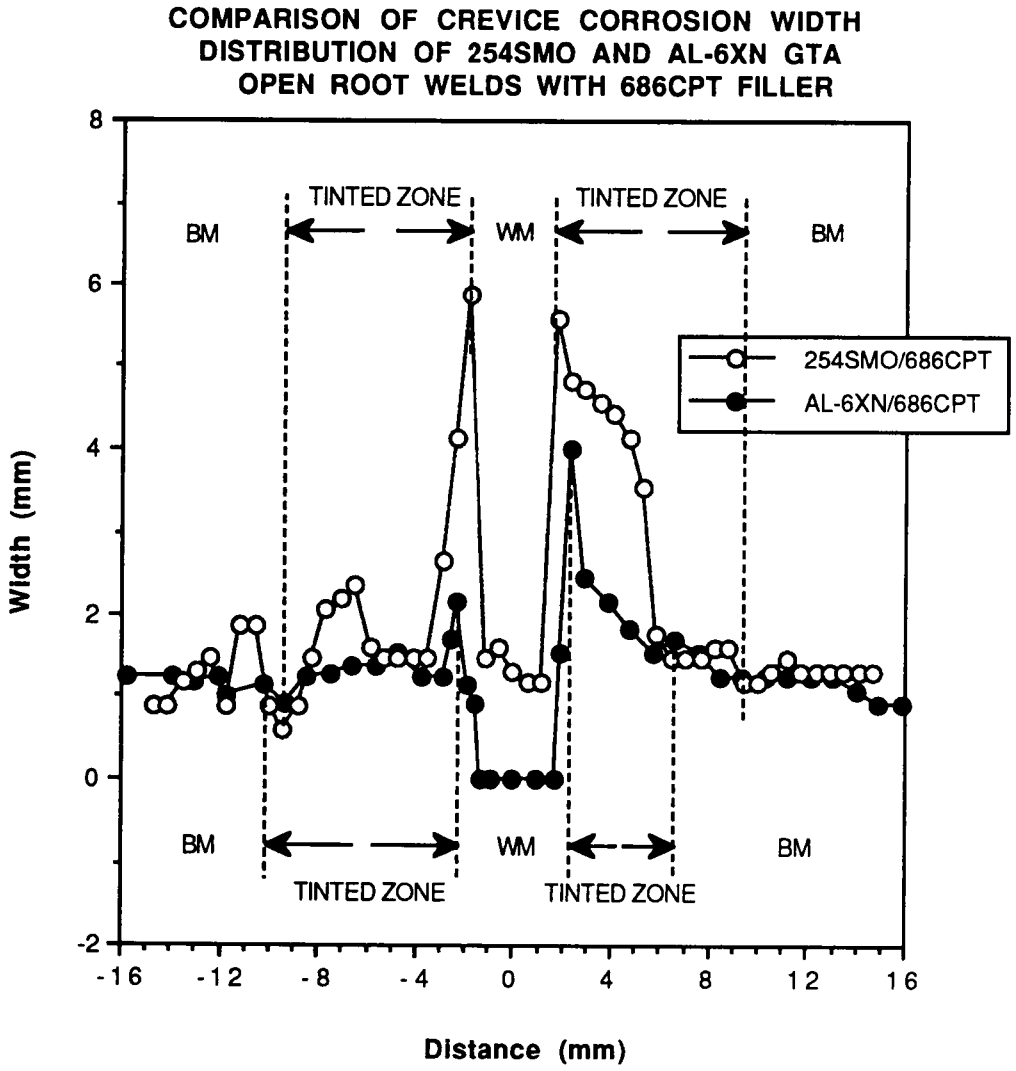


Figure 60. Comparison of crevice corrosion width distribution of 254SMO and AL-6XN GTA open root welds (686CPT filler), test at 45°C in 6% $FeCl_3$ for 72 hours.

4.3.2 Effect of surface condition on crevice corrosion behavior

Based on the pitting corrosion test results, the surface condition was seen to have a significant influence on the pitting corrosion behavior of the unmixed zone. Thus, it is hypothesized that surface condition, such as surface roughness and surface oxidation, may influence the crevice corrosion behavior of the unmixed zone.

To investigate the effect of surface condition, AL-6XN and 254SMO GTA open root welds (C-22 filler metal) were deposited on the sheet materials in both the as-received (mill surface) and as-ground (600 grit) condition. The specimens extracted from these welds were tested in both the as-welded and pickled (10%HNO_3 + 2%HF, 45°C, 1 hour) condition as defined below:

i) as-welded on as-received (mill) surface

ii) as-welded on 600 grit surface

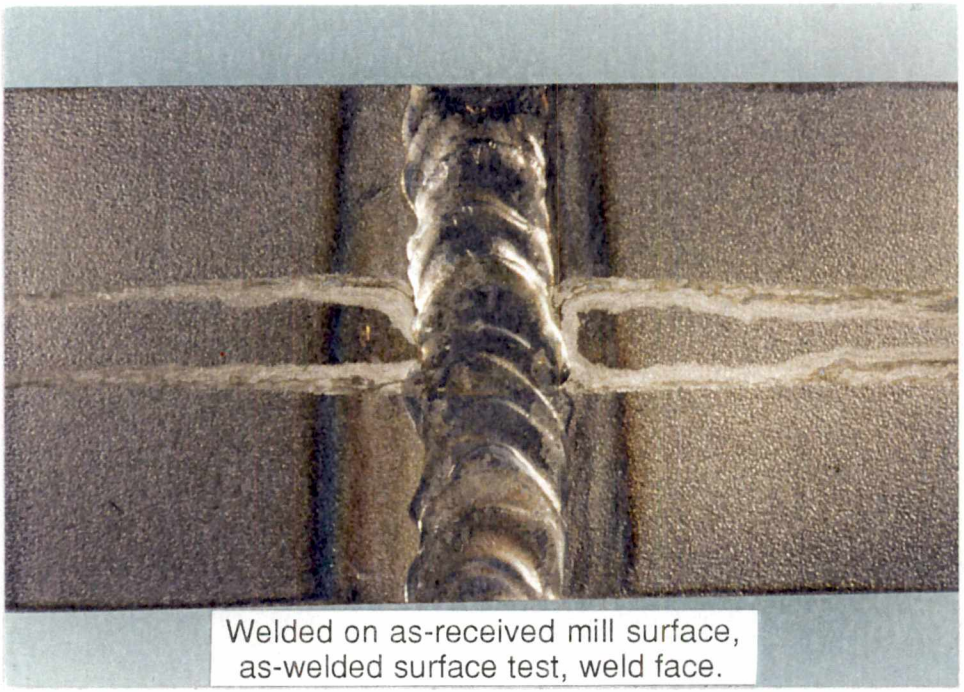
iii) pickled after welding on as-received mill surface

iv) pickled after welding on 600 grit surface

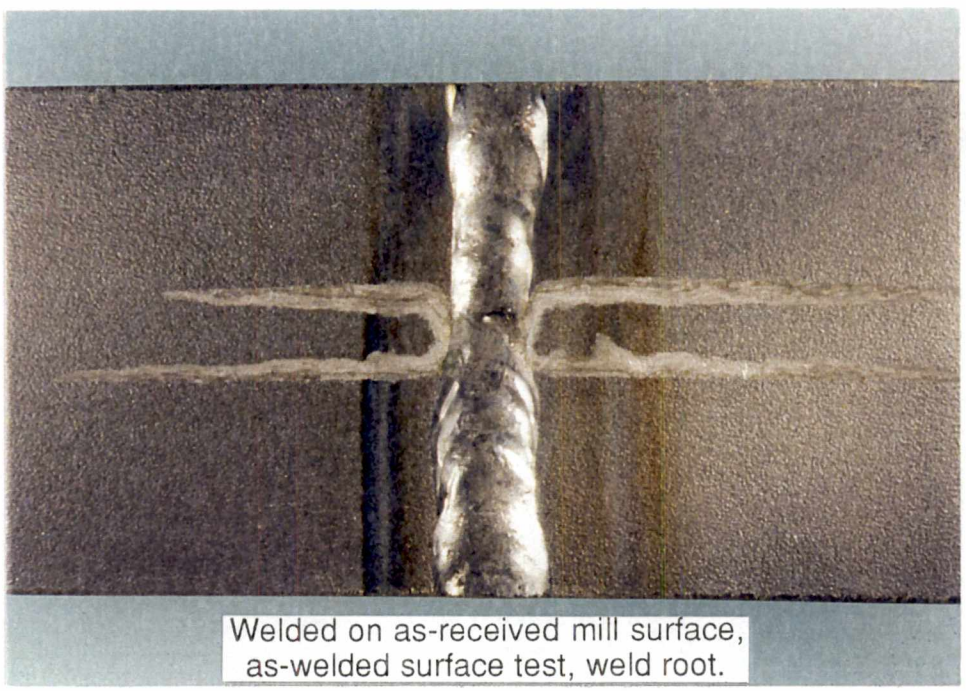
The crevice corrosion tests in 6% $FeCl_3$ at 23°C and 45°C for 72 hours were carried out.

To illustrate the results obtained, crevice corrosion test results at 23°C (6% $FeCl_3$, 72 hours) for AL-6XN welds in each surface condition are shown in Figure 61 (a, b, c and d) and these results are discussed below in detail.

Figure 61a and b shows the effect of surface roughness on crevice corrosion by comparing welds on the as-received (mill) surface and the 600 grit surface. It is evident that the unmixed zone, the heat tinted zone and the base metal are all corroded in both surface conditions. However, the extent of crevice corrosion in the non-oxidized heat tinted base metal regions was less

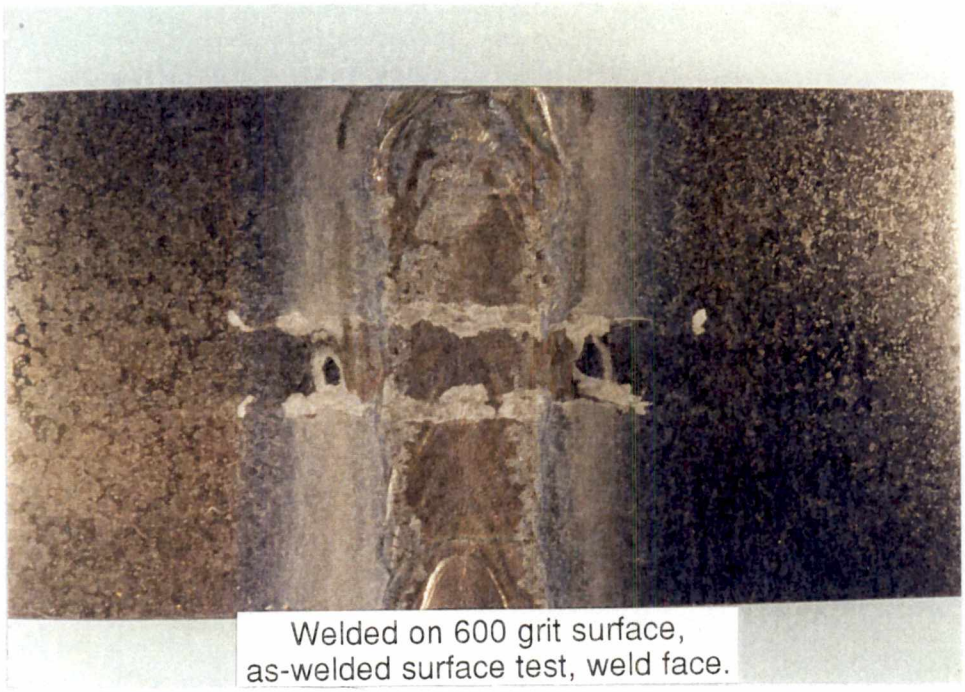


Welded on as-received mill surface,
as-welded surface test, weld face.

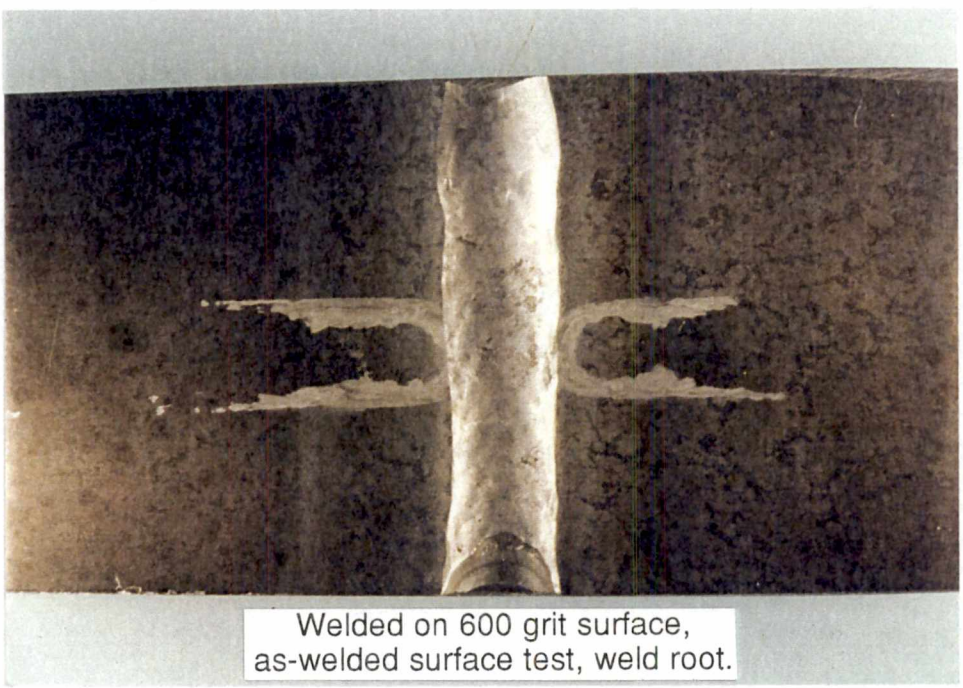


Welded on as-received mill surface,
as-welded surface test, weld root.

Figure 61. Crevice corrosion tested specimen - AL-6XN GTA open root weld (C-22 filler), test at 23°C in 6% $FeCl_3$ for 72 hours, (a) as-welded on as-received (mill) surface.

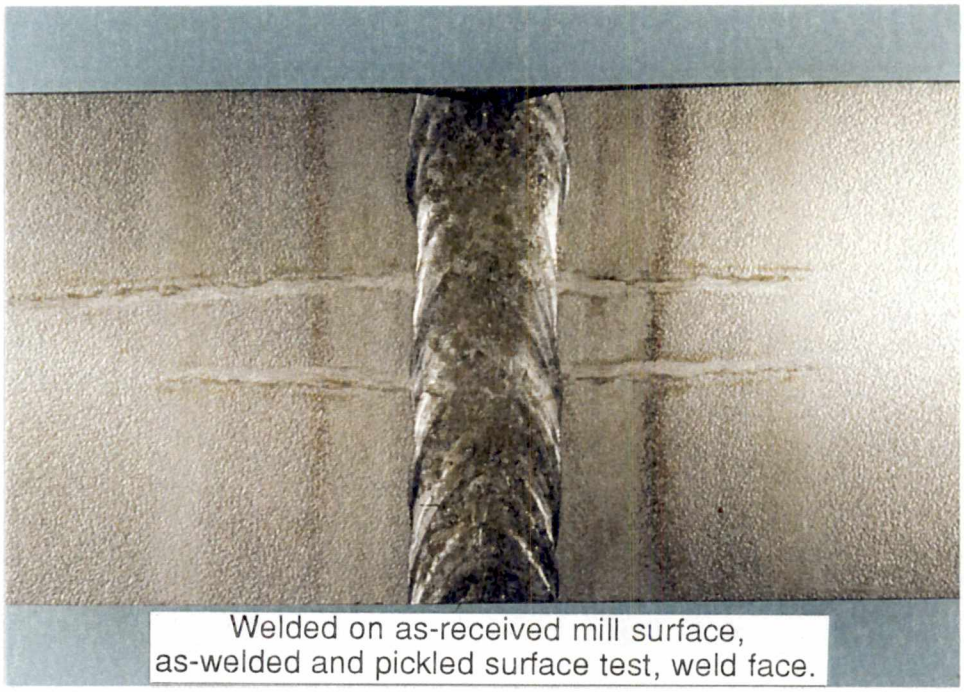


Welded on 600 grit surface,
as-welded surface test, weld face.

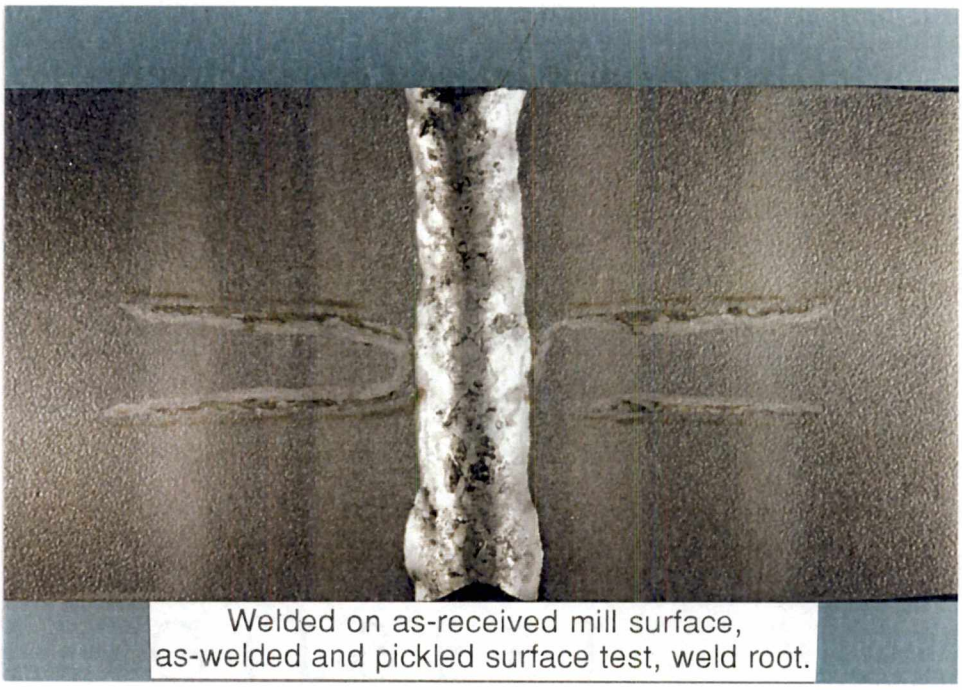


Welded on 600 grit surface,
as-welded surface test, weld root.

Figure 61 (cont'd). Crevice corrosion tested specimen - AL-6XN GTA open root weld (C-22 filler), test at 23°C in 6% $FeCl_3$ for 72 hours. (b) as-welded on 600 grit surface.

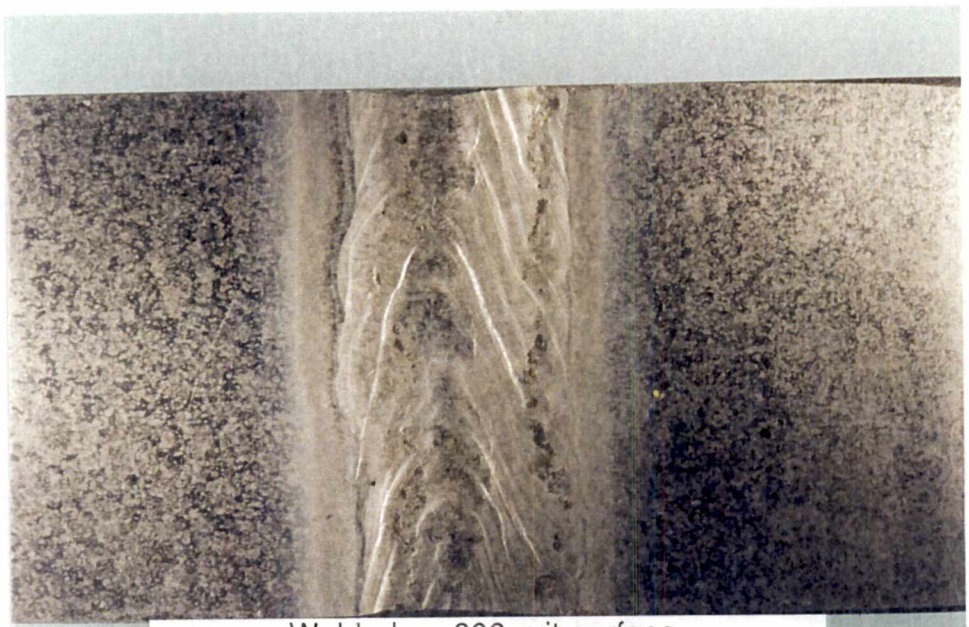


Welded on as-received mill surface,
as-welded and pickled surface test, weld face.

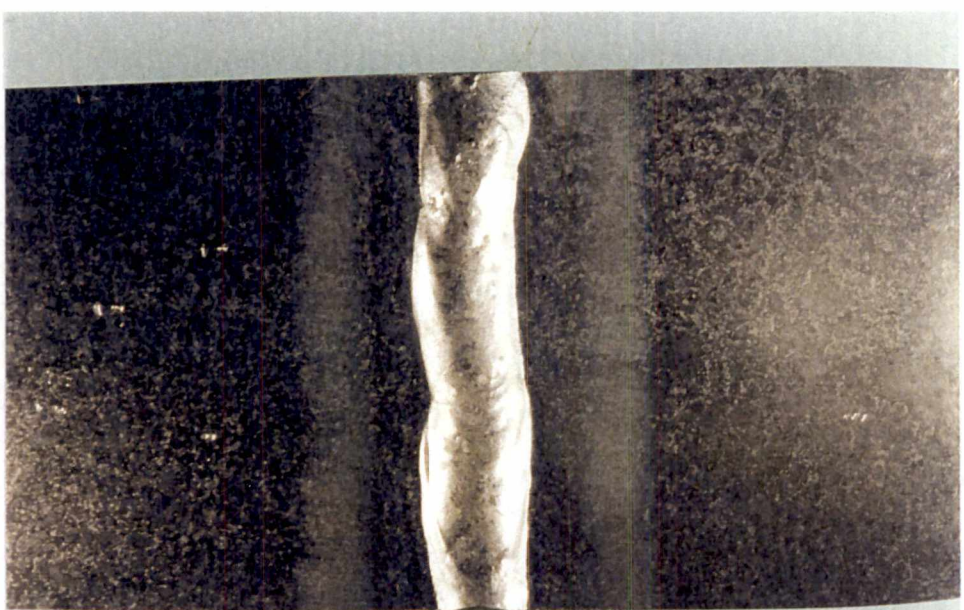


Welded on as-received mill surface,
as-welded and pickled surface test, weld root.

Figure 61 (cont'd). Crevice corrosion tested specimen - AL-6XN GTA open root weld (C-22 filler), test at 23°C in 6% $FeCl_3$ for 72 hours, (c) pickled after welding on as-received (mill) surface.



Welded on 600 grit surface,
as-welded and pickled surface test, weld face.



Welded on 600 grit surface,
as-welded and pickled surface test, weld root.

Figure 61 (cont'd). Crevice corrosion tested specimen - AL-6XN GTA open root weld (C-22 filler), test at 23°C in 6% $FeCl_3$ for 72 hours, (d) pickled after welding on 600 grit surface.

for the 600 grit surface than for the as-received (mill) surface. Thus, since the 600 grit surface is less rough than the mill surface, this result confirmed the fact that rougher surface are more susceptible to crevice corrosion.

Figure 61a and c shows the effect of surface oxide (heat tint) on crevice corrosion by comparing the as-welded mill surface and the pickled mill surface. It is evident that the unmixed zone, the heat tinted zone and the base metal are all corroded in both surface conditions. Therefore, it is apparent that pickling alone is not sufficient to reduce the extent of crevice corrosion in the unmixed zone. However, there is a smaller extent of crevice corrosion in the non-heat tinted base metal region for specimens which had been pickled compared to the original mill surface. This indicates that the addition pickling treatment provides a improvement over the mill pickling surface.

As shown in Figure 61d, the combination of grinding (to 600 grit) before welding and pickling after welding eliminates crevice corrosion in the unmixed zone and in fact in all other regions (72 hour, 6% $FeCl_3$, 23°C). Thus, it is concluded that the crevice corrosion resistance of the unmixed zone can be significantly improved by decreasing surface roughness by grinding (600 grit) before welding combined with removal of the heat tint (weld oxidation) by pickling after welding. But either decreasing surface roughness before welding alone or removing heat tint after welding alone does not eliminate the unmixed zone attack. However, it does improve the crevice corrosion resistance of the un-tinted base metal to some extent.

It is to be noted that the same test results were obtained for AL-6XN and 254SMO weldments tested at 45°C (6% $FeCl_3$, 72 hours).

4.3.3 Effect of Solution Heat Treatment on Crevice Corrosion Behavior of Unmixed Zone

To investigate the effects of solution treatment on crevice corrosion behavior, autogenous GTA BOP welds on AL-6XN, GTA open root welds on AL-6XN (C-22 filler), 254SMO (C-22 filler), and 654SMO (P16 filler) were tested in both the as-welded and solution treated (2100°F, 2150°F, and 2200°F for 30 min) conditions. Specimen surfaces were prepared by either pickling (10% HNO_3 + 2% HF, 43°C,1 hour) or 600 grit before testing. The corrosion specimens were assembled in the UT Crevice Corrosion Device at a torque of 32 in-oz. Six percent $FeCl_3$ (ASTM G48-B) was used for 72 hour immersion crevice corrosion tests at each test temperature. The effect of solution heat treatment on crevice corrosion behavior of the unmixed zone was evaluated by comparing the extent of crevice corrosion in the unmixed zone between the as-welded and the solution treated specimens.

Since the fusion zone in an autogenous weld has characteristics similar to the unmixed zone in dissimilar welds, crevice corrosion tests were first performed on AL-6XN autogenous welds at 45°C. The test results are depicted in Figures 62 (a, b, c and d) for the pickled specimens and 63 (a, b, c, and d) for the 600 grit specimens, respectively. It is obvious that more serious crevice corrosion occurred in the fusion zone of autogenous welds in the as-welded condition (without solution treatment). This is true for testing on pickled and 600 grit ground surfaces as presented in Figures 62a and 63a. Crevice corrosion was also observed in the base metal of the same samples, and the extent of the crevice corrosion in the base metal is higher on the rougher surface (pickled) than on the ground surface (600 grit).

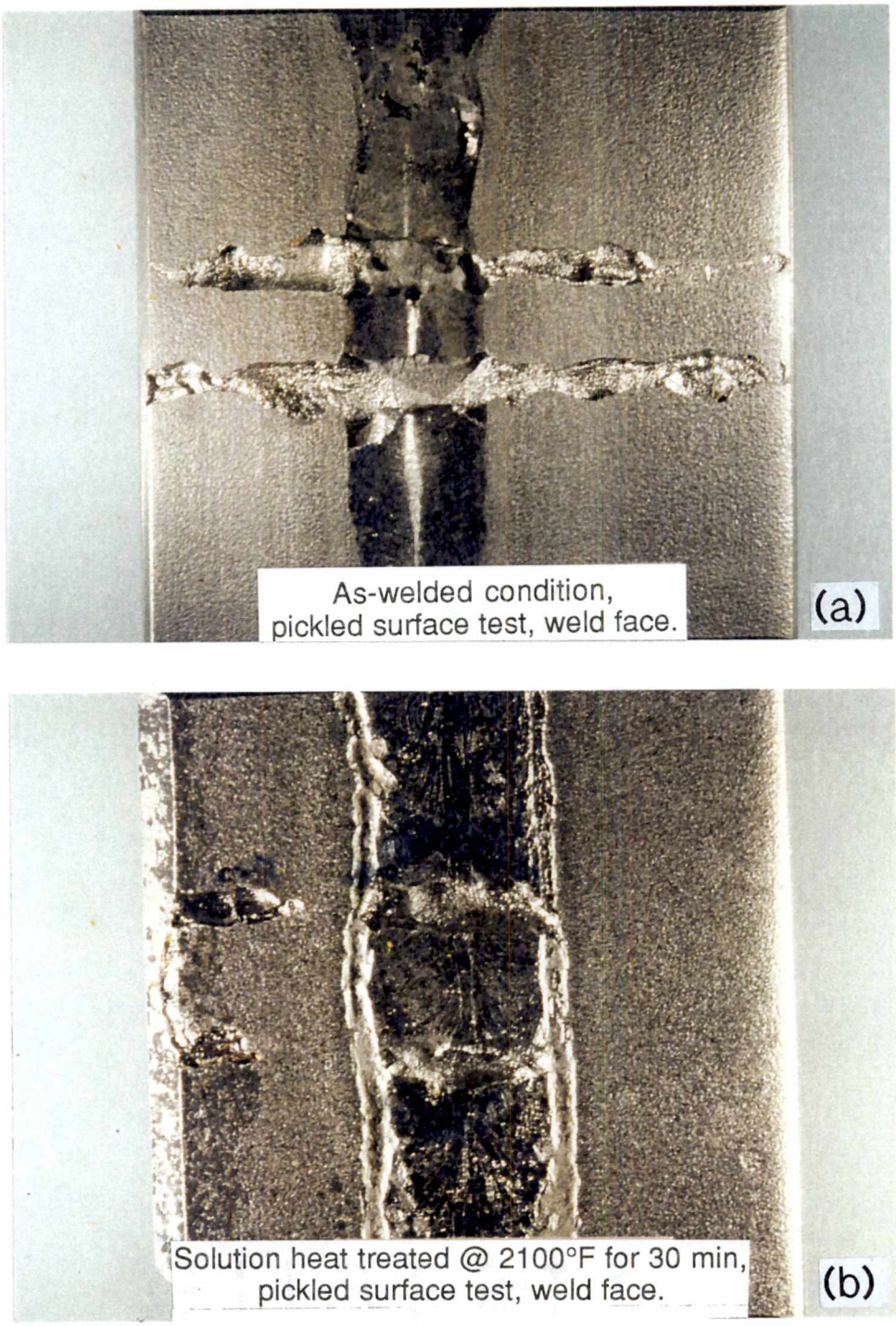
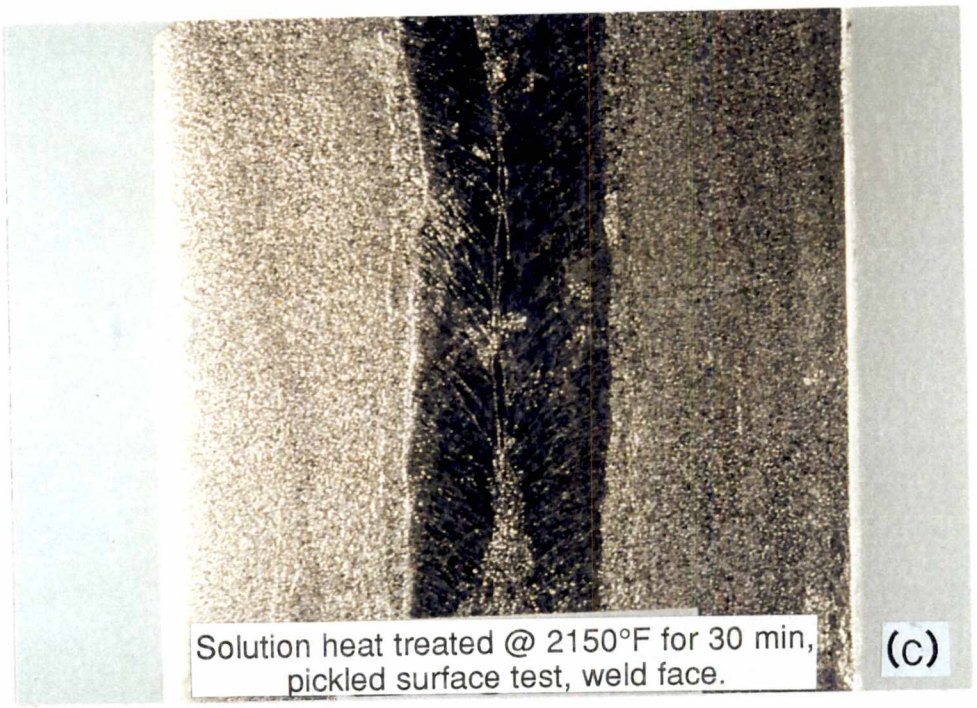


Figure 62. Crevice corrosion tested specimen - AL-6XN autogenous GTA BOP weld, test at 45°C in 6% $FeCl_3$ for 72 hours.



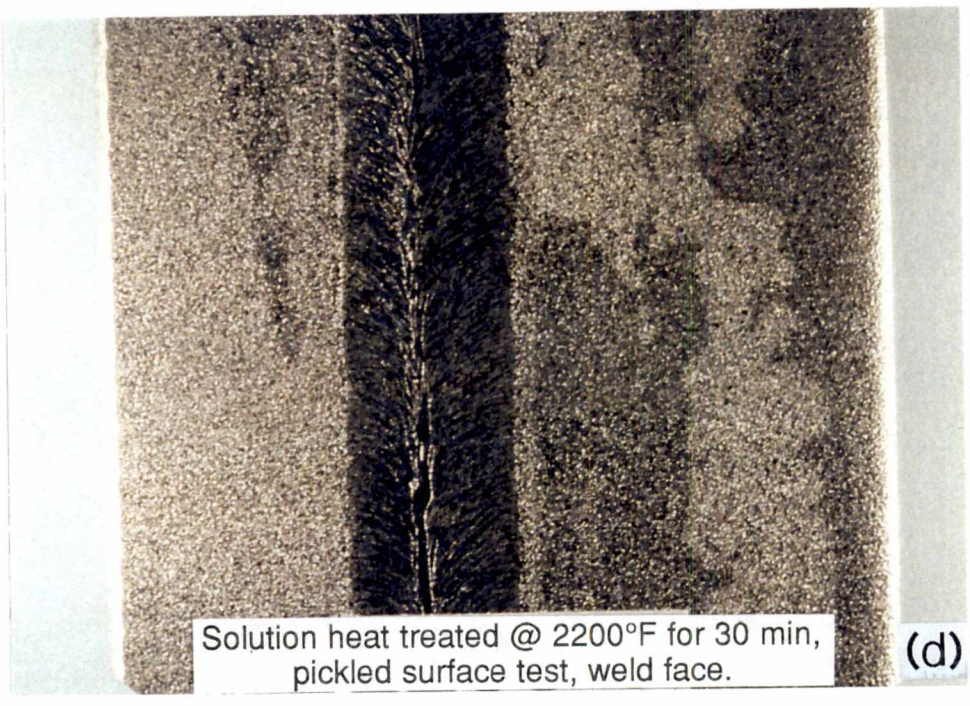


Figure 62 (cont'd). Crevice corrosion tested specimen - AL-6XN autogenous GTA BOP weld, test at 45°C in 6% $FeCl_3$ for 72 hours.

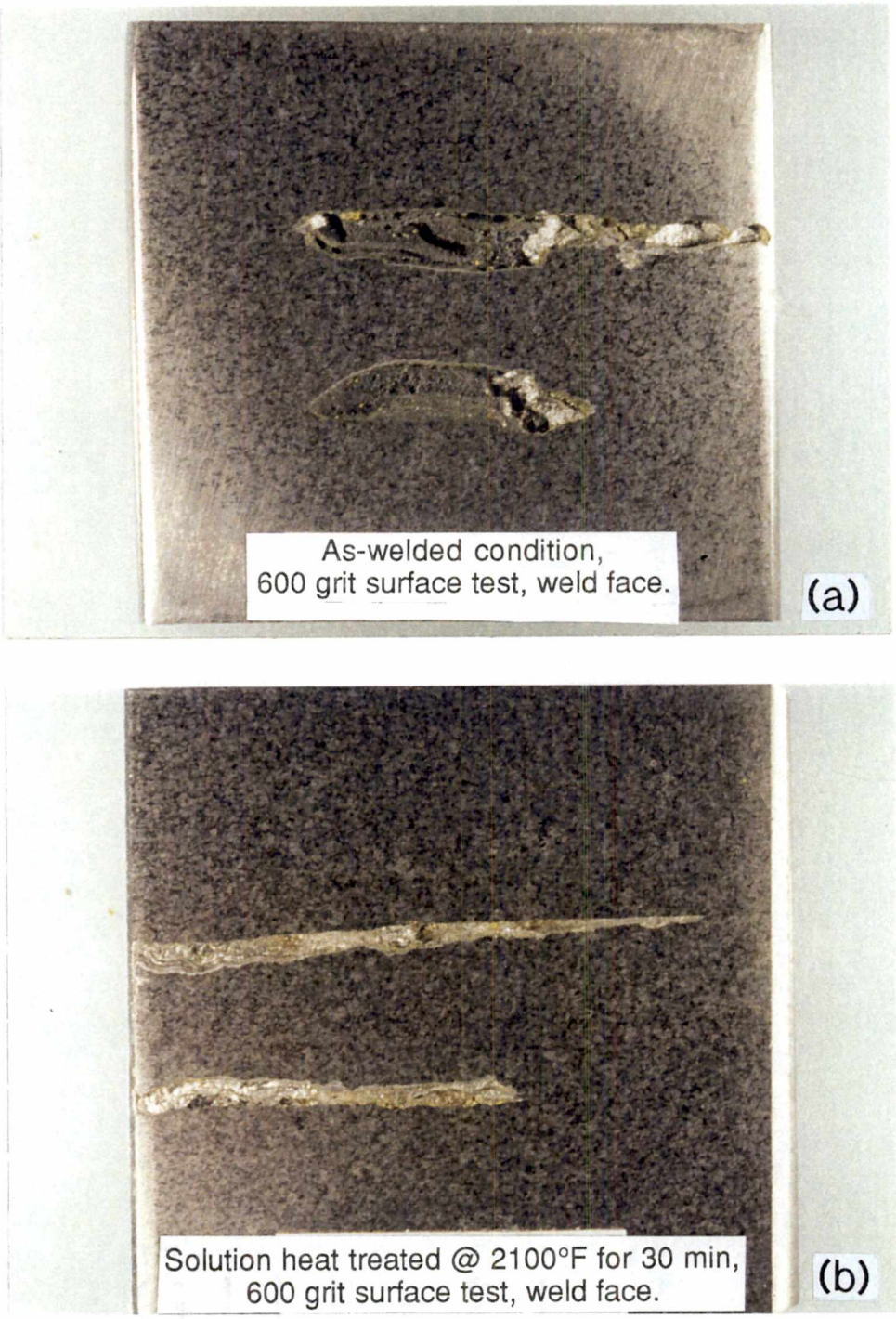


Figure 63. Crevice corrosion tested specimen - AL-6XN autogenous GTA BOP weld, test at 45°C in 6% $FeCl_3$ for 72 hours.



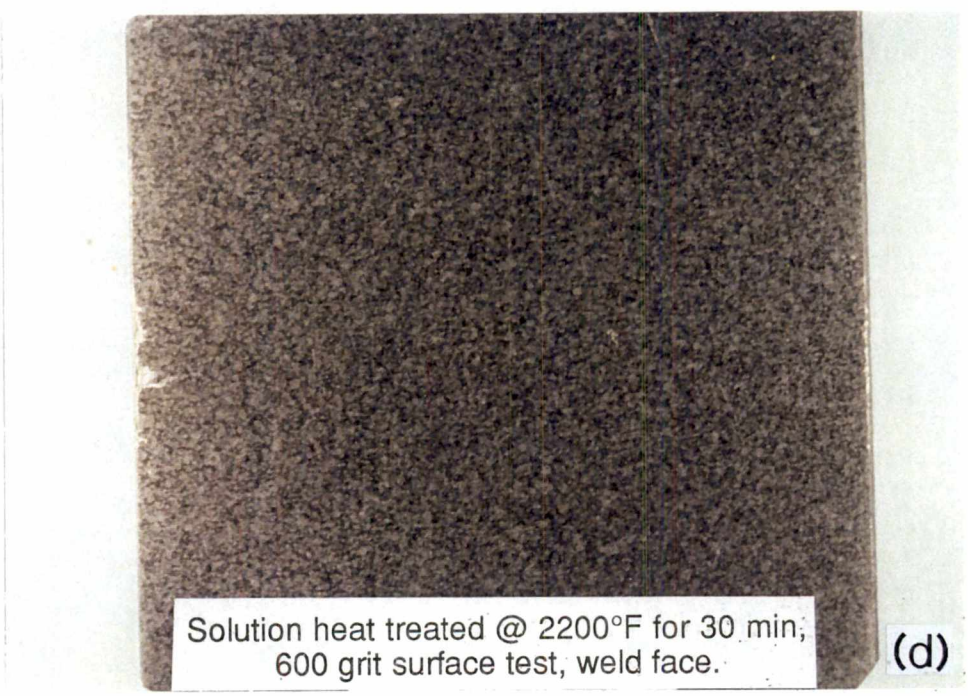


Figure 63 (cont'd). Crevice corrosion tested specimen - AL-6XN autogenous GTA BOP weld, test at 45°C in 6% $FeCl_3$ for 72 hours.

However, the crevice corrosion tendency of the autogenous welds was reduced by solution treatment. The influence of solution treatment on crevice corrosion behavior of the autogenous fusion zone and base metal is shown in Figure 62 (b, c, and d) for the pickled surface condition and Figure 63 (b, c, and d) for 600 grit ground surface condition. For the solution treated specimens (solution-treated at 2100°F), in the pickled condition, crevice corrosion was observed in the autogenous fusion zone and base metal (see Figure 62b). Only slight crevice corrosion occurred in the autogenous fusion zone for specimens solution treated at 2150°F (see Figure 62c) and no crevice corrosion occurred in either the autogenous fusion zone or base metal for the specimens solution treated at 2200°F (see Figure 62d). A similar result was found for the solution treated specimens with a 600 grit surface (see Figures 63b, c, and d). These results indicate that selection of a proper solution treatment temperature is extremely important in improving the crevice corrosion resistance of autogenous weld fusion zones by reducing segregation. Based on the above test results, the optimum solution heat treatment recommended for AL-6XN autogenous welds is 2200°F for 30 minutes. With this solution treatment, the crevice corrosion resistance of the autogenous fusion zone can be improved equivalent to that of the base metal.

To evaluate the effect of solution heat treatment on crevice corrosion behavior of the unmixed zone in dissimilar welds, 254SMO (C-22 filler), 654SMO (P16 filler) and AL-6XN (C-22 filler) GTA open root welds were studied in both the as-welded and solution treated condition. For 254SMO (C-22 filler) GTA open root welds, only the pickled surface condition (10% HNO_3 + 2% HF, 43°C,1 hour) was used for crevice corrosion testing. The test results after a 72

hour immersion in 6% $FeCl_3$ at 45°C are presented in Figures 64a, b, c and d for the as-welded and solution treated welds at 2100°F, 2150°F, and 2200°F, respectively. For the as-welded condition, crevice corrosion was more severe in the unmixed zone than in the other zones in terms of width and depth of the corroded region (see Figure 64a). However, no crevice corrosion occurred in the unmixed zone for the specimens solution treated at temperatures of 2100°F, 2150°F, and 2200°F (see Figures 64b, c, and d). This comparison again shows that solution treatment has a significant effect on preventing crevice corrosion in the unmixed zone. The crevice corrosion resistance of the unmixed zone can be made equivalent to that of the base metal by a thirty minute solution treatment at 2100°F.

For the solution treated specimens of AL-6XN (C-22 filler) and 654SMO (P16 filler) GTA open root welds, the heavy oxide on the surface of the solution treated coupons was difficult to be removed by pickling. Due to this condition, crevice corrosion tests were conducted only on a 600 grit prepared surface for the AL-6XN and 654SMO welds. Comparison crevice corrosion tests in the as-welded and solution treated condition were conducted in 6% $FeCl_3$ for 72 hours at 45°C for AL-6XN and at 80°C for 654SMO weld specimens.

For AL-6XN (C-22) and 654SMO (P16) weld specimens, the comparison test results between the as-welded and solution heat treated conditions for each material show that crevice corrosion is more severe in the unmixed zone than in other zones for the as-welded specimen, but no crevice corrosion occurs in the unmixed zone for any of the solution treated specimens (2100°F, 2150°F, and 2200°F for 30 min). As an example, Figures 65a and 65b show the tested sample appearances of 654SMO welds in the as-welded and solution treated

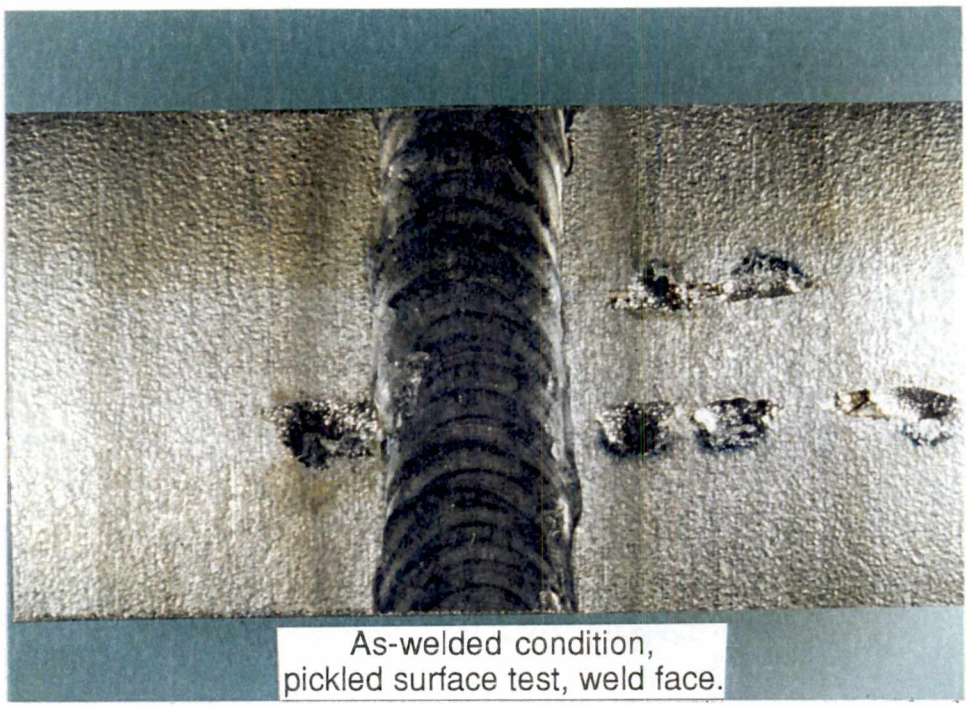
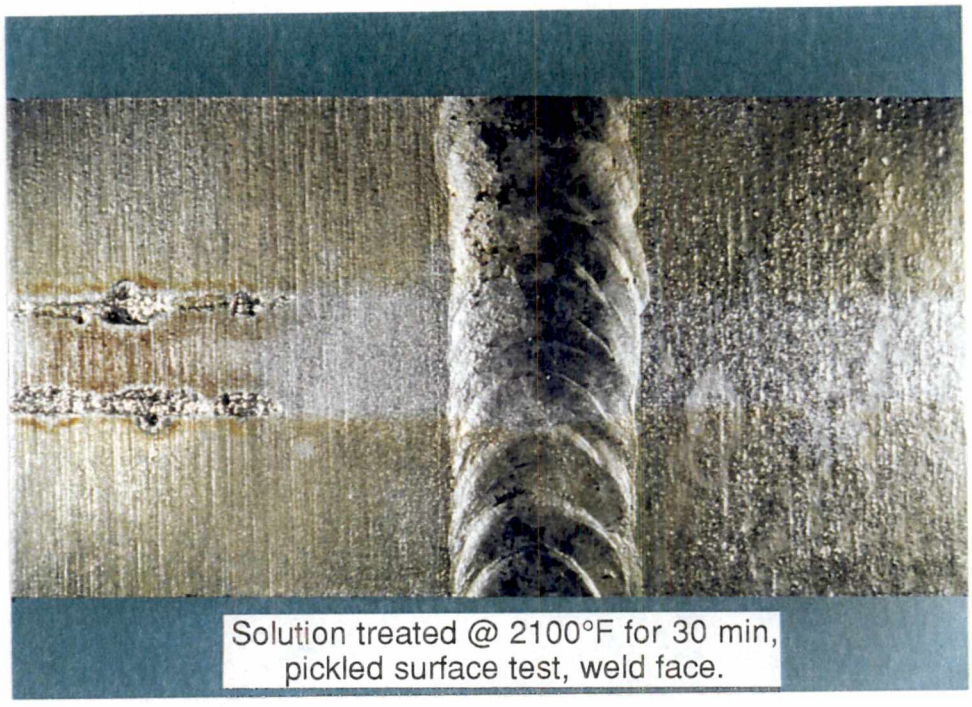




Figure 64. Crevice corrosion tested specimen - 254SMO GTA open root weld (C-22 filler), test at 45°C in 6% $FeCl_3$ for 72 hours, (a) as-welded.



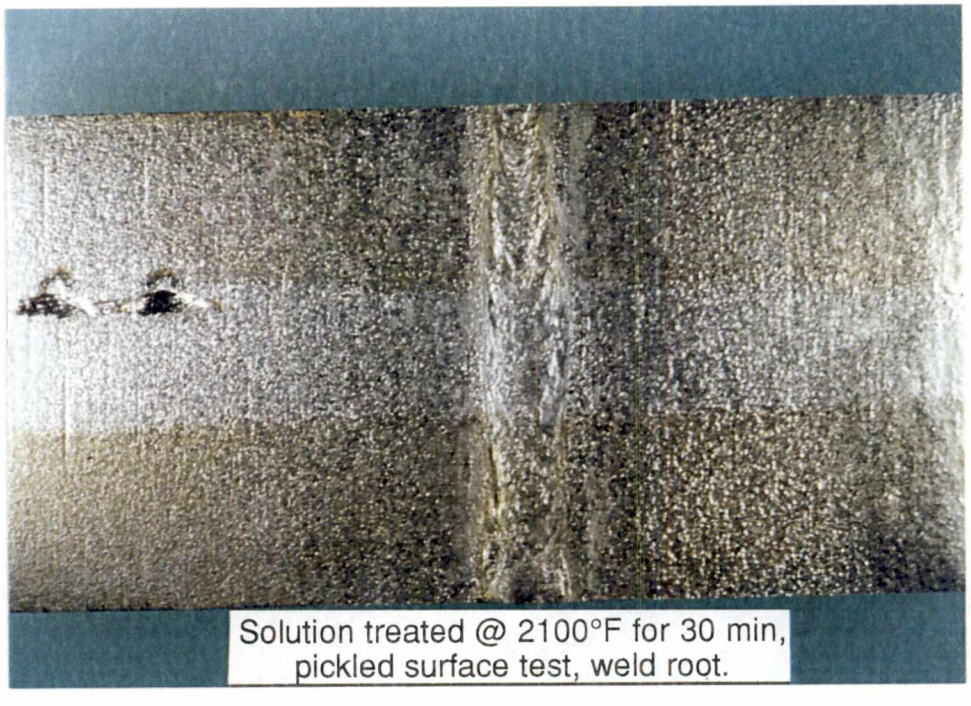


Figure 64(cont'd). Crevice corrosion tested specimen - 254SMO GTA open root weld (C-22 filler), test at 45°C in 6% $FeCl_3$ for 72 hours, (b) solution treated at 2100°F.



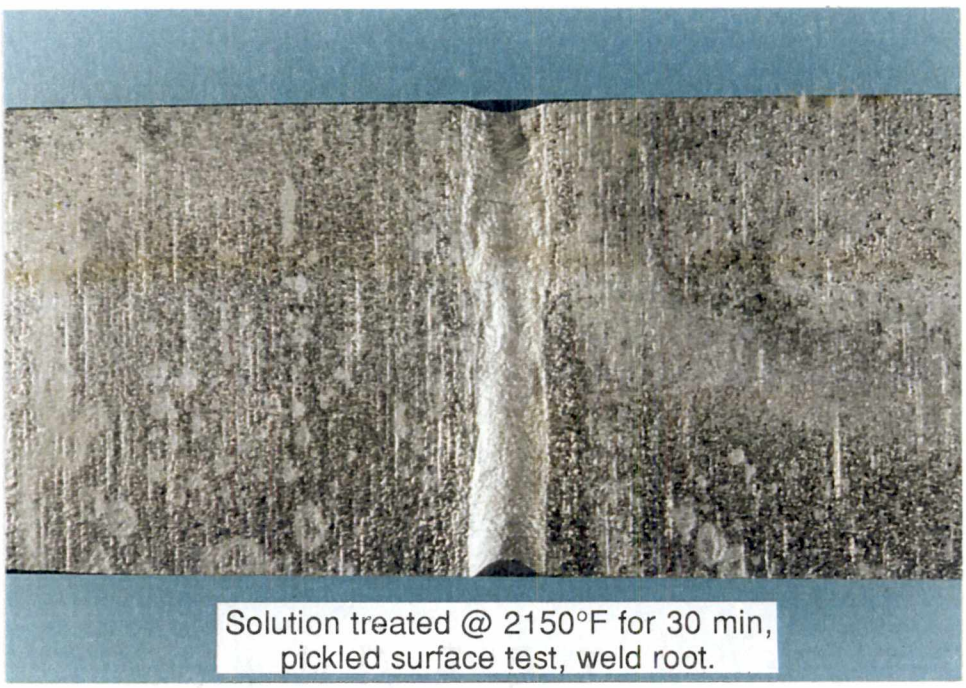
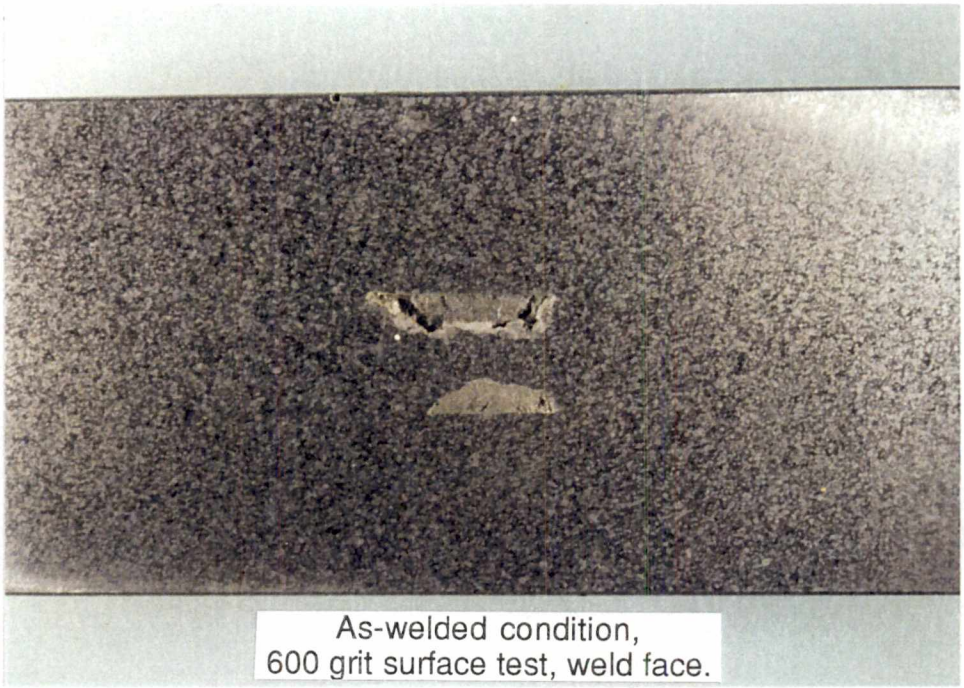


Figure 64 (cont'd). Crevice corrosion tested specimen - 254SMO GTA open root weld (C-22 filler), test at 45°C in 6% $FeCl_3$ for 72 hours, (c) solution treated at 2150°F.

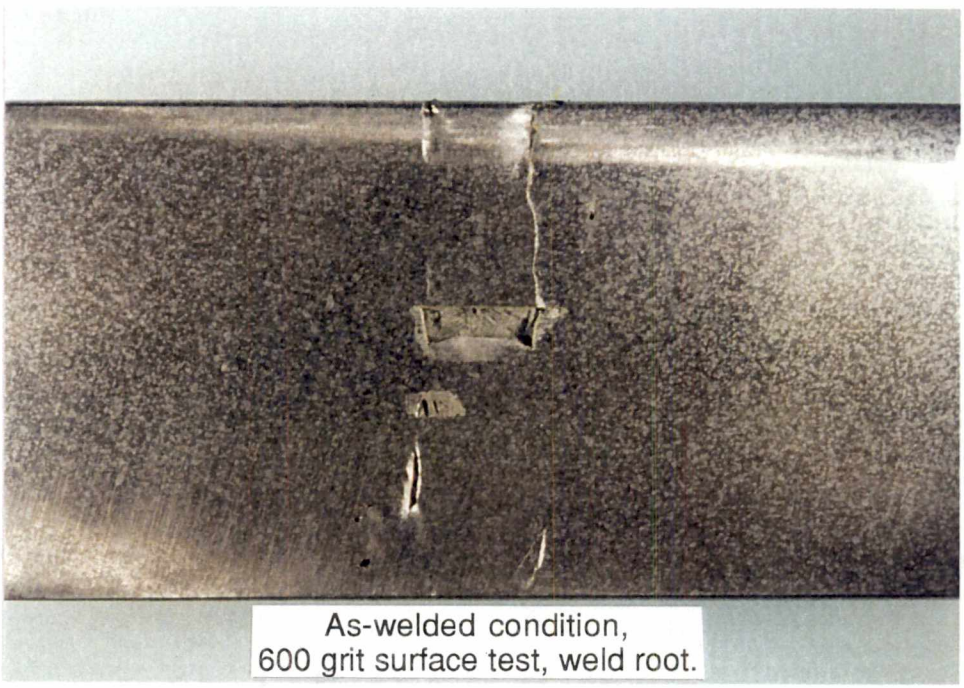




Figure 64 (cont'd). Crevice corrosion tested specimen - 254SMO GTA open root weld (C-22 filler), test at 45°C in 6% $FeCl_3$ for 72 hours, (d) solution treated at 2200°F.



As-welded condition,
600 grit surface test, weld face.

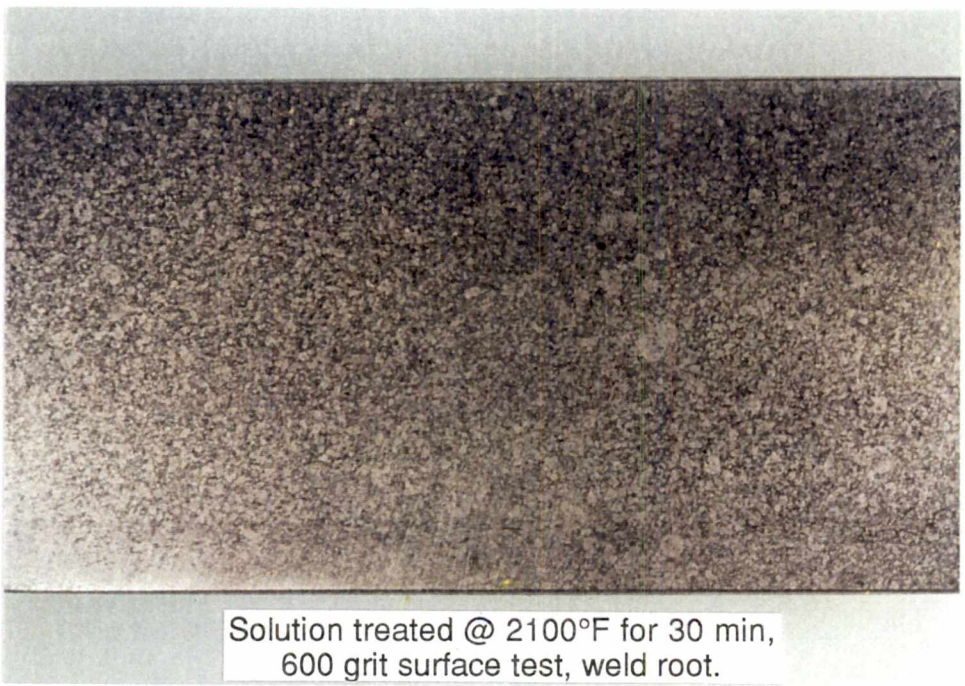


As-welded condition,
600 grit surface test, weld root.

Figure 65. Crevice corrosion tested specimen - 654SMO GTA open root weld (P16 filler), test at 80°C in 6% $FeCl_3$ for 72 hours, (a) as-welded.



Solution treated @ 2100°F for 30 min,
600 grit surface test, weld face.



Solution treated @ 2100°F for 30 min,
600 grit surface test, weld root.

Figure 65 (cont'd). Crevice corrosion tested specimen - 654SMO GTA open root weld (P16 filler), test at 80°C in 6% $FeCl_3$ for 72 hours, (b) solution treated at 2100°F.

conditions (2100°F for 30 min). It is observed that crevice corrosion is more severe in the unmixed zone on both weld face and root for the as-welded condition at 80°C. Also, pitting corrosion along the unmixed zone is evident on the root side of the specimen (see Figure 65a). However, after solution treatment (2100°F for 30 min), the unmixed zone and all the other region were free of crevice corrosion under the same test conditions (see Figure 65b). These results verify that solution treatment plays an important role in increasing the crevice corrosion resistance of the unmixed zone.

The crevice corrosion test results on the dissimilar welds show that solution treatment is remarkably effective in improving the crevice corrosion resistance of the unmixed zone by reducing the extent of segregation in unmixed zone. According to the test results, the minimum time temperature combination for solution heat treatment is 2100°F for 30 minutes for the dissimilar welds. With this treatment condition, crevice corrosion in the unmixed zone of all three weldments {254SMO (with C-22 filler, pickled surface), AL-6XN (C-22 filler, 600 grit surface) and 654SMO (P16 filler, 600 grit surface)}. is completely eliminated. However, for the autogenous fusion zone in AL-6XN GTA autogenous welds, a 2200°F solution heat treatment for 30 min is needed to avoid crevice corrosion in the fusion zone. 254SMO and 654SMO GTA BOP autogenous welds were not evaluated for the effect of solution heat treatment on the crevice corrosion, but it is anticipated that the results would be similar to AL-6XN GTA BOP autogenous welds.

4.3.4 Summary of Unmixed Zone Crevice Corrosion Behavior

The unmixed zone has the lowest crevice corrosion resistance compared

to other weld regions.

Surface condition, especially surface roughness and surface oxidation, remarkably influence the unmixed zone crevice corrosion behavior. A rougher surface or heavy oxidation exacerbates crevice corrosion in the unmixed zone. A combined decrease in surface roughness before welding by grinding (600 grit) and a removal of heat tint after welding by pickling can eliminate crevice corrosion in the unmixed zone.

Solution heat treatment provides a significant improvement of crevice corrosion resistance for the unmixed zone. For the GTA dissimilar welds, a thirty minute solution heat treatment at 2100°F is recommended to provide unmixed zone corrosion resistance equivalent to the base metal. In the case of GTA autogenous welds, a 2200°F solution heat treatment for 30 min is recommended for equivalence between the fusion zone and base metal in regard to crevice corrosion resistance. With the recommended solution treatment, the crevice corrosion resistance of the unmixed zone can be improved to be equivalent to that of the base metal.

Surface oxidation caused by solution heat treatment exacerbates crevice corrosion. Thus, oxidation protection during solution heat treatment is strongly recommended.

4.4 Effect of Welding Technique on the Unmixed Zone Corrosion Behavior

To investigate the effect of welding technique on the unmixed zone corrosion behavior, open root GTAW and GMAW welds (with different heat inputs) were deposited on AL-6XN (C-22 filler). The metallographic evaluation

showed that a wider unmixed zone was obtained for GTAW (average width 0.17 mm) than for GMAW (average width 0.09 mm) for the same heat input (10 KJ/in).

Pitting and crevice corrosion tests were conducted using the specimens extracted from both GTA and GMA weldments. The pitting results showed no difference in CPT for the unmixed zone between GTAW and GMAW regardless of heat input. In the crevice condition, corrosion occurs at the same temperature regardless of welding technique and heat input. However, the extent of pitting and crevice corrosion is influenced by welding technique and welding heat input through their effect on the width and distribution along the weld interface of the unmixed zone. The primary conclusions from the part of the study are:

i) In all dissimilar welds made in this study, regardless of welding process, heat input, filler metal and base metal an unmixed zone was formed.

ii) Both welding technique and heat input have an influence on the unmixed zone in terms of width and distribution.

iii) Neither welding technique nor heat input influenced the CPT and CCCT of the unmixed zone.

iv) Welding technique and heat input influence the severity of pitting and crevice corrosion through their effect on the width and distribution of the unmixed zone.

v) It is to be anticipated that the unmixed zone will not be eliminated by process or filler metal control. Only the extent of the unmixed zone can be controlled but the CPT and CCCT reduction below the base metal level is unavoidable.

Additional studies are necessary to further define the influence of welding technique and welding heat input on the severity of pitting and crevice corrosion in the unmixed zone.

4.5 Effect of Unmixed Zone on Mechanical Properties

Since the unmixed zone has different and distinct characteristics compared to the base metal in terms of its solidification substructure and alloying element segregation, the effect of the unmixed zone on mechanical properties is of interest. In the following section, the effect of the unmixed zone on hardness and ductility is discussed.

4.5.1 Effect of Unmixed Zone on Hardness

Evaluation of the hardness across the unmixed zone was conducted on AL-6XN GTA open root welds (Inconel 625 filler) and AL-6XN GTA BOP autogenous welds using a Leco M-400-G1 micro-hardness tester. A knoop indentor with a 100 gram load was selected due to the narrow width of the unmixed zone. The hardness values across various zones (base metal, unmixed zone, and weld fusion zone) was determined at 0.05 mm intervals for the AL-6XN GTA open root weld and at 0.1 mm intervals for the AL-6XN GTA BOP autogenous weld. The hardness distributions are presented in Figure 66 for the AL-6XN dissimilar weld and in Figure 67 for the autogenous weld, respectively. It is evident that the average hardness in both the unmixed zone in the AL-6XN dissimilar weld and the fusion zone in the AL-6XN autogenous weld are identical to that of the AL-6XN base metal (see Figures 66 and 67). This indicates that the

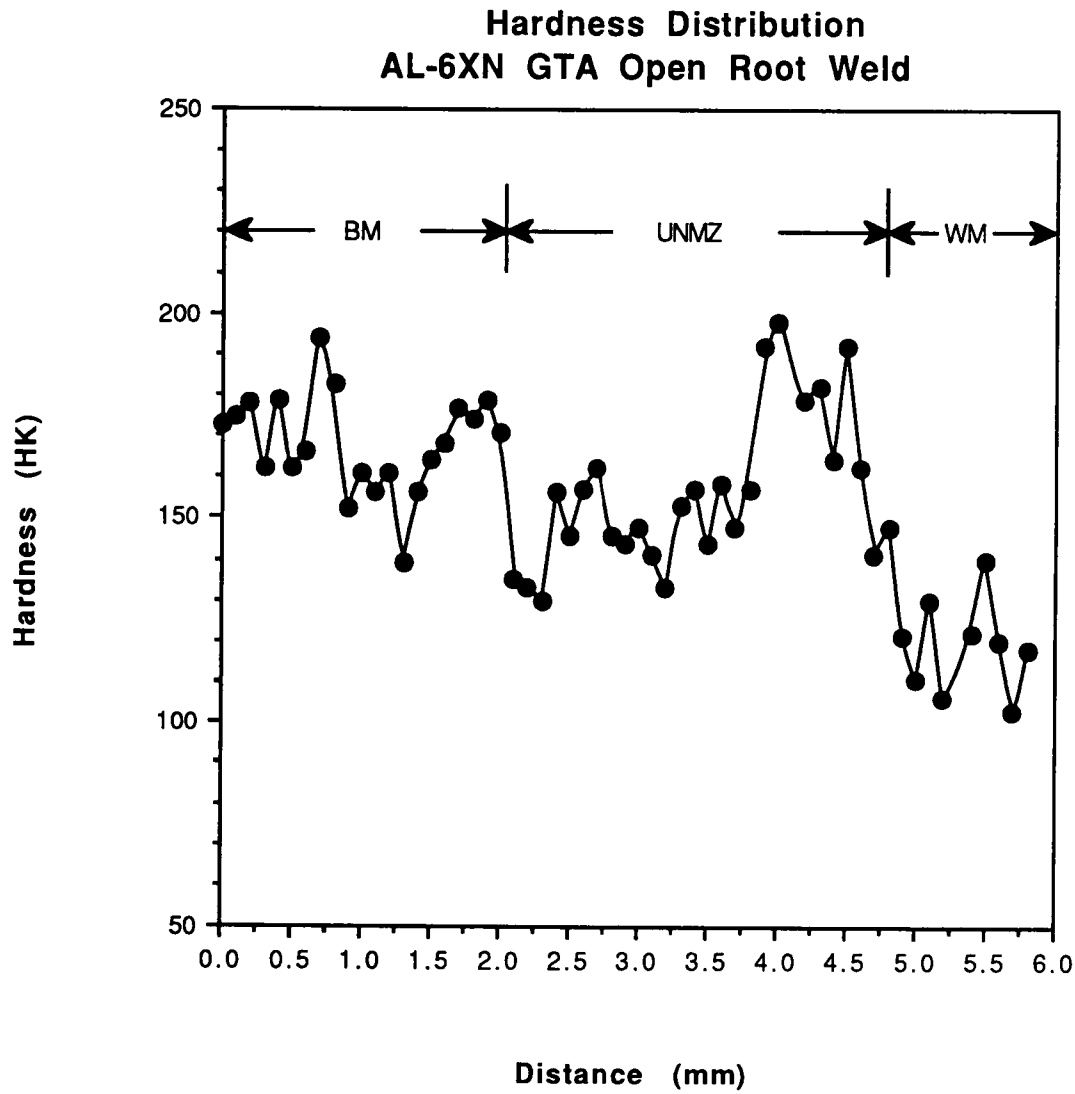


Figure 66. Hardness distribution across the unmixed zone in AL-6XN GTA open root weld (Inconel 625 filler metal).

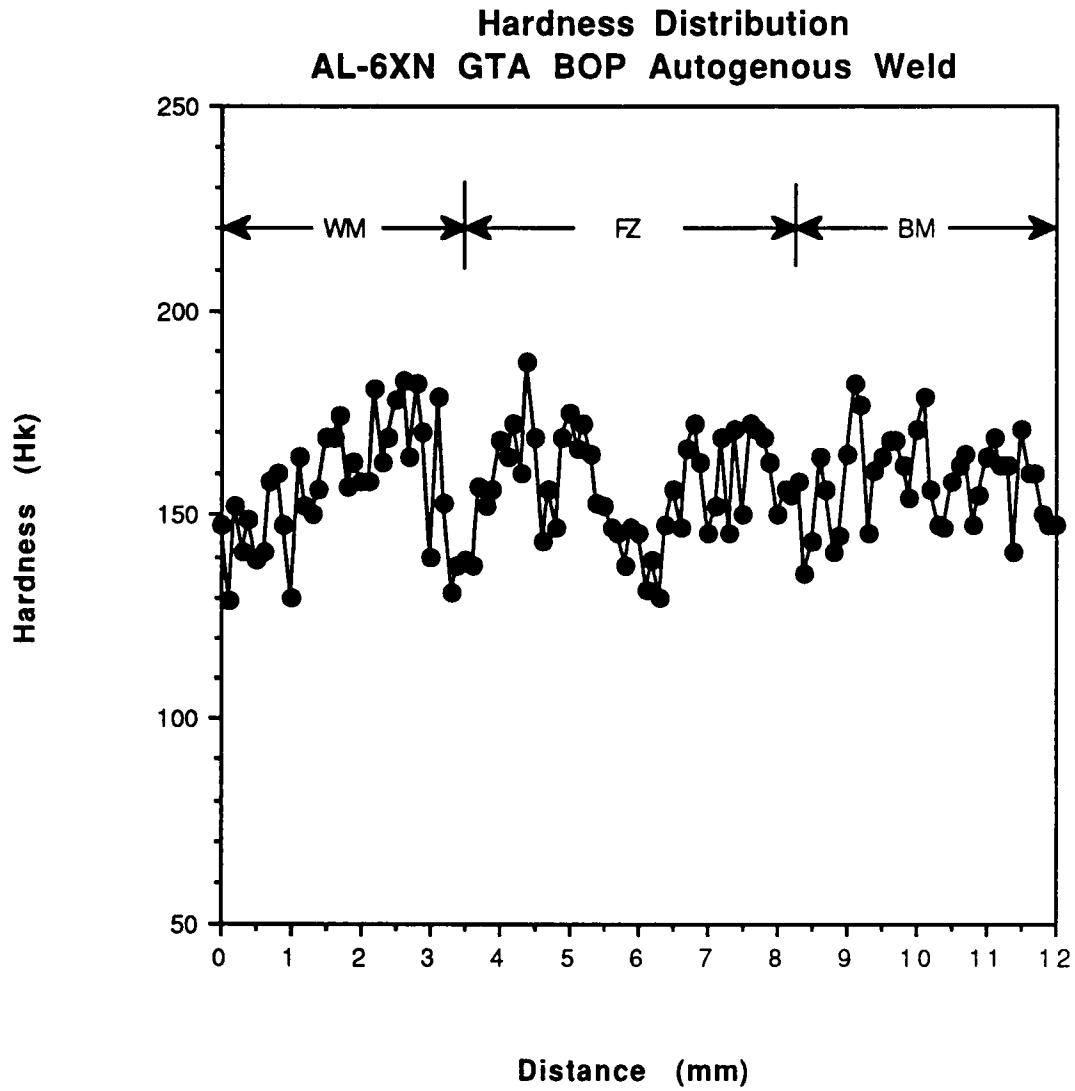


Figure 67. Hardness distribution across the weld fusion zone in AL-6XN autogenous GTA BOP weld.

formation of the unmixed zone along the weld interface will not influence the strength of the weld.

4.5.2 Effect of Unmixed Zone on Ductility

To determine the relative ductility of the unmixed zone and the other weld regions, bend tests (2t radius) were conducted on four types of AL-6XN (1/8" thick) welded coupons (3.5"X1.5"X1/8"):

i) Autogenous GTA BOP weld with the weld parallel to the longitudinal axis of the sample.

ii) Autogenous GTA BOP weld with the weld transverse to the longitudinal axis of the sample.

iii) GTA open root weld (C-22 filler) with the weld parallel to the longitudinal axis of the sample.

iv) GTA open root weld (C-22 filler) with the weld transverse to the longitudinal axis of the sample.

Face bend tests were carried out for autogenous welded specimens, while root bend tests were carried out for open root welded specimens because a uniform unmixed zone is located on weld root side. According to ASTM E190-64 the specimens were bent (3 point bending) in a U-shaped die by means of a centrally applied force. The specimen was forced into the die by a plunger with the a tip radius of 1/4" which provides 22% surface strain. After the bend test, the convex surface of each bent specimen was examined for cracks or other open defects using stereo microscopy at 70X. No cracks or defects were found in the unmixed zone or the other regions for all bend test specimens (2t radius, 180° bending angle). The tested specimens are shown in Figures 68a and b for

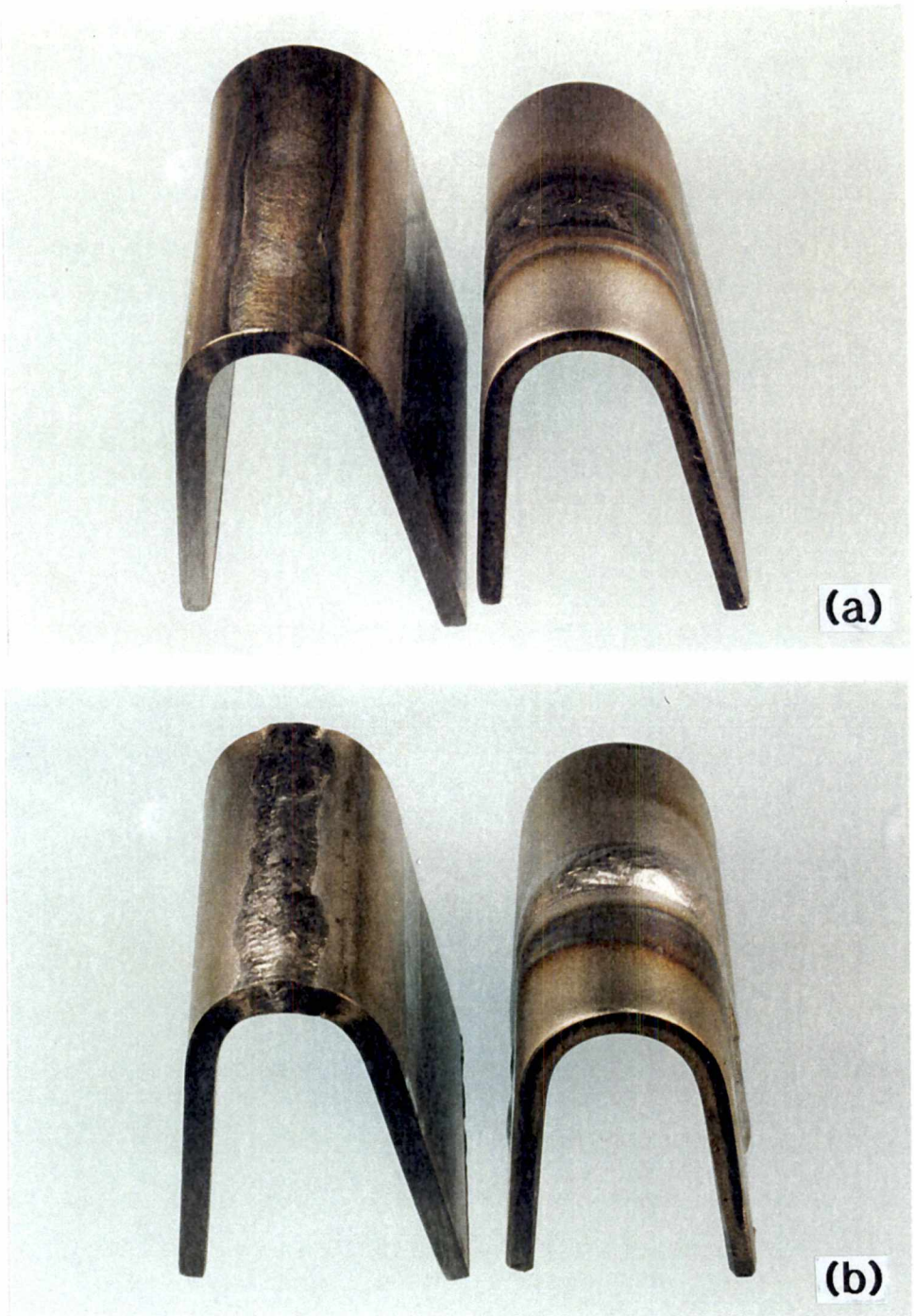


Figure 68. Bend tested specimens - (a) AL-6XN autogenous GTA BOP welded coupons, (b) AL-6XN GTA open root welded coupons (C-22 filler

autogenous GTA BOP weld and dissimilar GTA open root weld, respectively. This data indicates that the unmixed zone has the same bend ductility as all other weld regions.

4.5.3 Summary of the Effect of Unmixed Zone on Mechanical Properties

According to the results of microhardness testing and bend testing, the unmixed zone does not exhibit any difference in hardness and bend ductility compared to the base metal. Therefore, the existence of the unmixed zone should have little influence on the mechanical properties of the weld joint even though it has a significant effect on localized corrosion behavior.

CHAPTER V
CONCLUSIONS

5.1 Evaluation of Unmixed Zone

1) The unmixed zone is a weld region adjacent to the fusion boundary with chemical composition equivalent to the base metal, which has melted and re-solidified during welding. This zone exists in all dissimilar welds made in this study, regardless of welding process, heat input, filler metal and base metal.

2) The unmixed zone can be revealed using proper etchants and etching techniques. Electrolytically applied oxalic acid or glyceregia provide optimum as-etched revelation of the unmixed zone compared to chemically applied aqua regia.

3) Localized variation in the width distribution of the unmixed zone along weld interface has been observed in SMA BOP welds, GTA open root welds and GMA open root welds in the super-austenitic stainless steels. For SMA BOP dissimilar welds, the widest unmixed zone is near the weld root. For GTA and GMA open root welds, the widest unmixed zone is located near the sheet mid-plane and a relatively wide unmixed zone is also found at the face of the welds in some cases.

4) Wider unmixed zone is evident for welds fabricated using a filler metal with a higher melting range than those with a lower melting range.

5) Based on EDS, the Mo content is lowest in the core of the cellular dendrites in the unmixed zone. It is believed that this segregation of Mo, which occurs during solidification of the unmixed zone, plays an important role in the reduced corrosion resistance of the unmixed zone.

6) Solidification in the unmixed zone is epitaxial with the base metal.

7) After solution treatment, the solidification substructure in the unmixed zone is more difficult to define (as compared to the unmixed zone before solution treatment). This is caused by the reduction of segregation in the unmixed zone.

8) EDS studies on 654SMO welds (P16 filler) proves that a solution heat treatment (30 minutes at 2100°F) significantly homogenizes alloying elements in the unmixed zone by diffusion. It is believed that this homogenization of alloying elements plays an important role in improving pitting and crevice corrosion resistance in the unmixed zone.

9) Both welding technique and heat input have an influence on the unmixed zone in terms of width and distribution.

10) The extent of the unmixed zone can be controlled but the unmixed zone will not be eliminated by process or filler metal control.

5.2 Pitting Corrosion Behavior of Unmixed Zone

1) The CPT of the unmixed zone in SMA BOP dissimilar welds was determined to be 80°C for AL-6XN, 64°C for 254SMO and >101°C (boiling temperature of 10% $FeCl_3$ solution) for 654SMO, while the CPT of the base metals was determined to be 90°C for AL-6XN, 80°C for 254SMO and >101°C for 654SMO under the same test conditions (10% $FeCl_3$, 24 hours, 0.05μm specimen surface). Thus, the pitting resistance of the unmixed zone is inferior to that of base metal.

2). The CPT of the fusion zone in GTA BOP autogenous welds was determined to be 60°C for AL-6XN, 56°C for 254SMO and 101°C for 654SMO. Compared to the CPT of the unmixed zone for filler added welds (80°C for AL-6XN, 64°C for 254SMO and >101°C for 654SMO) under the same test conditions (10% $FeCl_3$, 24 hours, 0.05μm specimen surface), the pitting corrosion resistance of the fusion zone in GTA BOP autogenous welds is lower than that of unmixed zone in SMA BOP dissimilar welds.

3) The pitting corrosion resistance of the unmixed zone was evaluated using cyclic polarization test based on the measurement of the hysteresis loop area and passive current density in comparison with the respective base metal. The cyclic polarization test results prove that the pitting corrosion

resistance of the unmixed zone is inferior to that of the respective base metal, and the pitting corrosion resistance of the fusion zone in the autogenous welds is lower than that of the unmixed zone in the dissimilar welds. These test results are consistent with the test results obtained in immersion corrosion testing.

4) Pit initiation and propagation behavior in the unmixed zone can be defined as:

Step. 1: Pits initiate at the core of the cellular dendrites in the unmixed zone. The boundaries of the cellular dendrites remain un-corroded.

Step. 2: With increasing time, the cellular dendrite boundaries in the corroded area are attacked and a major pit is formed (which acts as a channel for further corrosion).

Step. 3: After the major pit is formed, pit propagation occurs beneath the surface with a typical "cave propagation" behavior.

Step 4: After a certain extent of "cave propagation" beneath the surface, corrosion breaks the surface through additional corrosion paths in the core of the cellular dendrites.

5) Pit propagation is always oriented vertically downward, independent of the weld or base metal orientation.

6) Surface finish has a significant influence on the pitting behavior. Greater surface roughness exacerbates pitting corrosion.

7) Solution treatment is remarkably effective in improving the pitting corrosion resistance of the unmixed zone. A thirty minute solution heat treatment at 2100°F is recommended for both dissimilar and autogenous welds to eliminate the pitting corrosion sensitivity in the unmixed zone. After solution treatment at 2100°F for 30 min, the pitting resistance of the unmixed zone in AL-6XN dissimilar welds ($CPT_{AL\text{-}6XN\text{-}UNMZ,\ 600\ grit}$ = 88°C) is equivalent to that of the respective base metal ($CPT_{BM,\ 600\ grit}$ = 88°C), while the pitting resistance of autogenous GTA fusion zone ($CPT_{AL\text{-}6XN\text{-}FZ,\ 600\ grit}$ = 82°C) is slightly lower than that of the respective base metal. {Note that in the as-welded condition, the CPT of the unmixed zone in AL-6XN dissimilar welds is 60°C and the CPT of autogenous GTA fusion zone is 50°C under the same test conditions (10% $FeCl_3$, 24 hours, 600 grit specimen surface)}.

8) Neither welding technique nor heat input influenced the CPT of the unmixed zone. Welding technique and heat input only influence the severity of pitting corrosion through their effect on the width and distribution of the unmixed zone.

5.3 Crevice Corrosion Behavior of Unmixed Zone

1) The unmixed zone in all three super-austenitic stainless steel weldments (AL-6XN, 254SMO and 654SMO) shows lower crevice corrosion resistance than the HAZ and base metal.

2) The unmixed zone in 654SMO weldments has better crevice corrosion resistance than that of AL-6XN and 254SMO weldments.

3) Specimen surface condition has a significant influence on crevice corrosion behavior of the unmixed zone. Decreasing surface roughness by grinding (600 grit) before welding and removing heat tint by pickling after welding can significantly improve the crevice corrosion resistance in the unmixed zone. However, only decreasing surface roughness by grinding (600 grit) before welding or only removing heat tint by pickling after welding can not effectively improve the crevice corrosion resistance in the unmixed zone.

4) Solution treatment can effectively improve the crevice corrosion resistance in the unmixed zone. A thirty minute solution heat treatment at 2100°F is recommended for dissimilar welds to eliminate crevice corrosion in the unmixed zone. A 2200°F solution heat treatment for 30 min is suggested for autogenous weld to avoid the crevice corrosion in autogenous fusion zone. After the recommended solution treatments, the crevice corrosion resistance of the unmixed zone and the autogenous fusion zone is basically equivalent to that of the base metal.

5) Surface oxidation resulting from solution heat treatment exacerbates crevice corrosion. Oxidation protection during solution treatment is strongly recommended.

6) Neither welding technique nor heat input influenced the CCCT of the unmixed zone. Welding technique and heat input only influence the severity of crevice corrosion through their effect on the width and distribution of the unmixed zone.

5.4 Effect of Unmixed Zone on Mechanical properties

1) There is no difference in average hardness either between the unmixed zone and the base metal or between the autogenous fusion zone and the base metal.

2) No cracks or defects were observed in the unmixed zone or other regions for all the bend test specimens at a 180° bend angle (2t radius). This result indicates that the unmixed zone has equivalent ductility compared to the other regions.

REFERENCES

REFERENCES

[1] Flasche, L. H. and Ahluwalia, H. S., "Localized Corrosion of the Unmixed Zone on Nickel-Base Alloy Weldments," Unpublished Research Report.

[2] Savage, W.F., Nippwa, E.F. and Szekeres, E.S. "A Study of Weld Interface Phenomena in a Low Alloy Steel," Weld Journal, 55, 1976, pp 260s-268s.

[3] Hibner, E. L., Hinshaw, E. B., and Lamb, S., "Weld Fabrication of a 6% Molybdenum Alloy to Avoid Corrosion in Bleach Plant Service," TAPPI Proceedings of the 1991 Engineering Conference.

[4] Kelly, J., "AL-6XN Alloy Physical, Mechanical and Corrosion Properties" Rolled Alloys, Inc., 1996.

[5] John, F. G., "AL-6XN ALLOY", Alligheny Ludlum.Corporation.

[6] "Trent AL-6XN Alloy Pipe and Tubing," Trent Tube, A Division of Crucible Materials Corp.

[7] Avesta Sheffield, "254 SMO-Plate, Sheet, Strip, Billet, Bar, Pipe, Tubing, Fittings and Casting," Avesta Sheffield Inc., 425 North Martingale Road, Suite 2000, Schaumburg, IL 60173.

[8] Avesta Sheffield, "654 SMO-a 7%Mo Steel with Excellent Corrosion Resistance in Hot Water and in Acids containing Halides," Avesta Sheffield Inc., 425 North Martingale Road, Suite 2000, Schaumburg, IL 60173.

[9] Wallen, B., Liljas, M. and Stenvall, P. "A New High Nitrogen Superaustenitic Stainless Steel for Use in Bleach Plant Washers and

other Aggressive Chloride Environments," National Association of Corrosion Engineers, Sweden, Avesta AB, S-77480 Avesta, 1992.

[10] "How to Weld Avesta Sheffield 254 SMO Stainless Steel," Avesta Sheffield Inc., 425 N. Martingale Rd., Suite 2000, Schaumburg, Illinois 60173.

[11] "Guidelines for the Welding of AvestaSheffield 654 SMO," Avesta Welding AB, Box 501, S-77427 Avesta, Sweden.

[12] Liljas, M. and Stenvall, P. "Welding of UNS S32654 - Corrosion Properties and Metallurgical Aspects," 12th International Corrosion Congress", Sept. 19-24, 1993, Houston, Tx (NACE).

[13] Baeslack, W. A., Lippold, J. C. and Savage, W. F. "Unmixed Zone Formation in Austenitic Stainless Steel Weldments," Welding Journal, 58, (6), June 1979, pp 168s-176s.

[14] Matthews, S. J. and Savage, W. F., "Heat-Affected Zone Inflitration by Dissimilar Liquid Weld Metal," Welding Journal, April 1971, pp 174s-182s.

[15] Lundin, C. D. Unpublished Research Rensselaer Polytechnic Institute, Troy, NY, 1964.

[16] Karlsson, L. and Arcini, H. "Formation of Unmixed Zones in Stainless Steel Welds," Innobation Stainless Steel Florence, Italy 11-14 October 1993, pp 3.273-3.278.

[17] Lukkri, J. and Moisio, T., "The Effect of the Welding Method on the Unmixed Zone of the Weld," Microstructural Science, Bolume 7, 1979, pp 333-344.

[18] Lundin, C. D. Unpublished Research University of Tennessee, Knoxville, TN, 1969.

[19] Takalo, T. and Moisio, T., "Fusion Line Attack at Low Corrosion Potentials in Austenitic Stainless Steel Welds," IIW Annual Assembly 1975, Public Session, Tel-Aviv, Israel, July 1975.

[20] Takalo, T. and Moisio, T., "Fusion Line Corrosion in Welds of Austenitic Stainless Steels," CHISA 1975, Prague, Czechoslovakia, August 1975.

[21] Tuthill, A. H. and Avery, R. E., "Corrosion Behavior of Stainless Steel and High-Alloy Weldments in Aggressive Oxidizing Environments," Welding Journal Research Supplement, February 1993, pp 41s-49s.

[22] Mliljas, Holmberg, B. and Ulander, A., "Welding of a High-molybdenum Austenitic Stainless Steel," Stainless Steels, 1984, pp 323-329.

[23] Gooch, T. "Welding Behavior and Weldability of Superaustenitic Stainless Steels," TWI, Cambridge, UK.

[24] Garner, A. H. , "Corrosion of Weldments in Pulp Bleach Plant ," Welding Journal, September 1986, pp 39-44.

[25] Garner, A., "Pitting Corrosion of High Alloy Stainless Steel Weldments in Oxidizing Environments," Welding Journal, January 1983, pp 27-34.

[26] Tuthill, A. H. and Garner, A., "Evaluation of Bleach Plant Piping Materials," Tappi Journal, June 1990, pp 147-151.

[27] Tuthill, A. H. and Avery, R. E., "Open Root Joint Welding of 6% Mo Pipe for Bleach Plant Service," TAPPI C & ME Metals Subcommittee Task Group Communication, January 1993, pp 1-7.

[28] Kearns, J. R. and Moller, G. E., "Optimizing the Corrosion Resistance of Welded Austenitic Stainless Alloys," The NACE Annual Conference and

Corrosion Show, March 11-15, 1991, Cincinnati Convention Center • CinCinnati, Ohio.

[29] Rabinsteimer, G. "The Welding of Fully Austenitic Stainless Steels with High Molybdenum Contents," Welding in the World, 27, (1/2), 1989.

[30] Gabrielli, C., Huet, F., Keddam, M. and Oltra, R. "Localized Corrosion as a Stochastic Process: A Review," Proceeding of the Second International Conference on Localized Corrosion, Orlando, Florida, June 1-5, 1987, pp 93-108.

[31] Sharland, S. M., Bishop, C. M., Balkwill, P. H. and Stewart, J. "A Process Governed be a Strange Attractor? " Proceeding of the Second International Conference on Localized Corrosion, Orlando, Florida, June 1-5, 1987, pp 109-115.

[32] Bertocci, U. "Statistics of Localized Breakdown Noise," Proceeding of the Second International Conference on Localized Corrosion, Orlando, Florida, June 1-5, 1987, pp 127-130.

[33] Smialowska, Z. S. "Pit Initiation," Proceeding of the Second International Conference on Localized Corrosion, Orlando, Florida, June 1-5, 1987, pp 41s-45s.

[34] Stamsbury, E. E. and Buchanan, R. A. "Fundamentals of Electrochemical Corrosion," Unpublished Text Book.

[35] Siebert, O. W. "Laboratory Electrochemical Test Methods," Laboratory Corrosion Tests and Standards. ASTM STP 866, G. S. Haynes and R. Baboian. Eds. American Society for Testing and Materials, Philadelphia, 1985, pp 65-90.

[36] Oldfield, J. W. " Test Techniques for Pitting and Crevice Corrosion Resistance of Stainless Steels and Nickel-Base Alloys in Chloride-Containing Environments," International Materials Reviews, Vol. 32, No. 3, 1987, pp 153-170.

[37] Smialowska, S. and Czachor, M. "The Analysis of Electrochemical Methods for the Determination of Characteristic Potentials of Pitting Corrosion," Localized Corrosion, National Association of Corrosion Engineers, 1971, pp 353-362.

[38] Hubbell, M., Price, C. and Heidersbach, R. "Crevice and Pitting Corrosion Tests for Stainless Steels: A Comparison of Short-Term Tests with Longer Exposures," Laboratory Corrosion Tests and Standards, ASTM STP866, 1983, pp 324-335.

[39] ASTM G61-78: "Standard Practice for Conducting Cyclic Potentiodynamic Polarization Measurements for Localized Corrosion," Pa, American Society for Testing and Materials.

[40] Lau, P. and Bernhardsson, S. "Electrochemical Techniques for the Study of Pitting and Crevice Corrosion Resistance of Stainless Steels," Electrochemical Techniques for Corrosion Engineering, National Association of Corrosion Engineers, 1986, pp 281-286.

[41] Brigham, R. J. and Tozer, E. W. "Temperature as a Pitting Criterion," National Association of Corrosion Engineers, Vol. 29, No. 1, January, 1973, pp 33-36.

[42] Macdonald, D. D., Liu, C., etc. "Prediction and Measurement of Pitting Damage Functions for Condensing Heat Exchangers," Corrosion-Vol. 50, No. 10, NACE International, 1994, pp 761-780.

[43] Odegard, L. and Fage, S. A., "The Toot Side Pitting Resistance of Stainless Steel Welds," Duplex Stainless Steels, Vol. 1, 28-30 Oct. 1991, Beaune Bourgogne, France, pp 451-460.

[44] Leinonen, J. I., Jarvenpaa, S. A. and Karjalainen, L. P., "Pitting Corrosion Properties of Autogenous TIG and Laser Welds in A 20Cr-22Ni-6Mo-N Steel," Stainless Steels, Proceeding of International Conference on Stainless Steels, 1991, Chiba, ISIJ, pp 373-378.

[45] Jarvenpaa, S. A., Leinonen, J. I.,Karjalainen, L. P. and Suutala, N., "Impact Toughness and Pitting corrosion Properties of Metal Arc, MIG and Plasma Welds in a 20Cr-22Ni-6Mo-N Steel," Stainless Steels, Proceeding of International Conference on Stainless Steels, 1991, Chiba, ISIJ, pp 379-386.

[46] ASTM G48: "Standard Test Methods for Pitting and Crevice Corrosion Resistance of Stainless Steels and Related Alloys by the Use of Ferric Chloride Solution," Pa, American Society for Testing and Materials.

[47] ASTM E190-64: "Standard Methods for Guided Bend Test for Ductility of Welds," Pa, American Society for Testing and Materials.

[48] McGannon, H. E., "The Making, Shaping and Treating of Steel", Ninth Edition, United States Steel, pp337-338.

VITA

Wei Liu, was born in Changchun City, Jilin Province, The People's Republic of China on March 23, 1959. She attended elementary school and then Changchun High School from which she graduated in July 1978. The following September she entered Jilin University and received the degree of Bachelor of Science in Physical Chemistry in July 1982. After she graduated from Jilin University, she worked in Department of Applied Chemistry in, Jilin University of Technology as an instructor and director of physical chemistry group until July 1991. The following August she came to Knoxville, Tennessee, United States of America to visit her husband. In January 1994, she was accepted as a graduate student in The University of Tennessee and received a Master of Science degree in Metallurgical Engineering in August 1996.

Now, she presently enrolled at The University of Tennessee, Knoxville.